Persoonia 46, 2021: 63–115
www.ingentaconnect.com/content/nhn/pimj

RESEARCH ARTICLE

ISSN (Online) 1878-9080
https://doi.org/10.3767/persoonia.2021.46.03

Evaluating species in *Botryosphaeriales*

W. Zhang[1], J.Z. Groenewald[2], L. Lombard[2], R.K. Schumacher[3], A.J.L. Phillips[4], P.W. Crous[2,5,*]

Key words

canker and leaf spot pathogens
Multi-Locus Sequence Typing (MLST)
new taxa
systematics

Abstract The *Botryosphaeriales* (*Dothideomycetes*) includes numerous endophytic, saprobic, and plant pathogenic species associated with a wide range of symptoms, most commonly on woody plants. In a recent phylogenetic treatment of 499 isolates in the culture collection (CBS) of the Westerdijk Institute, we evaluated the families and genera accommodated in this order of important fungi. The present study presents multigene phylogenetic analyses for an additional 230 isolates, using ITS, *tef1*, *tub2*, LSU and *rpb2* loci, in combination with morphological data. Based on these data, 58 species are reduced to synonymy, and eight novel species are described. They include *Diplodia afrocarpi* (*Afrocarpus*, South Africa), *Dothiorella diospyricola* (*Diospyros*, South Africa), *Lasiodiplodia acaciae* (*Acacia*, Indonesia), *Neofusicoccum podocarpi* (*Podocarpus,* South Africa), *N. rapaneae* (*Rapanea,* South Africa), *Phaeobotryon ulmi* (*Ulmus*, Germany), *Saccharata grevilleae* (*Grevillea,* Australia) and *S. hakeiphila* (*Hakea,* Australia). The results have clarified the identity of numerous isolates that lacked Latin binomials or had been deposited under incorrect names in the CBS collection in the past. They also provide a solid foundation for more in-depth future studies on taxa in the order. Sequences of the *tef1*, *tub2* and *rpb2* genes proved to be the most reliable markers. At the species level, results showed that the most informative genes were inconsistent, but that a combination of four candidate barcodes (ITS, *tef1*, *tub2* and *rpb2*) provided reliable resolution. Furthermore, given the large number of additional isolates included in this study, and newly generated multigene DNA datasets, several species could also be reduced to synonymy. The study illustrates the value of reassessing the identity of older collections in culture collections utilising modern taxonomic frameworks and methods.

Citation: Zhang W, Groenewald JZ, Lombard L, et al. 2021. Evaluating species in Botryosphaeriales. Persoonia 46: 63–115. https://doi.org/10.3767/persoonia.2021.46.03.
Effectively published online: 2 February 2021 [Received: 3 October 2020; Accepted: 18 January 2021].

INTRODUCTION

The *Botryosphaeriales* (*Dothideomycetes*) includes a phylogenetically and morphologically diverse assemblage of fungi occurring on many different hosts and have a wide global geographic distribution. They are found as pathogens or saprobes on both gymnosperms and angiosperms and occur mainly on the trunks and branches of woody plants (Phillips et al. 2013, Sarr et al. 2014, Zlatkovic et al. 2016, Lawrence et al. 2017, Scarlett et al. 2018, Zhu et al. 2018). However, they are occasionally also found on the leaves of herbaceous plants, and even on lichens (Denman et al. 2000, Mohali et al. 2007). Some species commonly occur as asymptomatic endophytes that become evident when their host plants are subjected to stress (Slippers & Wingfield 2007). Intriguingly, some species are known to cause opportunistic infections in humans, or have been isolated from sea grasses in marine environments (De Hoog et al. 2000, Sakayaroj et al. 2010).

The *Botryosphaeriales* was introduced by Schoch et al. (2006) who constructed a multigene phylogeny from 96 taxa in the *Dothideomycetes*. Those results showed that all species of '*Botryosphaeria*' and *Phyllosticta* clustered in a single clade that could not be associated with any order of fungi. Consequently, the new order, *Botryosphaeriales* was proposed and it included only the single family, *Botryosphaeriaceae*. Molecular evidence provided by Minnis et al. (2012) subsequently showed that a separate family, *Planistromellaceae,* also resided in the *Botryosphaeriales*. Wikee et al. (2013) resurrected *Phyllostictaceae* as a family in *Botryosphaeriales* to accommodate *Phyllosticta* and three new families, *Aplosporellaceae* (*Aplosporella* and *Bagnisiella*), *Melanopsaceae* (*Melanops*) and *Saccharataceae* (*Saccharata*), were introduced by Slippers et al. (2013). Later, Wyka & Broders (2016) added the *Septorioideaceae* (*Septorioides*) and Yang et al. (2017) introduced the *Endomelanconiopsisaceae* (*Endomelanconiopsis*) and *Pseudofusicoccumaceae* (*Pseudofusicoccum*), ultimately resulting in nine families in *Botryosphaeriales*. Slippers et al. (2017) reviewed the historical developments of species identification and taxonomy of the order and stressed that the biology of these species is still poorly understood. Phillips et al. (2019) considered a reduced dataset (LSU and ITS), and argued that the order should accommodate only the *Aplosporellaceae, Botryosphaeriaceae, Melanopsaceae, Phyllostictaceae, Planistromellaceae* and *Saccharataceae*.

Theissen & Sydow (1918) originally introduced the *Botryosphaeriaceae* as a subfamily in the *Pseudosphaeriaceae*, including *Phaeobotryon* and *Dibotryon*. Numerous genera were subsequently included, although without the support of DNA

[1] School of Geographical Science, Lingnan Normal University, Zhanjiang 524048, China.
[2] Westerdijk Fungal Biodiversity Institute, Uppsalalaan 8, 3584 CT Utrecht, The Netherlands; corresponding author e-mail: p.crous@wi.knaw.nl.
[3] Hölderlinstraße 25, 15517 Fürstenwalde / Spree, Germany.
[4] Universidade de Lisboa, Faculdade de Ciências, Biosystems and Integrative Sciences Institute (BioISI), Campo Grande, 1749-016 Lisbon, Portugal.
[5] Wageningen University and Research Centre (WUR), Laboratory of Phytopathology, Droevendaalsesteeg 1, 6708 PB Wageningen, The Netherlands.

sequence data. Liu et al. (2012) re-examined the type specimens of 15 genera, and based on morphology, accepted 29 genera in the *Botryosphaeriaceae*. Subsequently, Phillips et al. (2013) provided detailed descriptions and keys to 17 genera and 110 species known from culture at that time. A revision of the *Tiarosporella* complex resulted in the addition of four new genera (Crous et al. 2015), while *Alanphillipsia* and *Sardiniella* were introduced by Crous et al. (2013) and Linaldeddu et al. (2016a), respectively. Yang et al. (2017) introduced *Oblongocollomyces* and reduced *Spencermartinsia* to synonymy with *Dothiorella*. Following these various treatments, 33 genera are now recognized in *Botryosphaeriales*.

The culture collection (CBS) of the Westerdijk Fungal Biodiversity Institute (WI) in Utrecht, the Netherlands, accommodates numerous cultures of *Botryosphaeriales*. Many of these have been the subject of previous studies, but others have not yet been identified to species level or subjected to current taxonomic frameworks and methods. The aim of the present study was to name the unidentified *Botryosphaeriales* in the CBS collection that were not treated by Yang et al. (2017), and to resolve their taxonomy in light of currently available DNA sequence data and phylogenetic inference.

MATERIALS AND METHODS

Isolates

All isolates used in this study were sourced from the CBS culture collection of the WI in Utrecht, the Netherlands, and the working collection of Pedro Crous (CPC) housed at the WI (Table S1). DNA sequences for other strains not examined here but published in previous phylogenetic studies were retrieved from GenBank (Table S1).

DNA extraction, PCR amplification and sequencing

Total genomic DNA was extracted from 7-d-old axenic cultures, grown on 2 % malt extract agar (MEA) at room temperature, using the UltraClean Microbial DNA isolation kit (Mo Bio Laboratories, California, USA) following the protocols provided by the manufacturer. Partial gene sequences were determined for the internal transcribed spacer 1 and 2 including the intervening 5.8S nrDNA gene (ITS), the translation elongation factor 1-alpha gene (*tef1*), the beta-tubulin gene (*tub2*), the large subunit of the nuclear ribosomal RNA gene (LSU) and DNA directed RNA polymerase II second largest subunit gene (*rpb2*), using the primers listed in Table 1. Amplification protocols followed those of Pavlic et al. (2009), Phillips et al. (2013), Slippers et al. (2013) and Cruywagen et al. (2017). Amplicons were sequenced in both directions using a BigDye Terminator v. 3.1 Cycle Sequencing Kit (ThermoFisher Scientific) according to the manufacturer's instructions. Forward and reverse reads were paired and consensus sequences calculated in MEGA v. 7.0.21 (Kumar et al. 2016) and DNASTAR Lasergene SeqMan Pro v. 8.1.3. All new sequences and sequences that were longer or had nucleotide differences with published sequences were submitted to GenBank (Table S1).

Phylogenetic analyses

Sequence alignments of the five individual loci (ITS, *tef1*, *tub2*, LSU, *rpb2*) for the generic groups were made using MAFFT v. 7 (http://mafft.cbrc.jp/alignment/server/index.html) (Katoh & Standley 2013), and were then manually edited in MEGA v. 7.0.21. Maximum Likelihood (ML) and Bayesian analysis (BA) were used for phylogenetic inferences of the concatenated alignments. The ML analyses were executed on the CIPRES Science Gateway portal (https://www.phylo.org/) (Miller et al. 2012) using RAxML-HPC BlackBox v. 8.2.10 (Stamatakis 2014) and the Bayesian analyses locally using MrBayes v. 3.2.6 (Huelsenbeck & Ronquist 2001, Ronquist & Huelsenbeck 2003), respectively. For ML analyses, a GTR+GAMMA substitution model with 1 000 bootstrap iterations was set. For the Bayesian analyses, character sets were defined for each locus, and MrModel Test v. 2.2 (Nylander 2004) was used to determine their optimal nucleotide substitution model settings. Bayesian analyses were computed with four simultaneous Markov Chain Monte Carlo chains, 100 000 000 generations and a sampling frequency of 10 generations (*Botryosphaeria*, *Neofusicoccum parvum* complex, *Neoscytalidium*, *Phaeobotryon*, *Pseudofusicoccum* and *Saccharata* alignments) or 100 generations (*Diplodia*, *Dothiorella*, *Lasiodiplodia* and *Neofusicoccum* alignments), ending the run automatically when standard deviation of split frequencies fell below 0.01. The burn-in fraction was set to 0.25, after which the 50 % majority rule consensus trees and posterior probability (PP) values were calculated. The resulting trees were plotted using FigTree v. 1.4.2 (http://tree.bio.ed.ac.uk/software/figtree). Alignments and trees were deposited in TreeBASE (www.treebase.org; study S27596).

The individual gene trees were assessed for clade conflicts between the individual phylogenies (see next paragraph). For these assessments, Bayesian analyses were conducted as described above (with a sampling of every 10 generations for all analyses), as well as parsimony analyses using PAUP v. 4.0b10 (Swofford 2003) as explained in Braun et al. (2018). Species with missing data for a given gene were excluded from the analysis of that gene region. For all potential taxonomic novelties, their phylogenetic position, branch length to the closest sister

Table 1 Details of primer combinations used during this study for amplification and sequencing.

Locus[1]	Primer name	Sequence 5'→3'	Tm (°C)	Reference
ITS	ITS5	GGA AGT AAA AGT CGT AAC AAG G	52	White et al. (1990)
	ITS4	TCC TCC GCT TAT TGA TAT GC	52	White et al. (1990)
LSU	LR0R	ACC CGC TGA ACT TAA GC	52	Rehner & Samuels (1994)
	LR5	TCC TGA GGG AAA CTT CG	52	Vilgalys & Hester (1990)
tef1	EF1-728F	CAT CGA GAA GTT CGA GAA GG	54	Carbone & Kohn (1999)
	EF1-986R	TAC TTG AAG GAA CCC TTA CC	54	Carbone & Kohn (1999)
tub2	Bt-2a	GGT AAC CAA ATC GGT GCT GCT TTC	52	Glass & Donaldson (1995)
	Bt-2b	ACC CTC AGT GTA GTG ACC CTT GGC	52	Glass & Donaldson (1995)
rpb2	RPB2-6F	TGG GGK WTG GTY TGY CCT GC	60→58→54	Liu et al. (1999)
	fRPB2-7cR	CCC ATR GCT TGY TTR CCC AT	60→58→54	Liu et al. (1999)
	RPB2bot6F	GGT AGC GAC GTC ACT CCC	60→58→54	Sakalidis et al. (2011)
	RPB2bot7R	GGA TGG ATC TCG CAA TGC G	60→58→54	Sakalidis et al. (2011)
	RPB2-LasF	GGTAGCGACGTCACTCCT	60→58→54	Cruywagen et al. (2017)
	RPB2-LasR	GCGCAAATACCCAGAATCAT	60→58→54	Cruywagen et al. (2017)

[1] ITS: internal transcribed spacer regions and intervening 5.8S nrRNA gene;LSU: partial 28S nrRNA gene, large subunit; *tef1*: partial translation elongation factor 1-alpha gene; *tub2*: partial beta-tubulin gene; *rpb2*: partial DNA-directed RNA polymerase II second largest subunit.

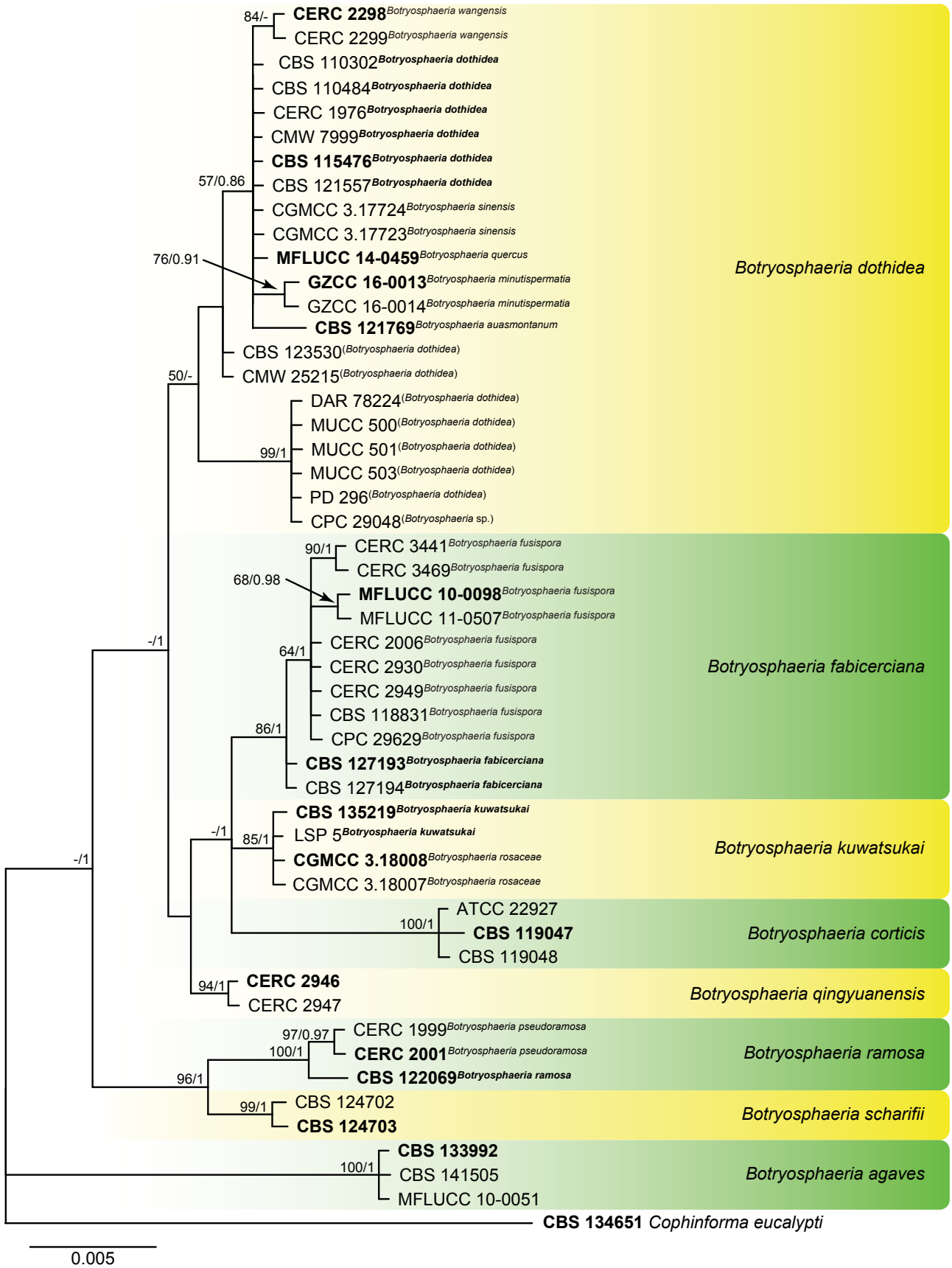

Fig. 1 Phylogenetic tree of *Botryosphaeria* resulting from a Bayesian analysis of the combined ITS, *tef1* and *tub2* sequence alignment. Maximum likelihood bootstrap support values (ML-BS > 50 %) and Bayesian posterior probabilities (PP > 0.85) are shown at the nodes. Ex-type strains and taxonomic novelties are indicated in **bold** font and the species are delimited with coloured blocks. The last accepted species names, or working species names in round parentheses, are shown in superscript where species were synonymised in this study; species names on which the name of the clade is based are in **bold** superscript. The tree was rooted to *Cophinforma eucalypti* (CBS 134651).

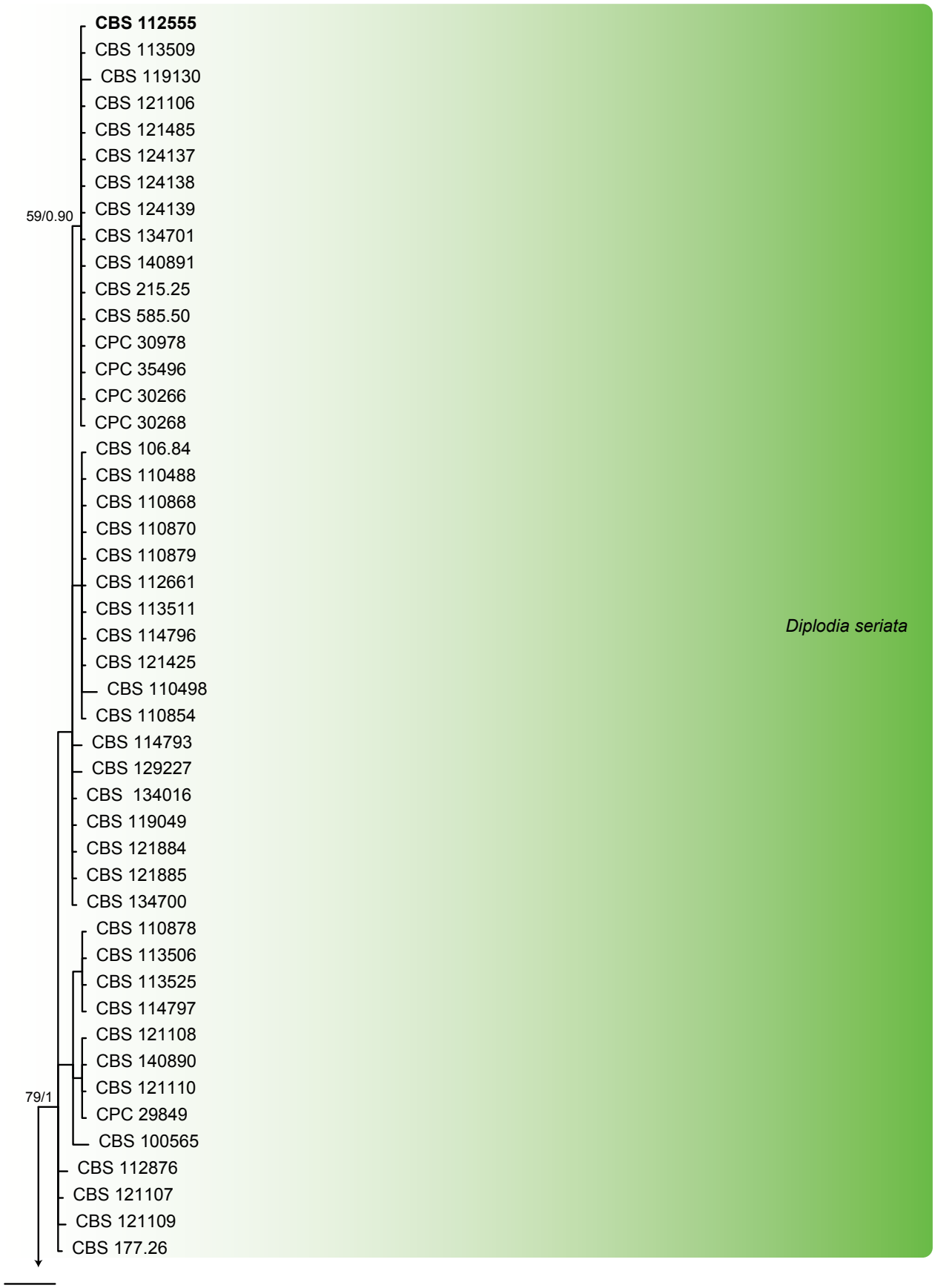

Fig. 2 Phylogenetic tree of *Diplodia* resulting from a Bayesian analysis of the combined ITS, *tef1* and *tub2* sequence alignment. Maximum likelihood bootstrap support values (ML-BS > 50 %) and Bayesian posterior probabilities (PP > 0.89) are shown at the nodes. Ex-type strains and taxonomic novelties are indicated in **bold** font and the species are delimited with coloured blocks. The last accepted species names, or working species names in round parentheses, are shown in superscript where species were synonymised in this study; species names on which the name of the clade is based are in **bold** superscript. The tree was rooted to *Lasiodiplodia theobromae* (CBS 164.96).

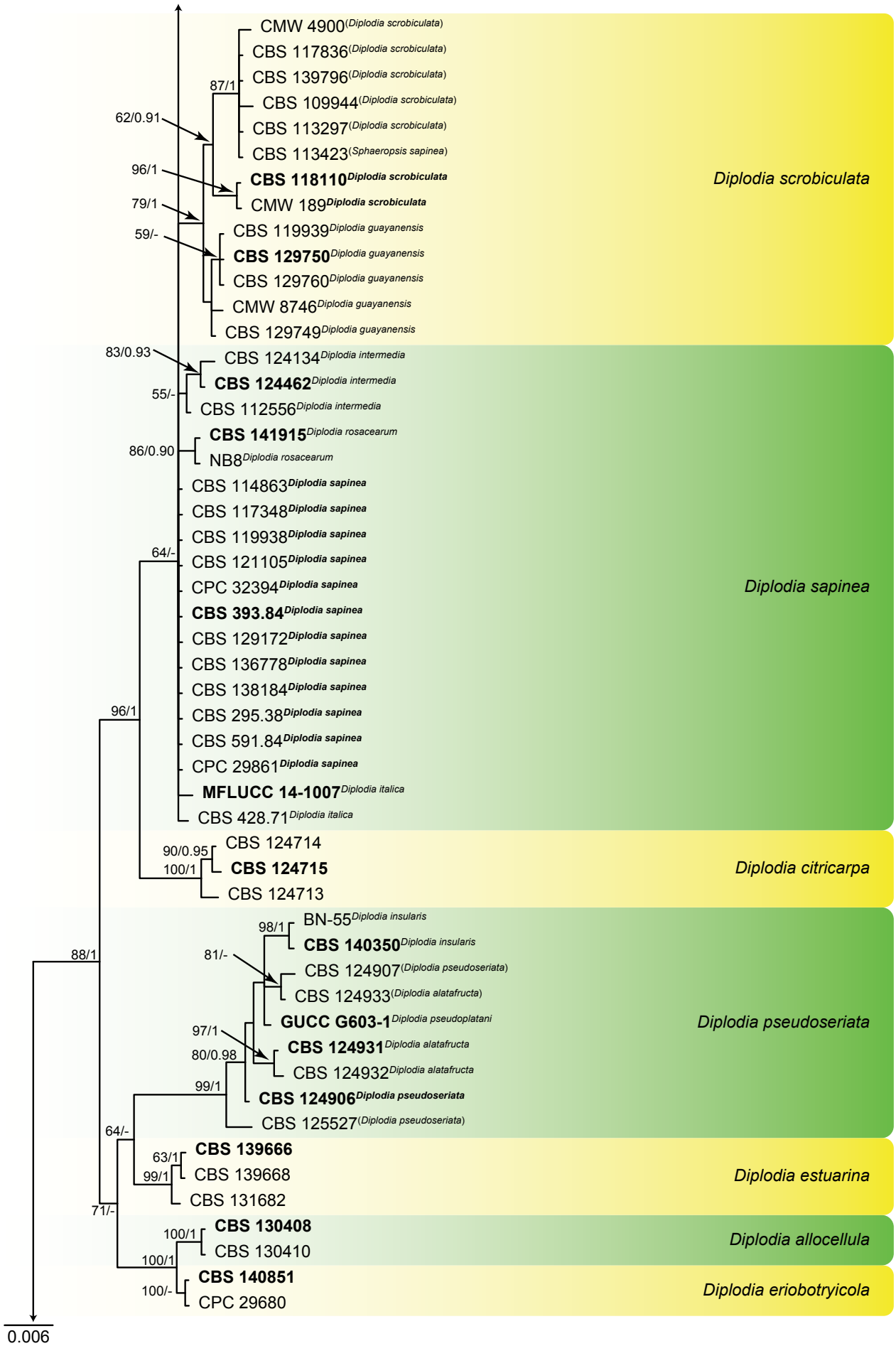
CMW 4900 (Diplodia scrobiculata)
CBS 117836 (Diplodia scrobiculata)
CBS 139796 (Diplodia scrobiculata)
CBS 109944 (Diplodia scrobiculata)
CBS 113297 (Diplodia scrobiculata)
CBS 113423 (Sphaeropsis sapinea)
CBS 118110 Diplodia scrobiculata
CMW 189 Diplodia scrobiculata
CBS 119939 Diplodia guayanensis
CBS 129750 Diplodia guayanensis
CBS 129760 Diplodia guayanensis
CMW 8746 Diplodia guayanensis
CBS 129749 Diplodia guayanensis
Diplodia scrobiculata
CBS 124134 Diplodia intermedia
CBS 124462 Diplodia intermedia
CBS 112556 Diplodia intermedia
CBS 141915 Diplodia rosacearum
NB8 Diplodia rosacearum
CBS 114863 Diplodia sapinea
CBS 117348 Diplodia sapinea
CBS 119938 Diplodia sapinea
CBS 121105 Diplodia sapinea
CPC 32394 Diplodia sapinea
CBS 393.84 Diplodia sapinea
CBS 129172 Diplodia sapinea
CBS 136778 Diplodia sapinea
CBS 138184 Diplodia sapinea
CBS 295.38 Diplodia sapinea
CBS 591.84 Diplodia sapinea
CPC 29861 Diplodia sapinea
MFLUCC 14-1007 Diplodia italica
CBS 428.71 Diplodia italica
Diplodia sapinea
CBS 124714
CBS 124715
CBS 124713
Diplodia citricarpa
BN-55 Diplodia insularis
CBS 140350 Diplodia insularis
CBS 124907 (Diplodia pseudoseriata)
CBS 124933 (Diplodia alatafructa)
GUCC G603-1 Diplodia pseudoplatani
CBS 124931 Diplodia alatafructa
CBS 124932 Diplodia alatafructa
CBS 124906 Diplodia pseudoseriata
CBS 125527 (Diplodia pseudoseriata)
Diplodia pseudoseriata
CBS 139666
CBS 139668
CBS 131682
Diplodia estuarina
CBS 130408
CBS 130410
Diplodia allocellula
CBS 140851
CPC 29680
Diplodia eriobotryicola
62/0.91
87/1
96/1
79/1
59/-
83/0.93
55/-
86/0.90
64/-
96/1
90/0.95
100/1
88/1
98/1
81/-
97/1
80/0.98
99/1
64/-
63/1
99/1
71/-
100/1
100/1
100/-
0.006

Fig. 2 (cont.)

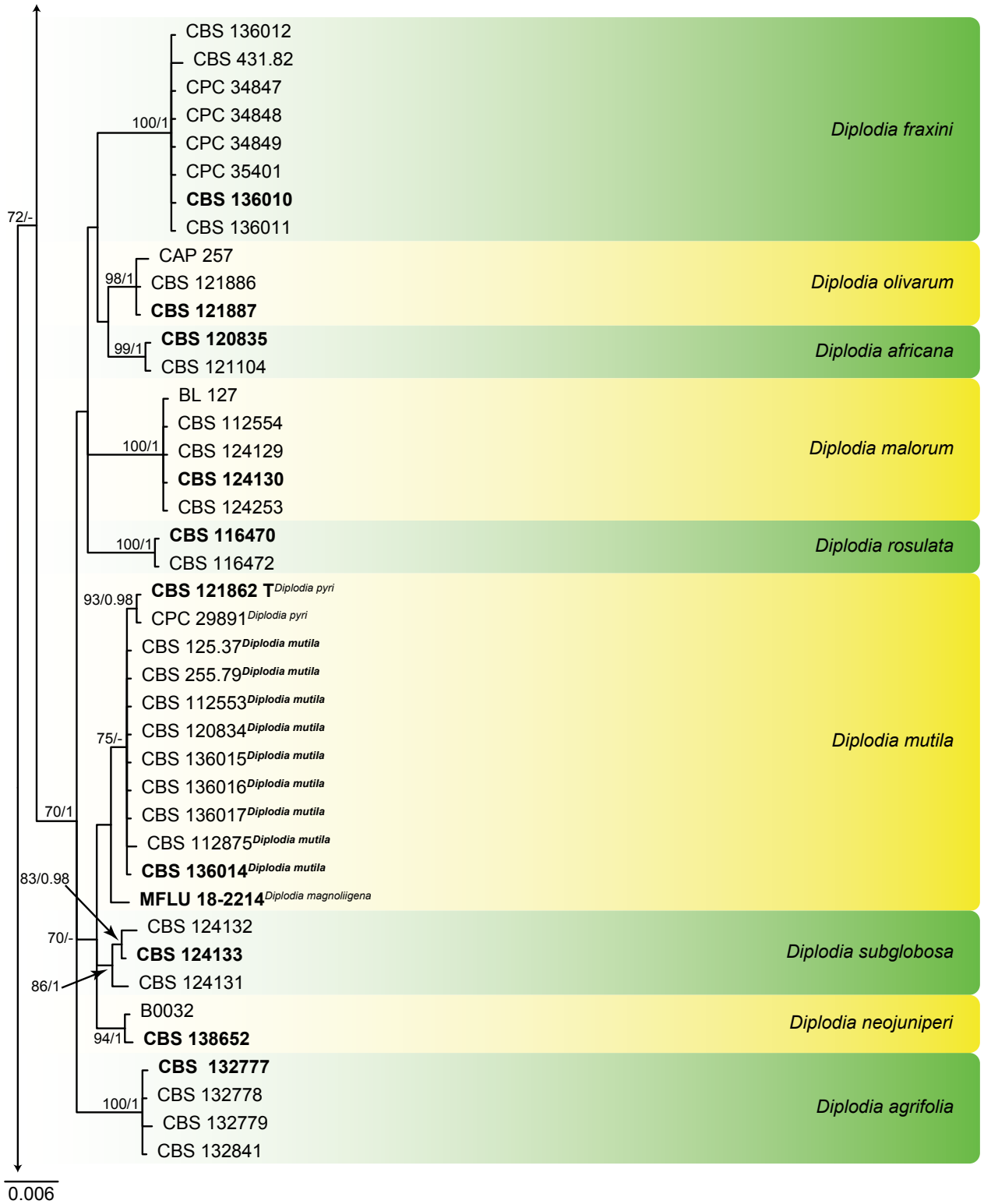
CBS 136012
CBS 431.82
CPC 34847
CPC 34848
CPC 34849
CPC 35401
CBS 136010
CBS 136011
Diplodia fraxini
CAP 257
CBS 121886
CBS 121887
Diplodia olivarum
CBS 120835
CBS 121104
Diplodia africana
BL 127
CBS 112554
CBS 124129
CBS 124130
CBS 124253
Diplodia malorum
CBS 116470
CBS 116472
Diplodia rosulata
CBS 121862 T Diplodia pyri
CPC 29891 Diplodia pyri
CBS 125.37 Diplodia mutila
CBS 255.79 Diplodia mutila
CBS 112553 Diplodia mutila
CBS 120834 Diplodia mutila
CBS 136015 Diplodia mutila
CBS 136016 Diplodia mutila
CBS 136017 Diplodia mutila
CBS 112875 Diplodia mutila
CBS 136014 Diplodia mutila
MFLU 18-2214 Diplodia magnoliigena
Diplodia mutila
CBS 124132
CBS 124133
CBS 124131
Diplodia subglobosa
B0032
CBS 138652
Diplodia neojuniperi
CBS 132777
CBS 132778
CBS 132779
CBS 132841
Diplodia agrifolia
100/1
72/-
98/1
99/1
100/1
100/1
93/0.98
75/-
70/1
83/0.98
70/-
86/1
94/1
100/1
0.006

Fig. 2 (cont.)

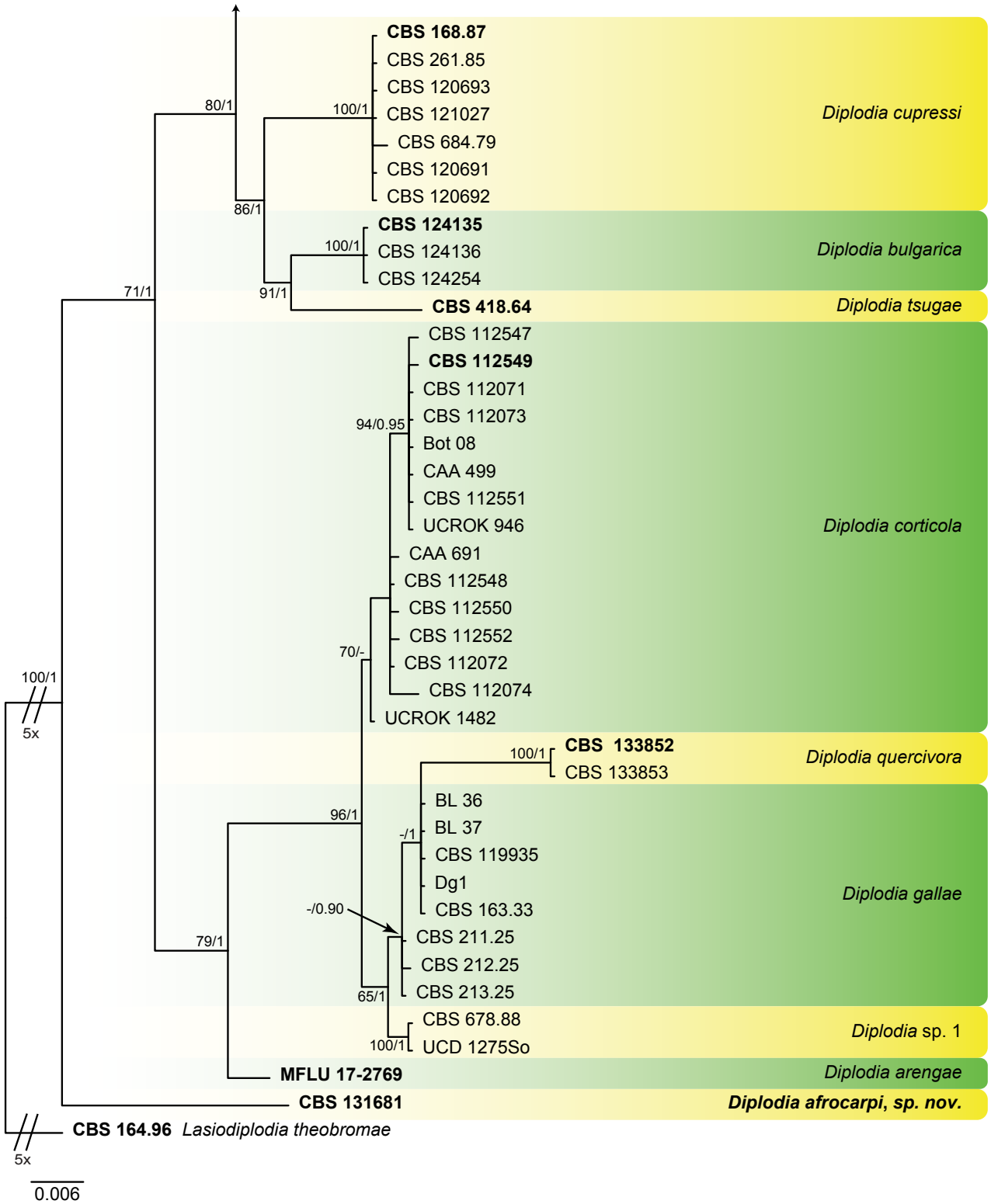
CBS 168.87
CBS 261.85
CBS 120693
CBS 121027
CBS 684.79
CBS 120691
CBS 120692
Diplodia cupressi
CBS 124135
CBS 124136
CBS 124254
Diplodia bulgarica
CBS 418.64
Diplodia tsugae
CBS 112547
CBS 112549
CBS 112071
CBS 112073
Bot 08
CAA 499
CBS 112551
UCROK 946
CAA 691
CBS 112548
CBS 112550
CBS 112552
CBS 112072
CBS 112074
UCROK 1482
Diplodia corticola
CBS 133852
CBS 133853
Diplodia quercivora
BL 36
BL 37
CBS 119935
Dg1
CBS 163.33
CBS 211.25
CBS 212.25
CBS 213.25
Diplodia gallae
CBS 678.88
UCD 1275So
Diplodia sp. 1
MFLU 17-2769
Diplodia arengae
CBS 131681
Diplodia afrocarpi, sp. nov.
CBS 164.96 Lasiodiplodia theobromae
80/1
100/1
86/1
100/1
91/1
71/1
94/0.95
70/-
100/1
5x
100/1
96/1
-/1
-/0.90
79/1
65/1
100/1
5x
0.006

Fig. 2 (cont.)

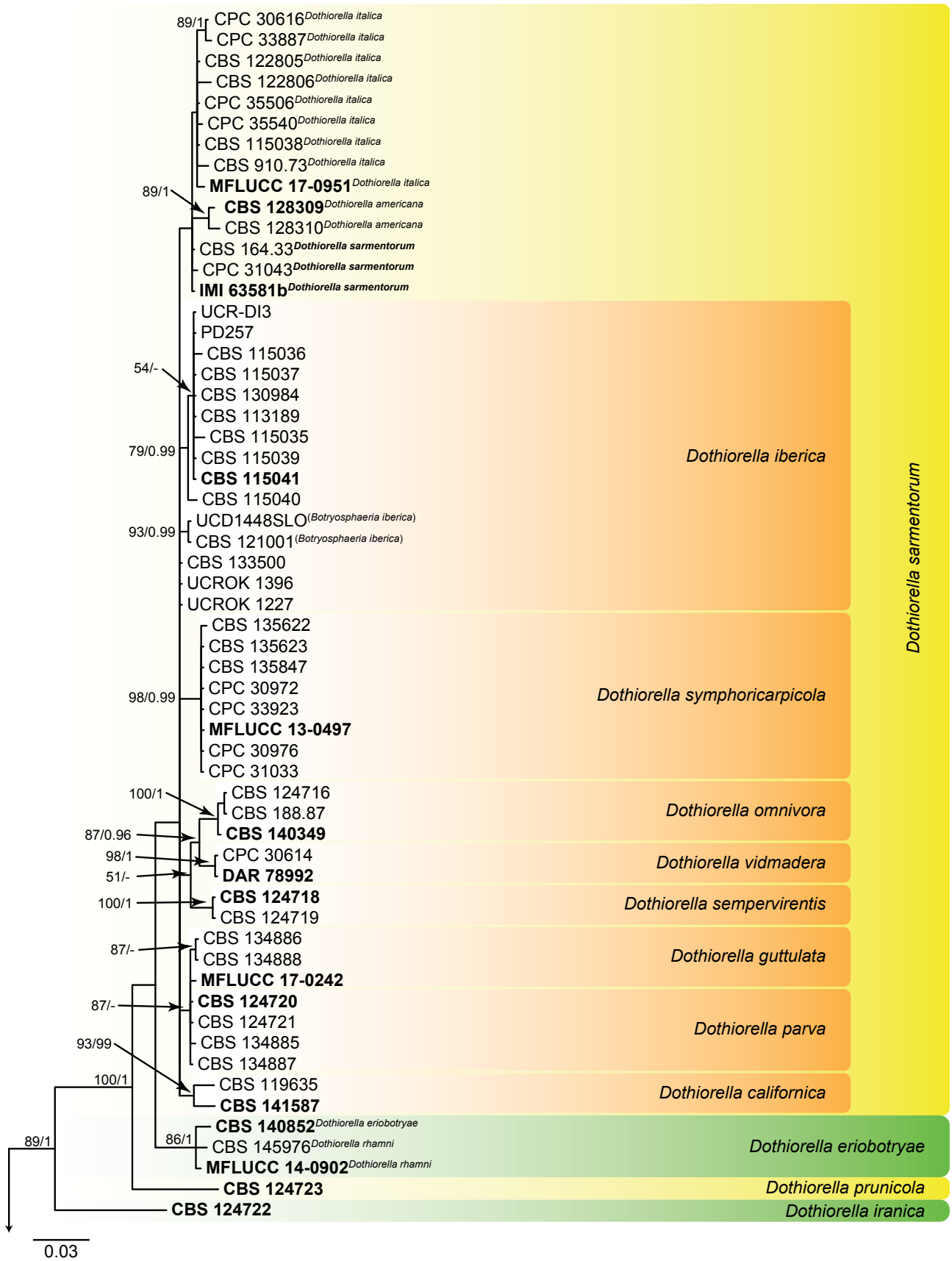

Fig. 3 Phylogenetic tree of *Dothiorella* resulting from a Bayesian analysis of the combined ITS, *tef1* and *tub2* sequence alignment. Maximum likelihood bootstrap support values (ML-BS > 50 %) and Bayesian posterior probabilities (PP > 0.90) are shown at the nodes. Ex-type strains and taxonomic novelties are indicated in **bold** font and the species are delimited with coloured blocks. The last accepted species names, or working species names in round parentheses, are shown in superscript where species were synonymised in this study; species names on which the name of the clade is based are in **bold** superscript. The tree was rooted to *Neofusicoccum luteum* (CBS 121482).

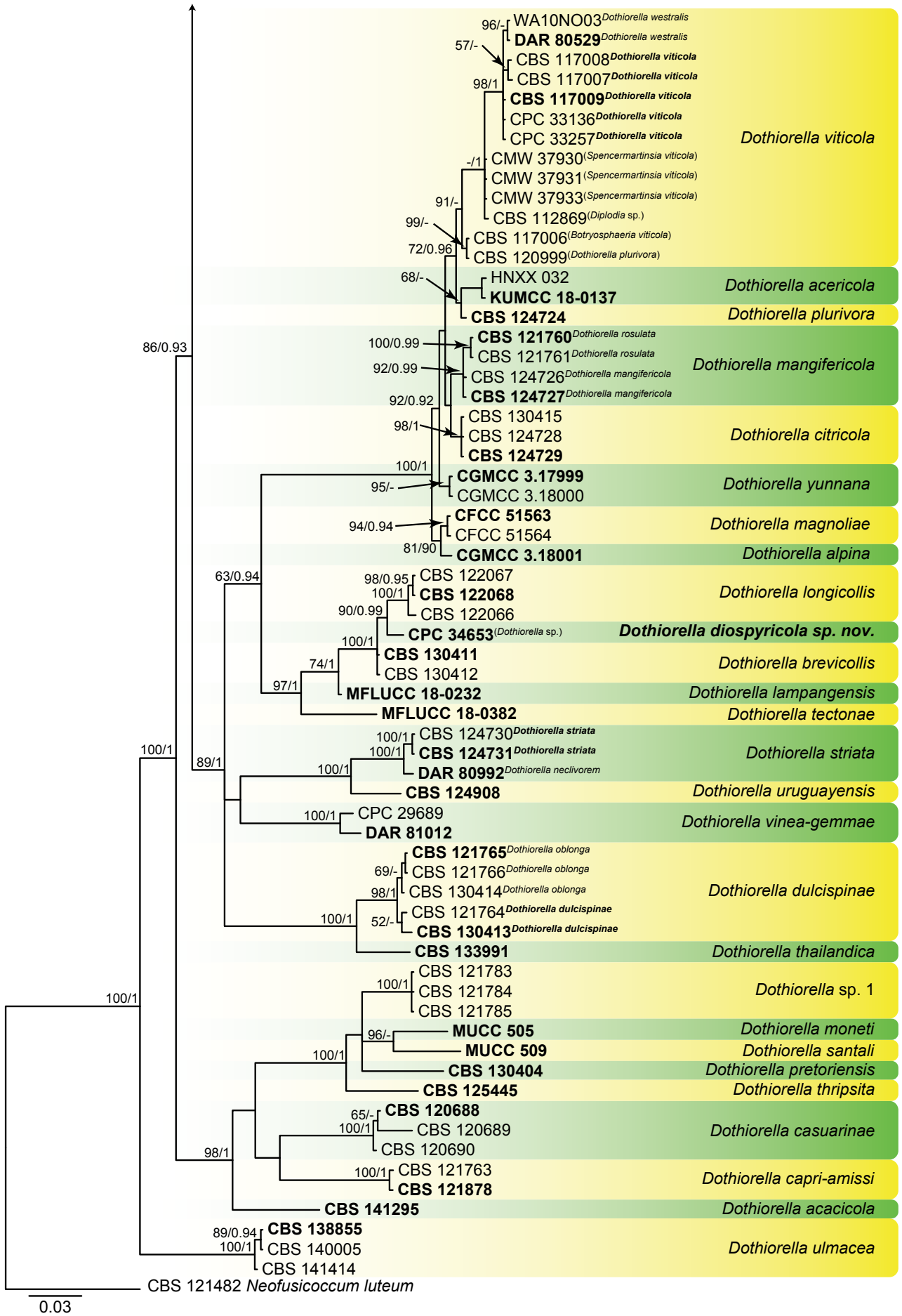
WA10NO03 Dothiorella westralis
DAR 80529 Dothiorella westralis
CBS 117008 Dothiorella viticola
CBS 117007 Dothiorella viticola
CBS 117009 Dothiorella viticola
CPC 33136 Dothiorella viticola
CPC 33257 Dothiorella viticola
CMW 37930 (Spencermartinsia viticola)
CMW 37931 (Spencermartinsia viticola)
CMW 37933 (Spencermartinsia viticola)
CBS 112869 (Diplodia sp.)
CBS 117006 (Botryosphaeria viticola)
CBS 120999 (Dothiorella plurivora)
Dothiorella viticola
HNXX 032
KUMCC 18-0137
Dothiorella acericola
CBS 124724
Dothiorella plurivora
CBS 121760 Dothiorella rosulata
CBS 121761 Dothiorella rosulata
CBS 124726 Dothiorella mangifericola
CBS 124727 Dothiorella mangifericola
Dothiorella mangifericola
CBS 130415
CBS 124728
CBS 124729
Dothiorella citricola
CGMCC 3.17999
CGMCC 3.18000
Dothiorella yunnana
CFCC 51563
CFCC 51564
Dothiorella magnoliae
CGMCC 3.18001
Dothiorella alpina
CBS 122067
CBS 122068
CBS 122066
Dothiorella longicollis
CPC 34653 (Dothiorella sp.)
Dothiorella diospyricola sp. nov.
CBS 130411
CBS 130412
Dothiorella brevicollis
MFLUCC 18-0232
Dothiorella lampangensis
MFLUCC 18-0382
Dothiorella tectonae
CBS 124730 Dothiorella striata
CBS 124731 Dothiorella striata
DAR 80992 Dothiorella neclivorem
Dothiorella striata
CBS 124908
Dothiorella uruguayensis
CPC 29689
DAR 81012
Dothiorella vinea-gemmae
CBS 121765 Dothiorella oblonga
CBS 121766 Dothiorella oblonga
CBS 130414 Dothiorella oblonga
CBS 121764 Dothiorella dulcispinae
CBS 130413 Dothiorella dulcispinae
Dothiorella dulcispinae
CBS 133991
Dothiorella thailandica
CBS 121783
CBS 121784
CBS 121785
Dothiorella sp. 1
MUCC 505
Dothiorella moneti
MUCC 509
Dothiorella santali
CBS 130404
Dothiorella pretoriensis
CBS 125445
Dothiorella thripsita
CBS 120688
CBS 120689
CBS 120690
Dothiorella casuarinae
CBS 121763
CBS 121878
Dothiorella capri-amissi
CBS 141295
Dothiorella acacicola
CBS 138855
CBS 140005
CBS 141414
Dothiorella ulmacea
CBS 121482 Neofusicoccum luteum
0.03

Fig. 3 (cont.)

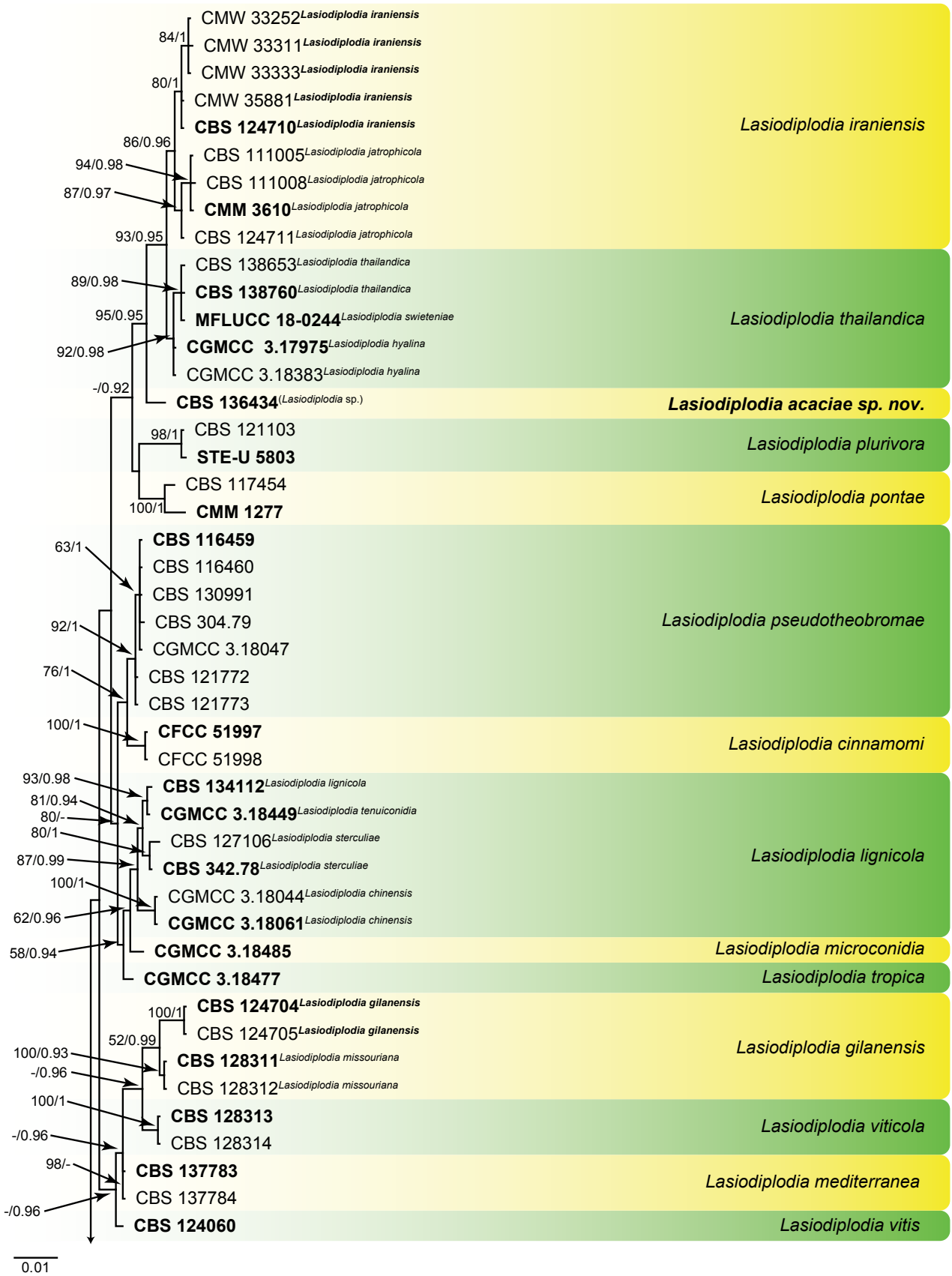

Fig. 4 Phylogenetic tree of *Lasiodiplodia* resulting from a Bayesian analysis of the combined ITS, *tef1*, *tub2* and *rpb2* sequence alignment. Maximum likelihood bootstrap support values (ML-BS > 50 %) and Bayesian posterior probabilities (PP > 0.90) are shown at the nodes. Ex-type strains and taxonomic novelties are indicated in **bold** font and the species are delimited with coloured blocks. Species in orange blocks are potential synonyms of the species under which these blocks are shown. The last accepted species names, or working species names in round parentheses, are shown in superscript where species were synonymised in this study; species names on which the name of the clade is based are in **bold** superscript. The tree was rooted to *Neodeightonia phoenicum* (CBS 122528).

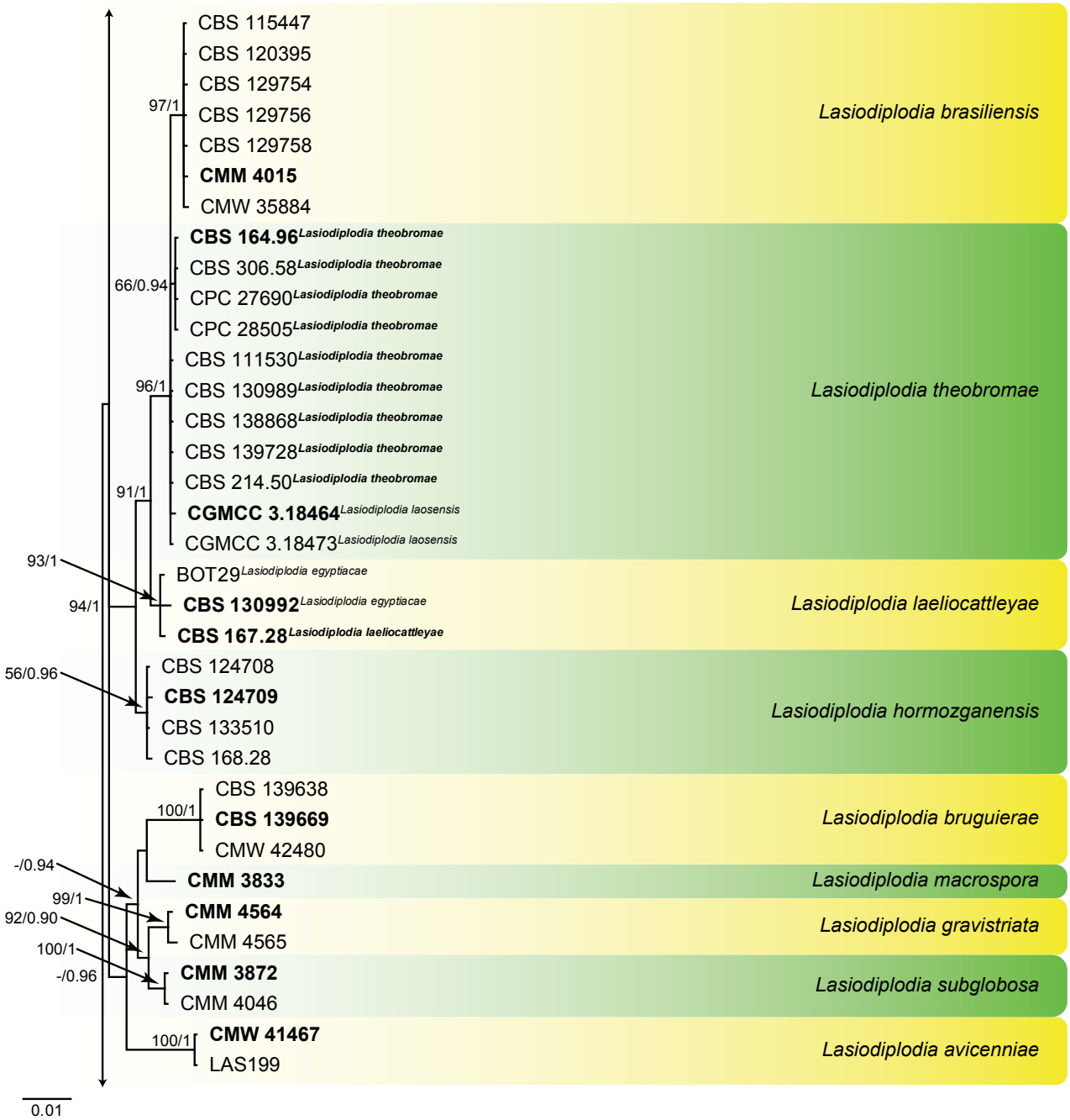
CBS 115447
CBS 120395
CBS 129754
97/1
CBS 129756
CBS 129758
CMM 4015
CMW 35884
Lasiodiplodia brasiliensis
CBS 164.96 Lasiodiplodia theobromae
CBS 306.58 Lasiodiplodia theobromae
66/0.94
CPC 27690 Lasiodiplodia theobromae
CPC 28505 Lasiodiplodia theobromae
CBS 111530 Lasiodiplodia theobromae
96/1
CBS 130989 Lasiodiplodia theobromae
CBS 138868 Lasiodiplodia theobromae
CBS 139728 Lasiodiplodia theobromae
CBS 214.50 Lasiodiplodia theobromae
91/1
CGMCC 3.18464 Lasiodiplodia laosensis
CGMCC 3.18473 Lasiodiplodia laosensis
Lasiodiplodia theobromae
93/1
BOT29 Lasiodiplodia egyptiacae
94/1
CBS 130992 Lasiodiplodia egyptiacae
CBS 167.28 Lasiodiplodia laeliocattleyae
Lasiodiplodia laeliocattleyae
56/0.96
CBS 124708
CBS 124709
CBS 133510
CBS 168.28
Lasiodiplodia hormozganensis
CBS 139638
100/1
CBS 139669
CMW 42480
Lasiodiplodia bruguierae
-/0.94
CMM 3833
Lasiodiplodia macrospora
99/1
92/0.90
CMM 4564
CMM 4565
Lasiodiplodia gravistriata
100/1
-/0.96
CMM 3872
CMM 4046
Lasiodiplodia subglobosa
100/1
CMW 41467
LAS199
Lasiodiplodia avicenniae
0.01

Fig. 4 (cont.)

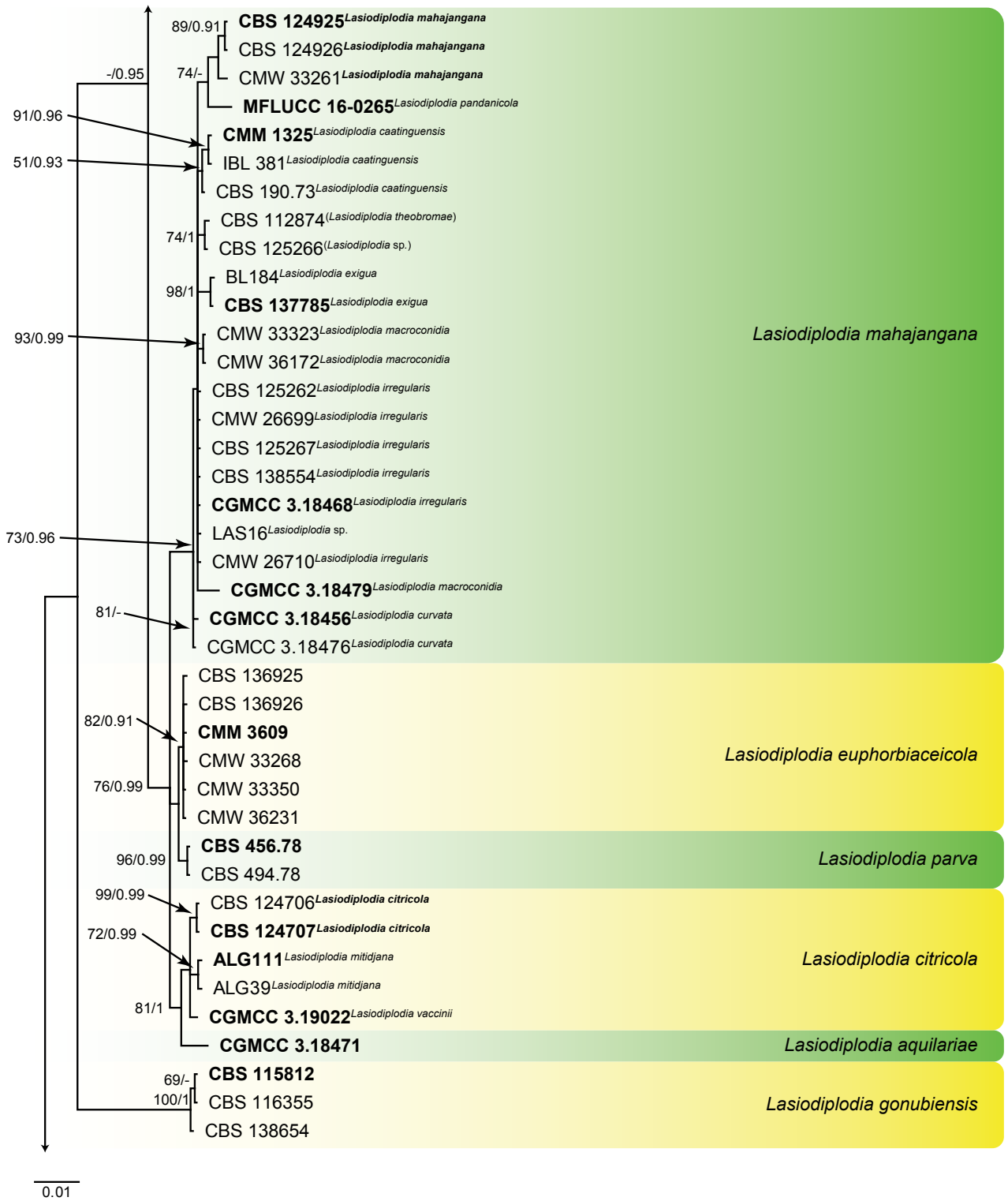
89/0.91
CBS 124925 Lasiodiplodia mahajangana
CBS 124926 Lasiodiplodia mahajangana
-/0.95
74/-
CMW 33261 Lasiodiplodia mahajangana
MFLUCC 16-0265 Lasiodiplodia pandanicola
91/0.96
CMM 1325 Lasiodiplodia caatinguensis
51/0.93
IBL 381 Lasiodiplodia caatinguensis
CBS 190.73 Lasiodiplodia caatinguensis
CBS 112874 (Lasiodiplodia theobromae)
74/1
CBS 125266 (Lasiodiplodia sp.)
BL184 Lasiodiplodia exigua
98/1
CBS 137785 Lasiodiplodia exigua
93/0.99
CMW 33323 Lasiodiplodia macroconidia
CMW 36172 Lasiodiplodia macroconidia
CBS 125262 Lasiodiplodia irregularis
CMW 26699 Lasiodiplodia irregularis
CBS 125267 Lasiodiplodia irregularis
CBS 138554 Lasiodiplodia irregularis
CGMCC 3.18468 Lasiodiplodia irregularis
73/0.96
LAS16 Lasiodiplodia sp.
CMW 26710 Lasiodiplodia irregularis
CGMCC 3.18479 Lasiodiplodia macroconidia
81/-
CGMCC 3.18456 Lasiodiplodia curvata
CGMCC 3.18476 Lasiodiplodia curvata
Lasiodiplodia mahajangana
CBS 136925
CBS 136926
82/0.91
CMM 3609
CMW 33268
76/0.99
CMW 33350
CMW 36231
Lasiodiplodia euphorbiaceicola
96/0.99
CBS 456.78
CBS 494.78
Lasiodiplodia parva
99/0.99
CBS 124706 Lasiodiplodia citricola
72/0.99
CBS 124707 Lasiodiplodia citricola
ALG111 Lasiodiplodia mitidjana
ALG39 Lasiodiplodia mitidjana
81/1
CGMCC 3.19022 Lasiodiplodia vaccinii
Lasiodiplodia citricola
CGMCC 3.18471
Lasiodiplodia aquilariae
69/-
CBS 115812
100/1
CBS 116355
CBS 138654
Lasiodiplodia gonubiensis
0.01

Fig. 4 (cont.)

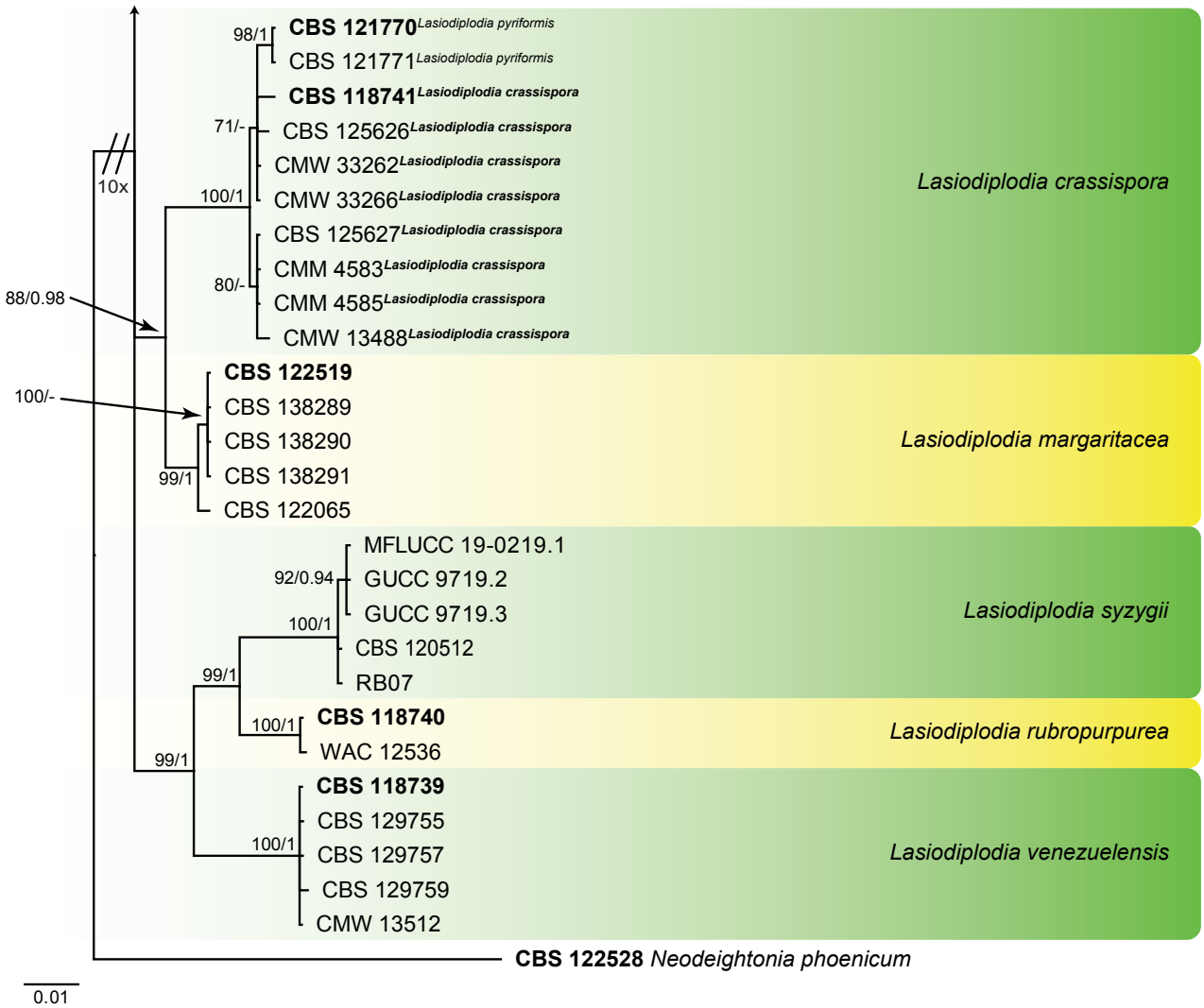
98/1
CBS 121770 Lasiodiplodia pyriformis
CBS 121771 Lasiodiplodia pyriformis
CBS 118741 Lasiodiplodia crassispora
71/-
CBS 125626 Lasiodiplodia crassispora
CMW 33262 Lasiodiplodia crassispora
10x
100/1
CMW 33266 Lasiodiplodia crassispora
CBS 125627 Lasiodiplodia crassispora
CMM 4583 Lasiodiplodia crassispora
80/-
88/0.98
CMM 4585 Lasiodiplodia crassispora
CMW 13488 Lasiodiplodia crassispora
Lasiodiplodia crassispora
100/-
CBS 122519
CBS 138289
CBS 138290
99/1
CBS 138291
CBS 122065
Lasiodiplodia margaritacea
MFLUCC 19-0219.1
92/0.94
GUCC 9719.2
GUCC 9719.3
100/1
CBS 120512
99/1
RB07
Lasiodiplodia syzygii
100/1
CBS 118740
WAC 12536
Lasiodiplodia rubropurpurea
99/1
CBS 118739
CBS 129755
100/1
CBS 129757
CBS 129759
CMW 13512
Lasiodiplodia venezuelensis
CBS 122528 Neodeightonia phoenicum
0.01

Fig. 4 (cont.)

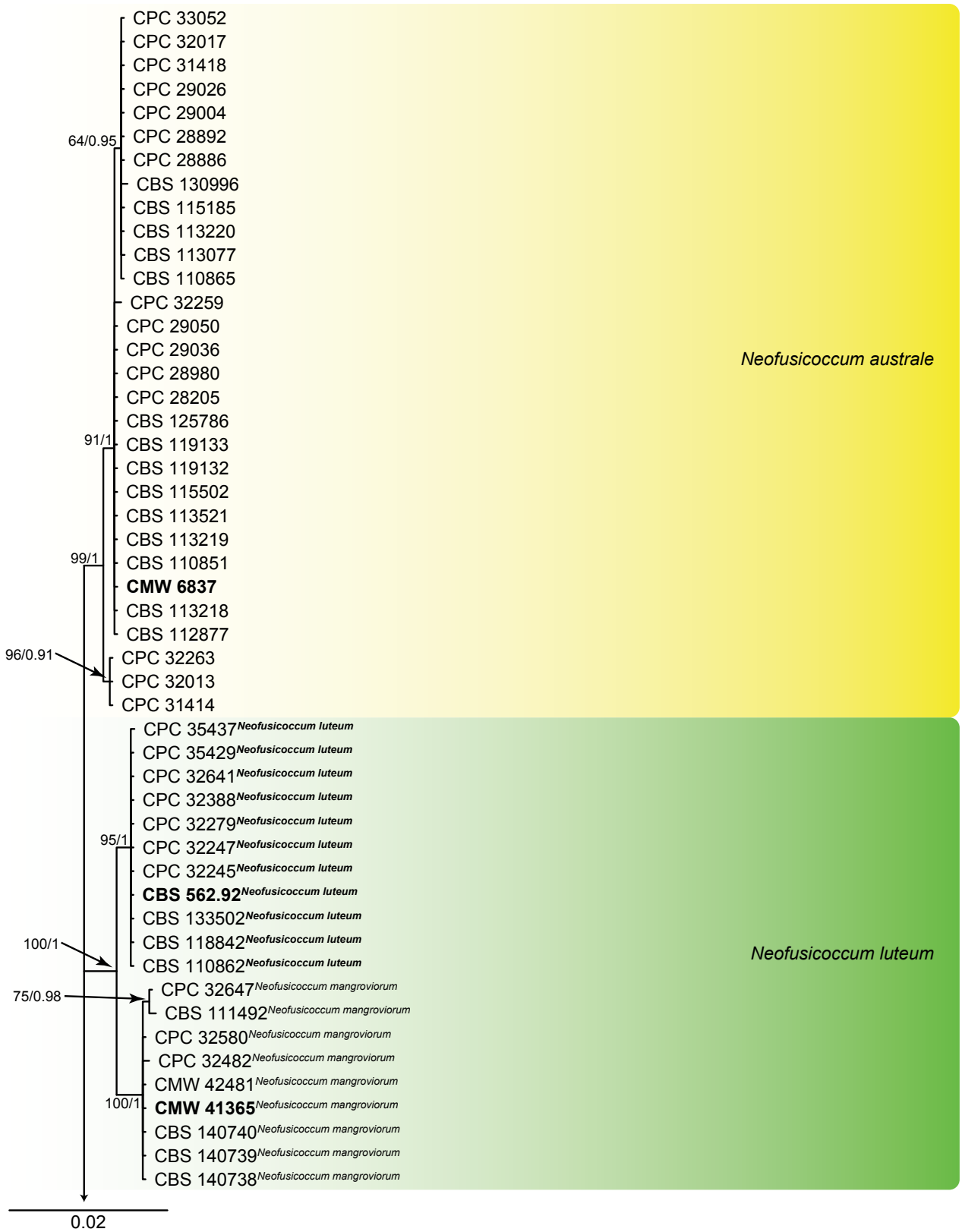

Fig. 5 Phylogenetic tree of *Neofusicoccum* resulting from a Bayesian analysis of the combined ITS, *tef1*, *tub2* and *rpb2* sequence alignment. Maximum likelihood bootstrap support values (ML-BS > 50 %) and Bayesian posterior probabilities (PP > 0.90) are shown at the nodes. Ex-type strains and taxonomic novelties are indicated in **bold** font and the species are delimited with coloured blocks. The last accepted species names, or working species names in round parentheses, are shown in superscript where species were synonymised in this study; species names on which the name of the clade is based are in **bold** superscript. The tree was rooted to *Botryosphaeria dothidea* (CBS 115476).

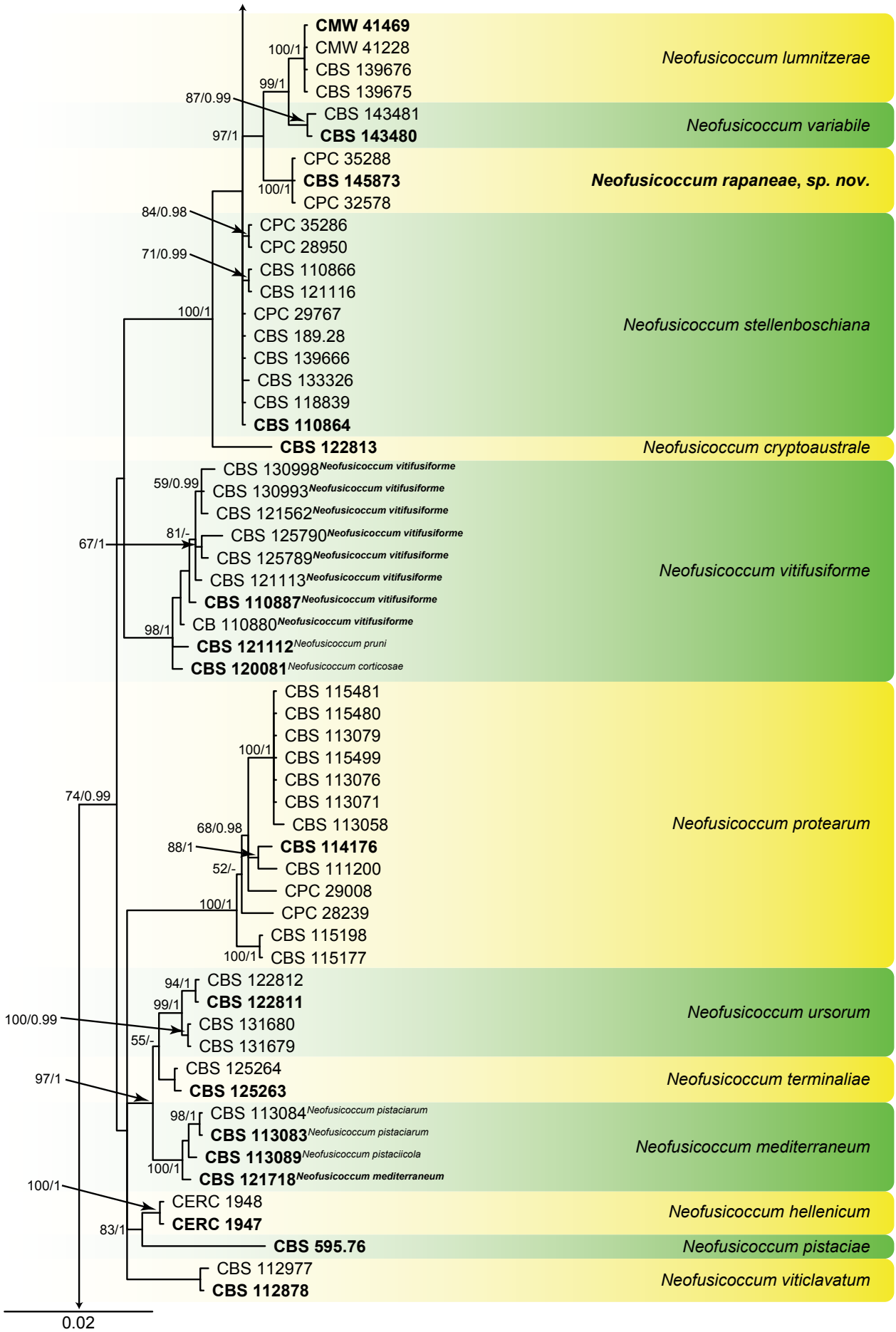
CMW 41469
CMW 41228
CBS 139676
CBS 139675
CBS 143481
CBS 143480
CPC 35288
CBS 145873
CPC 32578
CPC 35286
CPC 28950
CBS 110866
CBS 121116
CPC 29767
CBS 189.28
CBS 139666
CBS 133326
CBS 118839
CBS 110864
CBS 122813
CBS 130998 Neofusicoccum vitifusiforme
CBS 130993 Neofusicoccum vitifusiforme
CBS 121562 Neofusicoccum vitifusiforme
CBS 125790 Neofusicoccum vitifusiforme
CBS 125789 Neofusicoccum vitifusiforme
CBS 121113 Neofusicoccum vitifusiforme
CBS 110887 Neofusicoccum vitifusiforme
CB 110880 Neofusicoccum vitifusiforme
CBS 121112 Neofusicoccum pruni
CBS 120081 Neofusicoccum corticosae
CBS 115481
CBS 115480
CBS 113079
CBS 115499
CBS 113076
CBS 113071
CBS 113058
CBS 114176
CBS 111200
CPC 29008
CPC 28239
CBS 115198
CBS 115177
CBS 122812
CBS 122811
CBS 131680
CBS 131679
CBS 125264
CBS 125263
CBS 113084 Neofusicoccum pistaciarum
CBS 113083 Neofusicoccum pistaciarum
CBS 113089 Neofusicoccum pistaciicola
CBS 121718 Neofusicoccum mediterraneum
CERC 1948
CERC 1947
CBS 595.76
CBS 112977
CBS 112878
87/0.99
97/1
100/1
99/1
84/0.98
71/0.99
100/1
59/0.99
81/-
67/1
98/1
74/0.99
100/1
68/0.98
88/1
52/-
100/1
100/1
94/1
99/1
100/0.99
55/-
97/1
98/1
100/1
100/1
83/1
0.02
Neofusicoccum lumnitzerae
Neofusicoccum variabile
Neofusicoccum rapaneae, sp. nov.
Neofusicoccum stellenboschiana
Neofusicoccum cryptoaustrale
Neofusicoccum vitifusiforme
Neofusicoccum protearum
Neofusicoccum ursorum
Neofusicoccum terminaliae
Neofusicoccum mediterraneum
Neofusicoccum hellenicum
Neofusicoccum pistaciae
Neofusicoccum viticlavatum

Fig. 5 (cont.)

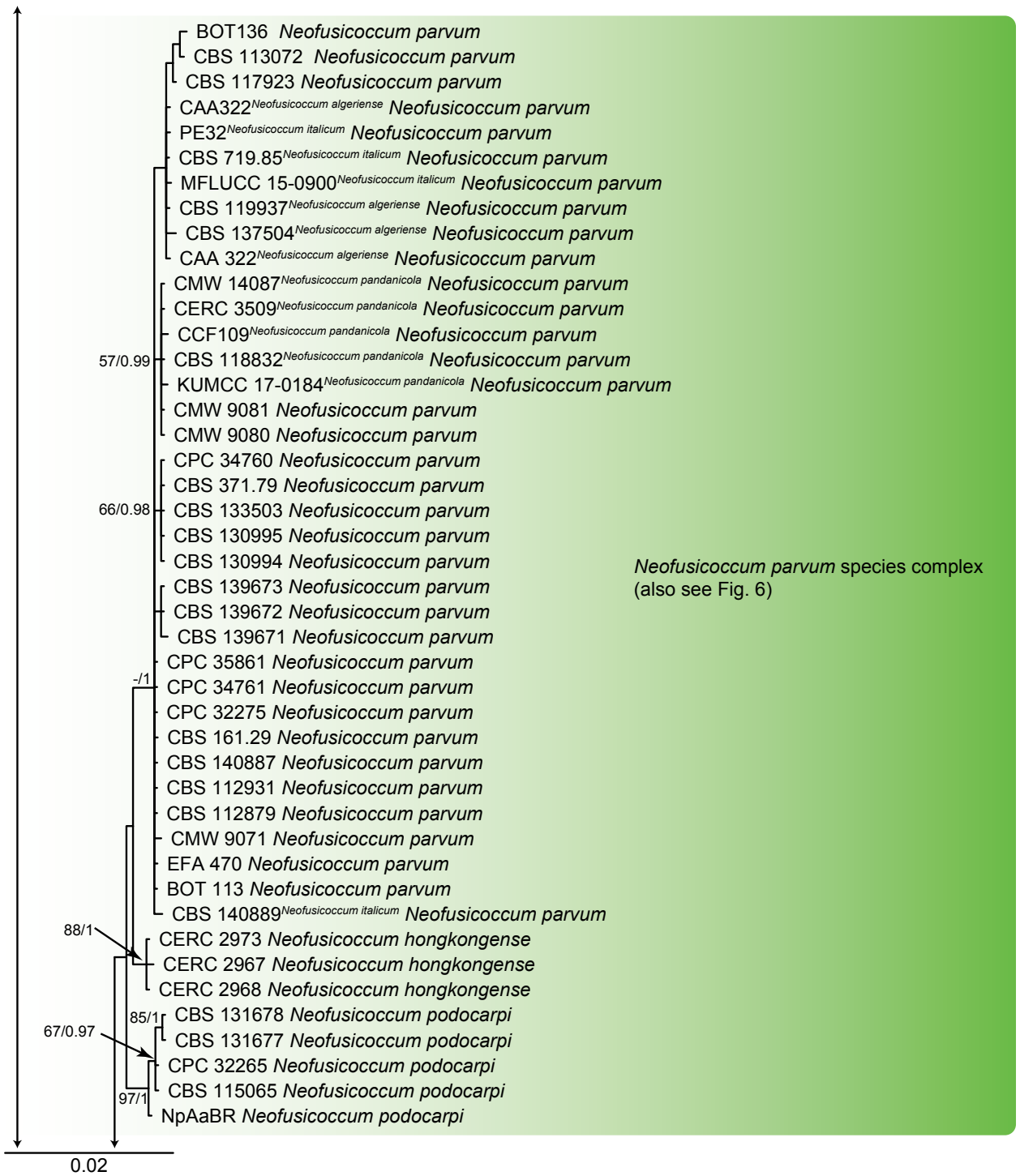
BOT136 Neofusicoccum parvum
CBS 113072 Neofusicoccum parvum
CBS 117923 Neofusicoccum parvum
CAA322 Neofusicoccum algeriense Neofusicoccum parvum
PE32 Neofusicoccum italicum Neofusicoccum parvum
CBS 719.85 Neofusicoccum italicum Neofusicoccum parvum
MFLUCC 15-0900 Neofusicoccum italicum Neofusicoccum parvum
CBS 119937 Neofusicoccum algeriense Neofusicoccum parvum
CBS 137504 Neofusicoccum algeriense Neofusicoccum parvum
CAA 322 Neofusicoccum algeriense Neofusicoccum parvum
CMW 14087 Neofusicoccum pandanicola Neofusicoccum parvum
CERC 3509 Neofusicoccum pandanicola Neofusicoccum parvum
CCF109 Neofusicoccum pandanicola Neofusicoccum parvum
57/0.99
CBS 118832 Neofusicoccum pandanicola Neofusicoccum parvum
KUMCC 17-0184 Neofusicoccum pandanicola Neofusicoccum parvum
CMW 9081 Neofusicoccum parvum
CMW 9080 Neofusicoccum parvum
CPC 34760 Neofusicoccum parvum
CBS 371.79 Neofusicoccum parvum
66/0.98
CBS 133503 Neofusicoccum parvum
CBS 130995 Neofusicoccum parvum
CBS 130994 Neofusicoccum parvum
CBS 139673 Neofusicoccum parvum
CBS 139672 Neofusicoccum parvum
CBS 139671 Neofusicoccum parvum
CPC 35861 Neofusicoccum parvum
-/1
CPC 34761 Neofusicoccum parvum
CPC 32275 Neofusicoccum parvum
CBS 161.29 Neofusicoccum parvum
CBS 140887 Neofusicoccum parvum
CBS 112931 Neofusicoccum parvum
CBS 112879 Neofusicoccum parvum
CMW 9071 Neofusicoccum parvum
EFA 470 Neofusicoccum parvum
BOT 113 Neofusicoccum parvum
CBS 140889 Neofusicoccum italicum Neofusicoccum parvum
88/1
CERC 2973 Neofusicoccum hongkongense
CERC 2967 Neofusicoccum hongkongense
CERC 2968 Neofusicoccum hongkongense
85/1
CBS 131678 Neofusicoccum podocarpi
67/0.97
CBS 131677 Neofusicoccum podocarpi
CPC 32265 Neofusicoccum podocarpi
CBS 115065 Neofusicoccum podocarpi
97/1
NpAaBR Neofusicoccum podocarpi
Neofusicoccum parvum species complex
(also see Fig. 6)
0.02

Fig. 5 (cont.)

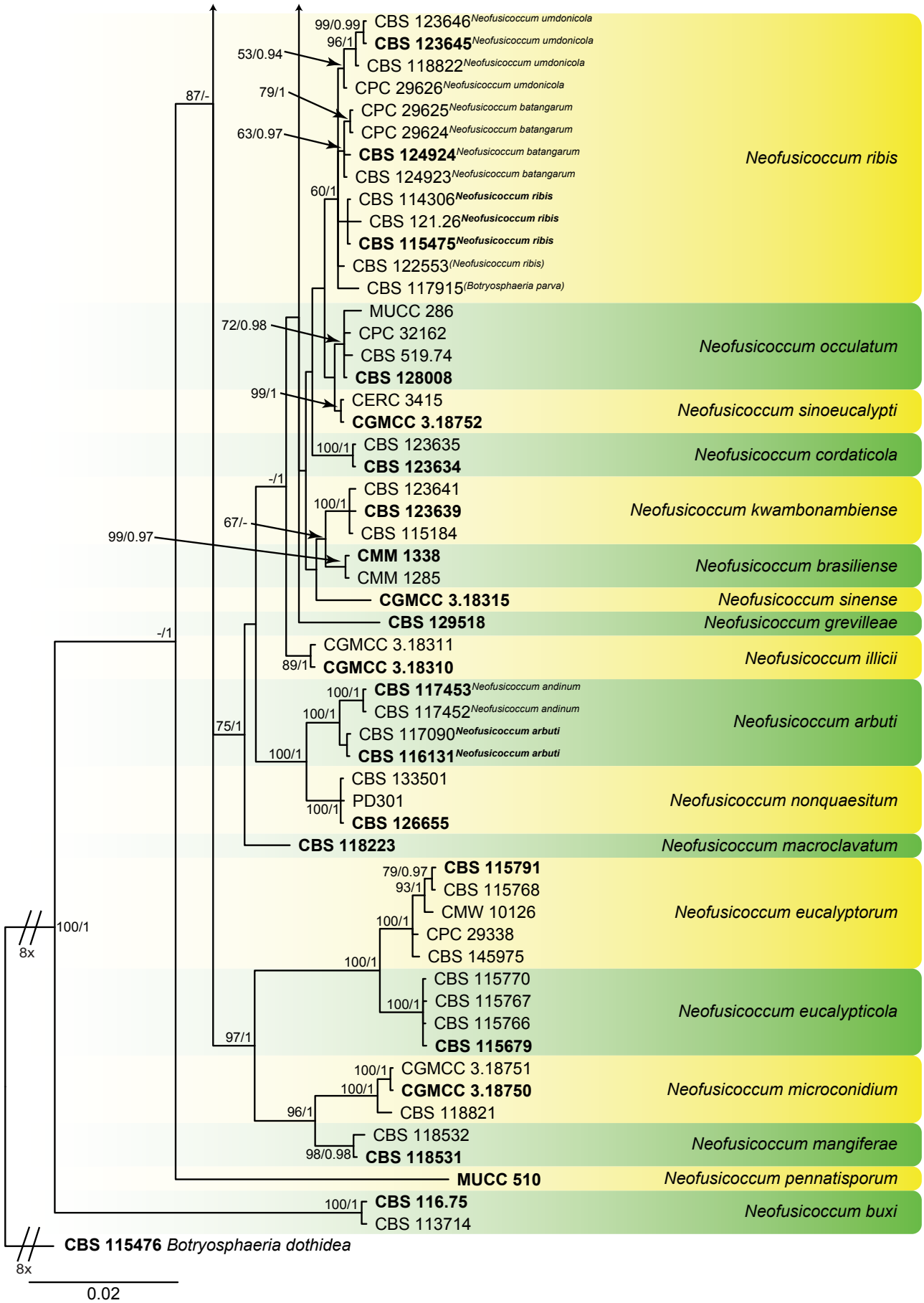
99/0.99
96/1
CBS 123646 Neofusicoccum umdonicola
CBS 123645 Neofusicoccum umdonicola
CBS 118822 Neofusicoccum umdonicola
CPC 29626 Neofusicoccum umdonicola
53/0.94
79/1
87/-
CPC 29625 Neofusicoccum batangarum
CPC 29624 Neofusicoccum batangarum
63/0.97
CBS 124924 Neofusicoccum batangarum
CBS 124923 Neofusicoccum batangarum
60/1
CBS 114306 Neofusicoccum ribis
CBS 121.26 Neofusicoccum ribis
CBS 115475 Neofusicoccum ribis
CBS 122553 (Neofusicoccum ribis)
CBS 117915 (Botryosphaeria parva)
Neofusicoccum ribis
72/0.98
MUCC 286
CPC 32162
CBS 519.74
CBS 128008
Neofusicoccum occulatum
99/1
CERC 3415
CGMCC 3.18752
Neofusicoccum sinoeucalypti
100/1
CBS 123635
CBS 123634
Neofusicoccum cordaticola
-/1
CBS 123641
100/1
CBS 123639
67/-
CBS 115184
Neofusicoccum kwambonambiense
99/0.97
CMM 1338
CMM 1285
Neofusicoccum brasiliense
CGMCC 3.18315
Neofusicoccum sinense
CBS 129518
Neofusicoccum grevilleae
-/1
CGMCC 3.18311
89/1
CGMCC 3.18310
Neofusicoccum illicii
100/1
CBS 117453 Neofusicoccum andinum
CBS 117452 Neofusicoccum andinum
100/1
75/1
CBS 117090 Neofusicoccum arbuti
100/1
CBS 116131 Neofusicoccum arbuti
Neofusicoccum arbuti
CBS 133501
PD301
100/1
CBS 126655
Neofusicoccum nonquaesitum
CBS 118223
Neofusicoccum macroclavatum
79/0.97
CBS 115791
93/1
CBS 115768
CMW 10126
100/1
CPC 29338
CBS 145975
Neofusicoccum eucalyptorum
100/1
100/1
8x
100/1
CBS 115770
CBS 115767
CBS 115766
CBS 115679
Neofusicoccum eucalypticola
97/1
100/1
CGMCC 3.18751
100/1
CGMCC 3.18750
96/1
CBS 118821
Neofusicoccum microconidium
CBS 118532
98/0.98
CBS 118531
Neofusicoccum mangiferae
MUCC 510
Neofusicoccum pennatisporum
100/1
CBS 116.75
CBS 113714
Neofusicoccum buxi
CBS 115476 Botryosphaeria dothidea
8x
0.02

Fig. 5 (cont.)

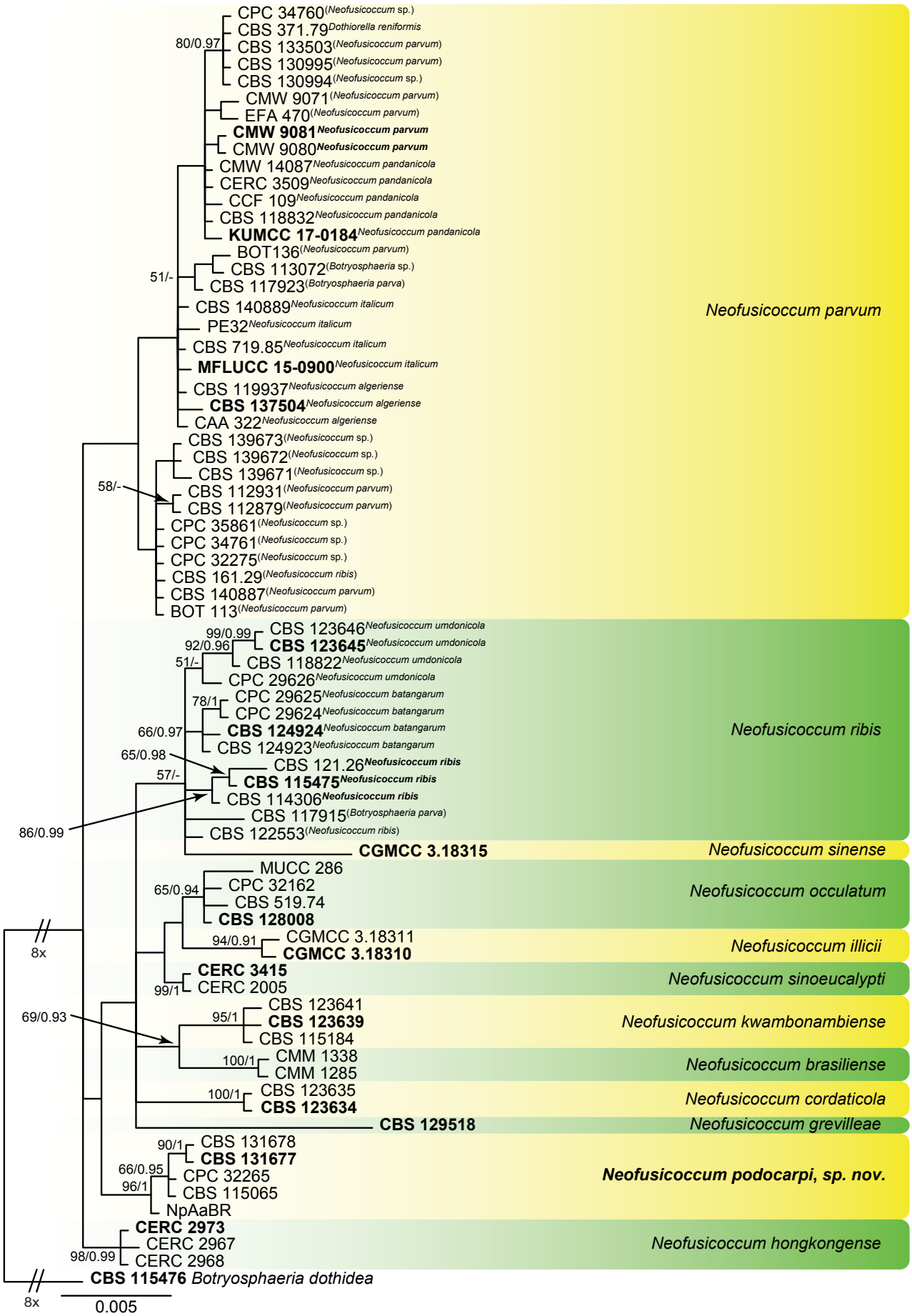

Fig. 6 Phylogenetic tree of *Neofusicoccum parvum* species complex resulting from a Bayesian analysis of the combined ITS, *tef1*, *tub2* and *rpb2* sequence alignment. Maximum likelihood bootstrap support values (ML-BS > 50 %) and Bayesian posterior probabilities (PP > 0.90) are shown at the nodes. Ex-type strains and taxonomic novelties are indicated in **bold** font and the species are delimited with coloured blocks. The last accepted species names, or working species names in round parentheses, are shown in superscript where species were synonymised in this study; species names on which the name of the clade is based are in **bold** superscript. The tree was rooted to *Botryosphaeria dothidea* (CBS 115476).

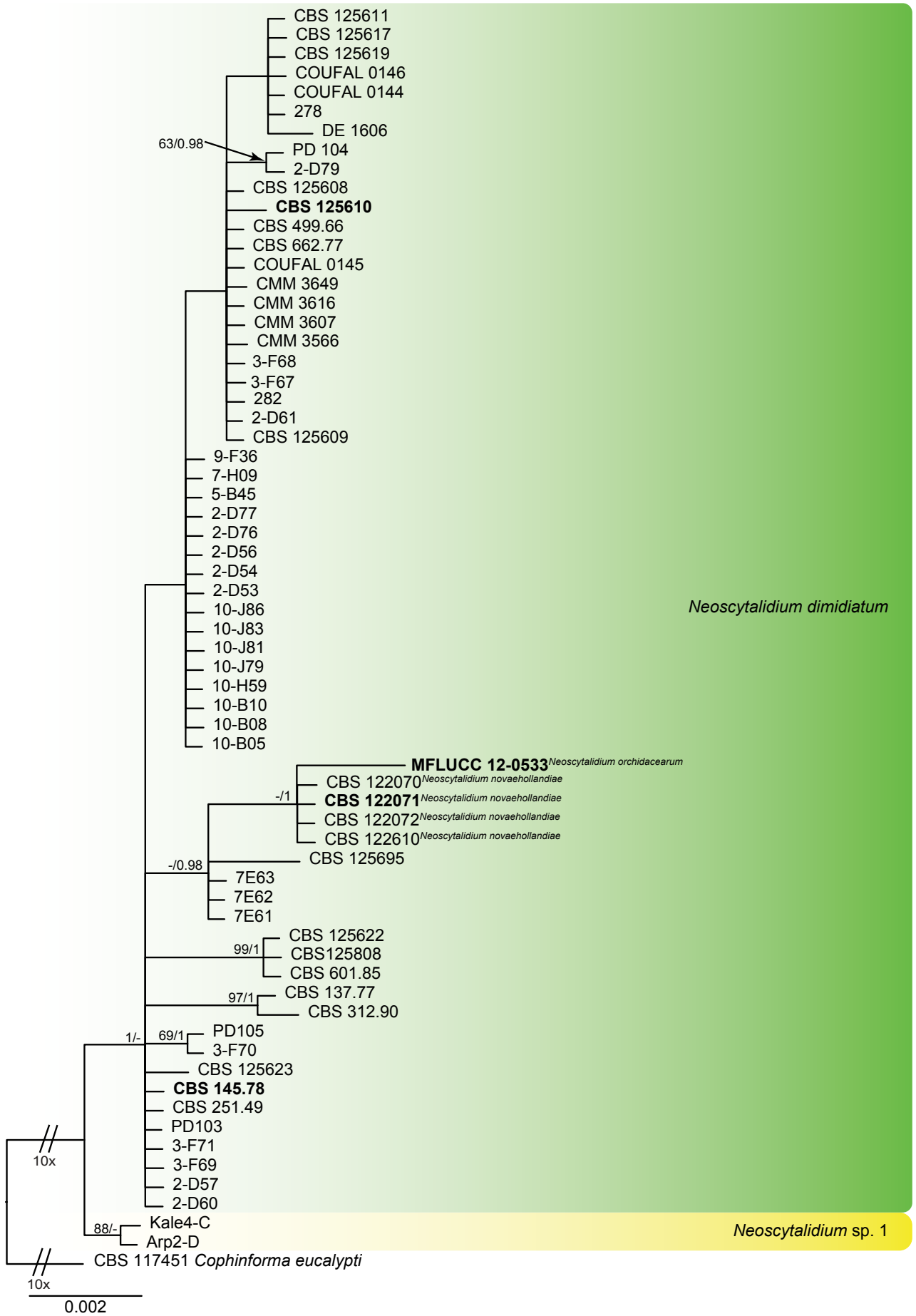

Fig. 7 Phylogenetic tree of *Neoscytalidium* resulting from a Bayesian analysis of the combined ITS, *tef1*, *tub2* sequence alignment. Maximum likelihood bootstrap support values (ML-BS > 50 %) and Bayesian posterior probabilities (PP > 0.90) are shown at the nodes. Ex-type strains and taxonomic novelties are indicated in **bold** font and the species are delimited with coloured blocks. The last accepted species names, or working species names in round parentheses, are shown in superscript where species were synonymised in this study; species names on which the name of the clade is based are in **bold** superscript. The tree was rooted to *Botryosphaeria dothidea* (CBS 117451).

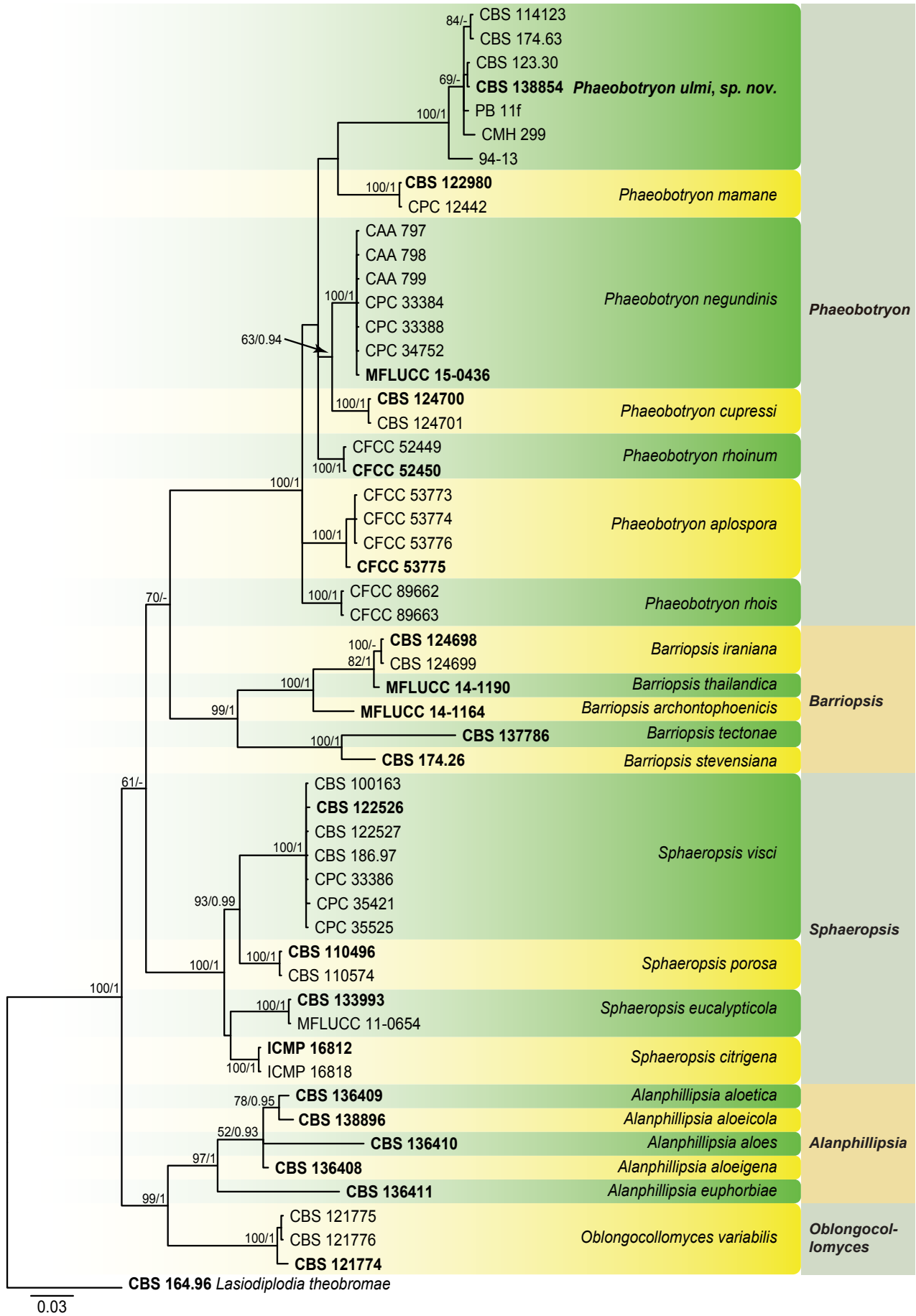

Fig. 8 Phylogenetic tree of *Phaeobotryon*, *Alanphillipsia*, *Barriopsis*, *Oblongocollomyces* and *Sphaeropsis* resulting from a Bayesian analysis of the combined ITS, LSU and *tef1* sequence alignment. Maximum likelihood bootstrap support values (ML-BS > 50 %) and Bayesian posterior probabilities (PP > 0.90) are shown at the nodes. Ex-type strains and taxonomic novelties are indicated in **bold** font and the species are delimited with coloured blocks. The last accepted species names, or working species names in round parentheses, are shown in superscript where species were synonymised in this study; species names on which the name of the clade is based are in **bold** superscript. The tree was rooted to *Cophinforma eucalypti* (CBS 117451).

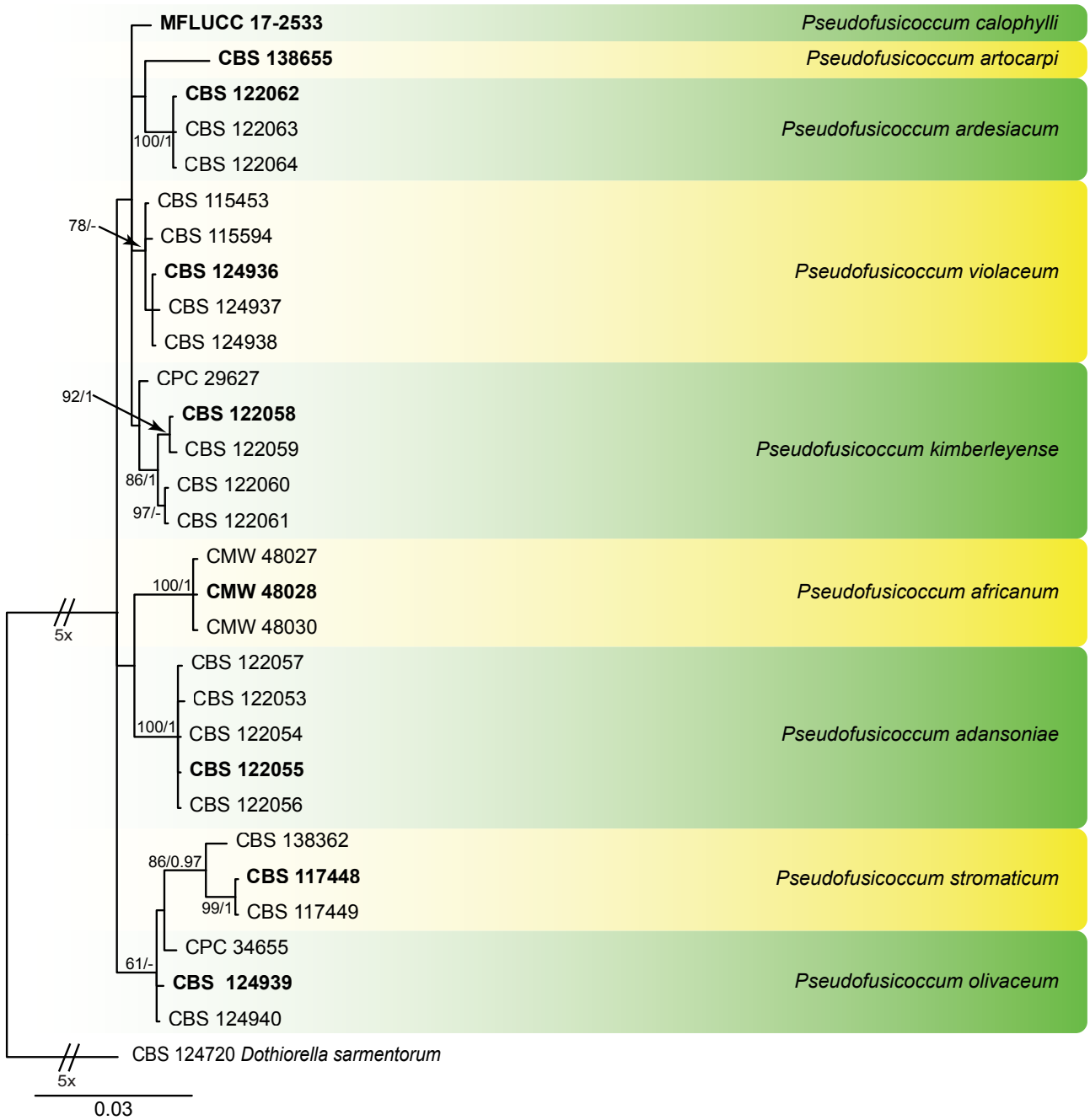

Fig. 9 Phylogenetic tree of *Pseudofusicoccum* resulting from a Bayesian analysis of the combined ITS, LSU, *tef1* sequence alignment. Maximum likelihood bootstrap support values (ML-BS > 50 %) and Bayesian posterior probabilities (PP > 0.90) are shown at the nodes. Ex-type strains and taxonomic novelties are indicated in **bold** font and the species are delimited with coloured blocks. The tree was rooted to *Dothiorella parva* (CBS124720).

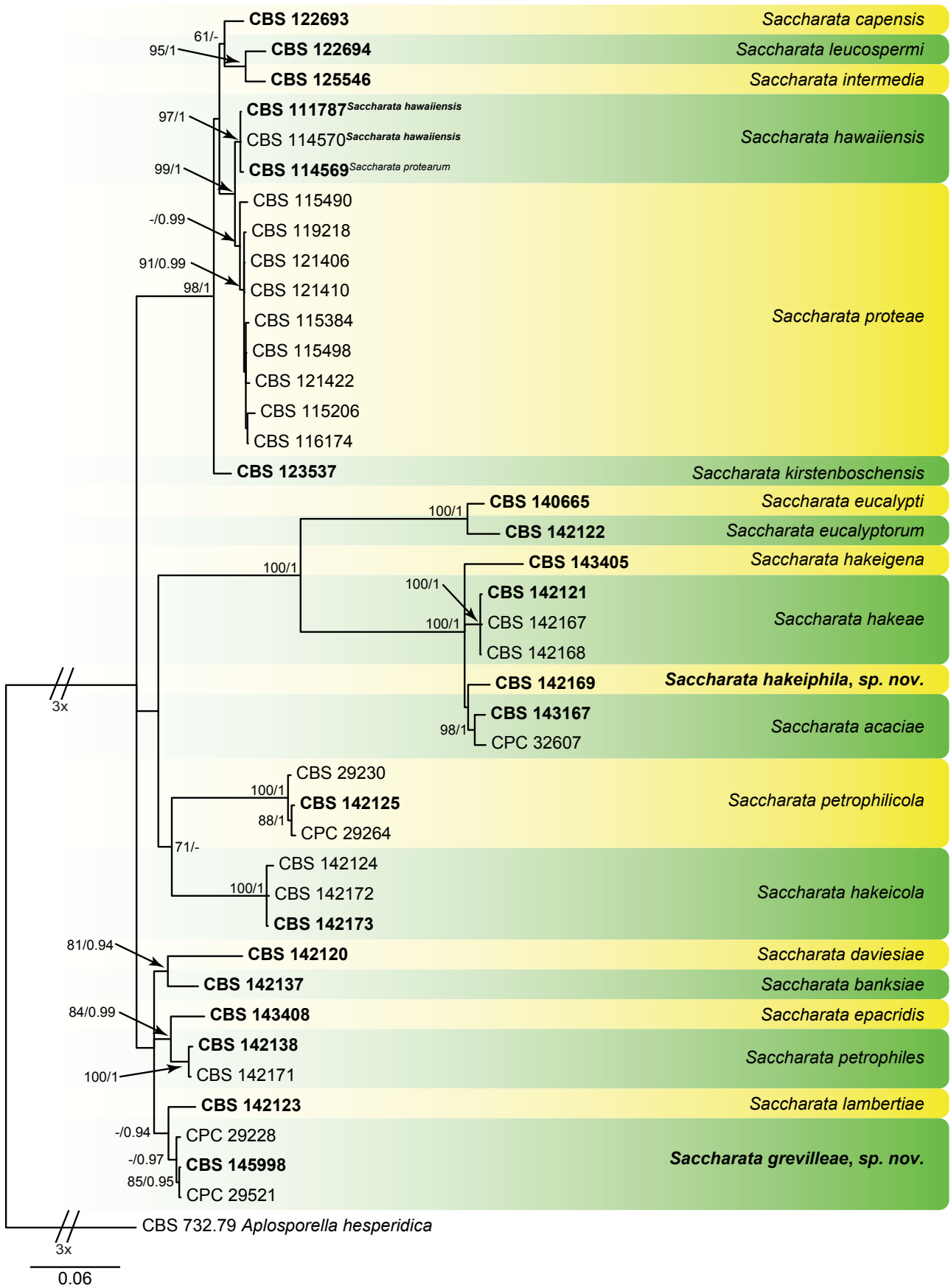

Fig. 10 Phylogenetic tree of *Saccharata* resulting from a Bayesian analysis of the combined ITS, *tef1* and *rpb2* sequence alignment. Maximum likelihood bootstrap support values (ML-BS > 50 %) and Bayesian posterior probabilities (PP > 0.90) are shown at the nodes. Ex-type strains and taxonomic novelties are indicated in **bold** font and the species are delimited with coloured blocks. The last accepted species names, or working species names in round parentheses, are shown in superscript where species were synonymised in this study; species names on which the name of the clade is based are in **bold** superscript. The tree was rooted to *Aplosporella hesperidiaca* (CBS732.79).

Table 2 Substitution models used for Bayesian analyses in this study.

Analysis	Figure number	Number of ingroup sequences	Number of generations	Number of trees used	Substitution models used for Bayesian analyses[1] / Number of unique site patterns				
					ITS	*tef1*	*tub2*	LSU	*rpb2*
Botryosphaeria 3-gene	Fig. 1	50	255 000	38 252	GTR+I / 55	GTR+G / 96	HKY+I / 45		
Diplodia 3-gene	Fig. 2	179	5515 000	82 728	GTR+I+G / 128	HKY+I+G / 141	GTR+I+G / 126	–	–
Dothiorella 3-gene	Fig. 3	122	1820 000	27 302	HKY+I+G / 130	GTR+G / 213	GTR+I+G / 141	–	–
Lasiodiplodia 4-gene	Fig. 4	147	3180 000	477 002	SYM+I+G / 75	HKY+I+G / 118	GTR+I / 98	–	GTR+G / 155
Neofusicoccum 4-gene	Fig. 5	207	13585 000	203 778	GTR+I+G / 128	HKY+G / 171	GTR+I+G / 127	–	GTR+G / 149
Neofusicoccum 4-gene	Fig. 6	74	2520 000	378 002	GTR+I+G / 52	HKY+G / 72	GTR+I+G / 53	–	GTR+G / 49
Neoscytalidium 3-gene	Fig. 7	65	470 000	70 502	F81 / 78	HKY+I / 24	F81 / 21	–	–
Alanphillipsia, *Barriopsis*, *Oblongocollomyces*, *Phaeobotryon* and *Sphaeropsis* 3-gene	Fig. 8	53	940 000	141 002	SYM+I+G / 114	HKY+G / 242	–	HKY+I+G / 59	–
Pseudofusicoccum 3-gene	Fig. 9	29	385 000	57 752	K80+I / 52	HKY+I / 62	GTR+I / 32	–	–
Saccharata 3-gene	Fig. 10	40	625 000	93 752	GTR+I+G / 162	HKY+G / 150	–	–	GTR+G / 296

[1] ITS: internal transcribed spacer regions and intervening 5.8S nrRNA gene; *tef1*: partial translation elongation factor 1-alpha gene; *tub2*: partial beta-tubulin gene; LSU: partial 28S nrRNA gene, large subunit; *rpb2*: partial DNA-directed RNA polymerase II second largest subunit.

species and support values for the clustering were evaluated. For the parsimony analyses, the first equally most parsimonious tree was used as reference when multiple equally most parsimonious trees were obtained (trees not shown, available in TreeBASE under study S27596). These results are discussed under the species notes and the tree statistics are presented in Table S2. The Bayesian trees are shown as Fig. S1–S10 and are also available in TreeBASE under study S27596. To determine sequence similarity, blast2 searches were performed on the NCBI blast website using the query sequence (from the ex-type strain of the proposed novelty) against all other sequences in the alignment for a given gene in each genus alignment after removing all gaps in the alignment.

Species of *Botryosphaeriaceae* were recognised based on the following criteria:

i Phylogenetic trees were constructed for individual genes and concatenated alignments to identify distinct lineages and to check for conflict in the position on the tree;

ii Per lineage or previously accepted species in that lineage, a distance matrix between the ex-type strain or a representative strain in the absence of a sequence for the ex-type strain were constructed using Geneious v. 11.1.5 (both showing pairwise sequence similarity as well as number of differences) and blast2 searches were also used on the NCBI blast website (https://blast.ncbi.nlm.nih.gov/Blast.cgi) for sequence comparisons.

The values in the distance matrix were conditionally coloured in Microsoft Excel for two scenarios: In the first scenario all similarity values greater than 99.4 % (simulates a 'strict criteria' situation where a small number of nucleotide differences due to sequencing error are allowed, in this case three or four nucleotides in 600 nucleotides) were coloured red and species that coloured red for all available loci were considered synonyms; in the second scenario, similarity values lower than 99 % were coloured green and those greater than 99 % were coloured red. Any species that had green cells for all available genes was considered distinct. Finally, all remaining species (i.e., those having both green and red values depending on the gene) were again examined by looking at their position in the different trees, their nucleotide differences and the original publication to determine the basis on which the authors described the species. In many instances, it was found that only one gene, most often *tef1*, was responsible for separation of the given species from its relatives, and in such cases the species was tentatively accepted. Support values proved to be a poor criterion in the present study, as many of the clades were found to have little to poor support. This is partly due to the missing data present in the dataset as not all loci were available for all species, but also partly due to the extremely close genetic similarity of many of the included species. Fixed Single Nucleotide Polymorphisms (SNPs) were also not always useful as the number of available sequences for a given species varied. In closely related species complexes it was therefore not always possible to assign unambiguous fixed nucleotide positions, except for maybe the two closest neighbours.

Morphology

To induce sporulation, isolates were inoculated onto sterile pine needles (Smith et al. 1996) and placed on synthetic nutrient-poor agar (PNA), 2 % potato dextrose agar (PDA), MEA, oatmeal agar (OA), and incubated at 25 °C under near-UV light for 2–4 wk (see Crous et al. 2019 for recipes). Slide preparations were made in clear lactic acid. Morphological observations of reproductive structures were made using a Nikon AZ100 dissecting microscope and a Nikon Eclipse 80i compound microscope with differential interference contrast (DIC) illumination, both equipped with a Nikon DS-Ri2 high definition colour digital

camera. Measurements of conidiomata, conidiophores and conidiogenous cells were made to determine the smallest and the largest values. For the isolates selected as holotype, the lengths and widths of 50 conidia per isolate were determined, and 25 measurements were made for the remaining isolates in each taxon. Average (mean), standard deviation (SD), minimum (min) and maximum (max) measurements are presented as (min–) (mean–SD)–(mean+SD) (–max). Colony morphology was characterised from cultures grown on MEA, OA and PDA after 1 wk at 25 °C in the dark, and colony colour was determined using the colour charts of Rayner (1970).

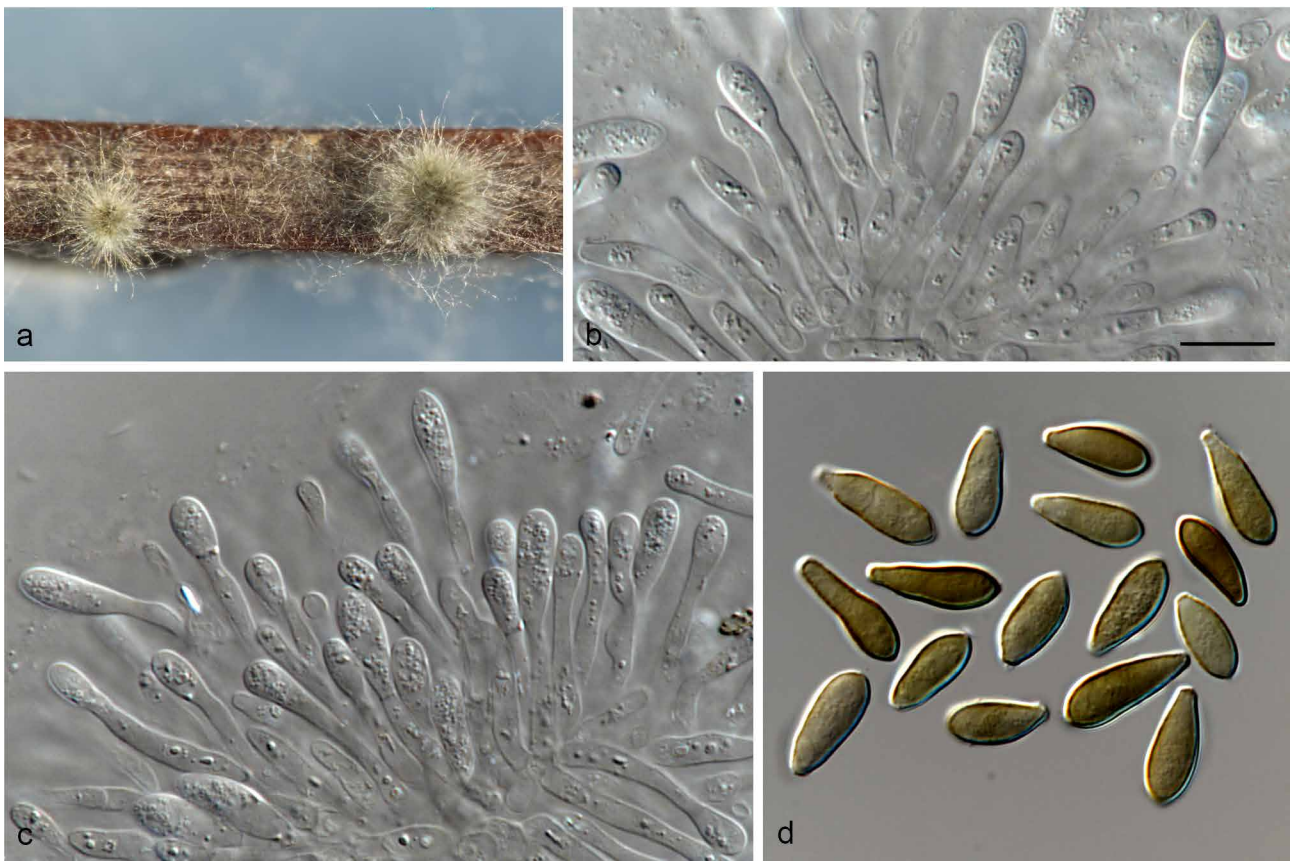

Fig. 11 *Botryosphaeria dothidea* (CBS 123530). a. Colony sporulating on PNA; b–c. conidiogenous cells and developing conidia; d. mature, brown conidia. — Scale bar: b = 10 µm, scale bar of b applies to b–d.

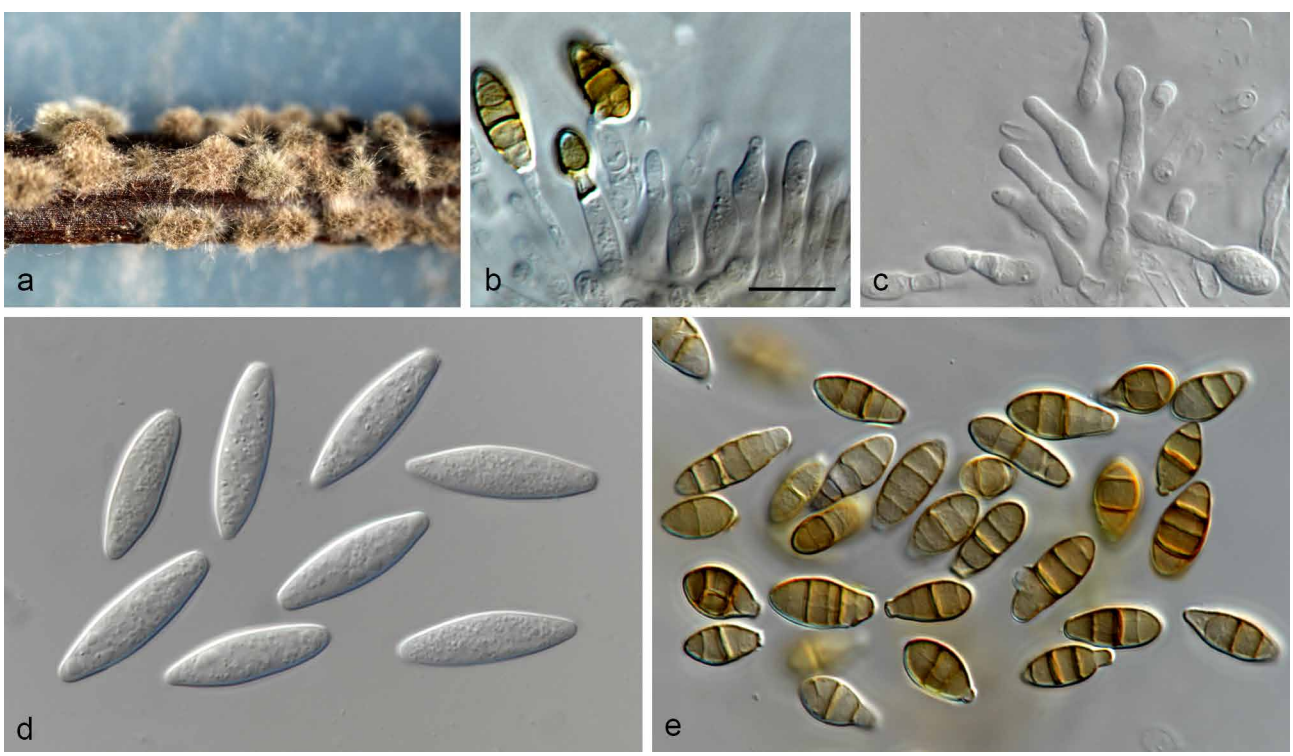

Fig. 12 *Botryosphaeria dothidea* (CBS 145971). a. Colony sporulating on PNA; b–c. conidiogenous cells and developing conidia; d. hyaline conidia; e. brown pigmented, septate conidia. — Scale bar: b = 10 µm, scale bar of b applies to b–e.

RESULTS

In total, 10 multigene phylogenies (Fig. 1–10) were generated (see TreeBASE; study S27596). Statistics and models used for the different datasets are shown in Table 2. The Bayesian tree from each alignment is presented, with the bootstrap support values from the RAxML analyses plotted in addition at the nodes. The phylogenetic analyses treated the following genera: *Botryosphaeria* (Fig. 1), *Diplodia* (Fig. 2), *Dothiorella* (Fig. 3), *Lasiodiplodia* (Fig. 4), *Neofusicoccum* (Fig. 5, 6), *Neoscytalidium* (Fig. 7), *Phaeobotryon*, *Barriopsis*, *Sphaeropsis*, *Alanphillipsia* and *Oblongocollomyces* (Fig. 8), *Pseudofusicoccum* (Fig. 9) and *Saccharata* (Fig. 10). Taxonomic novelties were revealed in *Botryosphaeria* (one species) *Diplodia* (one species), *Dothiorella* (one species), *Lasiodiplodia* (one species), *Neofusicoccum* (two species), *Phaeobotryon* (one species) and *Saccharata* (two species).

Taxonomy

Based on the phylogenetic analyses conducted in this study, eight species are delineated as new, with morphological descriptions provided below. Several isolates appeared to represent distinct taxa based on the multigene analyses, but were not formally named. This was due to the limited number of nucleotide or morphological differences, or the fact that several cryptic lineages appeared to represent older, well established names. Nevertheless, descriptions and illustrations are provided for those isolates to facilitate a revision of these genera in the future. Justification for reducing previously accepted species to synonymy are provided below.

Botryosphaeria dothidea (Moug.: Fr.) Ces. & De Not., Comment. Soc. Crittog. Ital. 1: 212. 1863 — Fig. 11, 12

Basionym. *Sphaeria dothidea* Moug. In: Fries, Syst. Mycol. (Lundae) 2 (2): 423. 1823.

New synonyms. *Botryosphaeria auasmontanum* F.J.J. van der Walt et al., Persoonia 33: 162. 2014.

Botryosphaeria minutispermatia Ariyaw. et al., Phytotaxa 275: 40. 2016.

Botryosphaeria quercus Wijayaw. et al., Fungal Diversity 77: 63. 2016.

Botryosphaeria sinensis Y.P. Zhou & Y. Zhang ter (as '*sinensia*'), Phytotaxa 245: 45. 2016.

Botryosphaeria wangensis G.Q. Li & S.F. Chen, Persoonia 40: 84. 2017 (2018).

Botryosphaeria qinlingensis C.M. Tian & L.Y. Liang, Mycotaxon 134: 469. 2019.

Isolate CBS 123530. *Conidiomata* pycnidial, produced on PNA, solitary, globose to ovoid, dark brown to black, up to 730 µm wide, 680 µm high, embedded in needle tissue, semi-immersed to superficial, unilocular, with a central ostiole. *Conidiophores* absent or reduced to a supporting cell. *Conidiogenous cells* holoblastic, discrete, hyaline, cylindrical to lageniform, phialidic with periclinal thickening, (9–)12.5–18.5(–20.5) × (2–)2.5–3.5(–4) µm. *Paraphyses* not seen. *Conidia* hyaline, thin-walled, smooth with granular contents, aseptate, narrowly or irregularly fusoid, base subtruncate to bluntly rounded, apex subobtuse, becoming brown when mature, (9–)10.5–14(–16) × (3.5–)4–5(–6) µm (av. = 12.5 × 4.8 µm, n = 50; L/W = 2.6).

Culture characteristics — Colonies on PDA have fluffy aerial mycelia with an irregular margin, with appressed moderately dense mycelial mat, smoke grey to olivaceous, covering the dish after 6 d at 25 °C in the dark. Colonies on MEA have fluffy aerial mycelia with an uneven margin, with an appressed mycelial mat that is sparse to moderately dense, smoke grey in the centre, white towards the margin, covering the dish after 5 d at 25 °C in the dark. Colonies on OA have fluffy aerial mycelia with an uneven margin, with appressed mycelial mat and moderately dense, pale grey centre with white region, covering the dish after 5 d at 25 °C in the dark.

Isolate CPC 29048. *Conidiomata* pycnidial, produced on PNA, solitary, globose to ovoid, dark brown to black, up to 610 µm wide, 540 µm high, embedded in needle tissue, semi-immersed to superficial, unilocular, with a central ostiole. *Conidiophores* absent. *Conidiogenous cells* holoblastic, discrete, hyaline, cylindrical to lageniform, phialidic with periclinal thickening, (8.5–)10–17(–18.5) × 2–3(–3.5) µm. *Paraphyses* not seen. *Conidia* hyaline, thin-walled, smooth with granular contents, aseptate, narrowly fusoid, base subtruncate to bluntly rounded, apex subobtuse, (17–)19–23(–25) × (4.5–)5.5–6.5(–7.5) µm (av. = 21 × 6.2 µm, n = 50; L/W = 3.4). *Dichomera* synasexual morph with pigmented, brown conidia, thin-walled, transversely 2–7-septate, with 1–2 oblique septa, (11–)13.5–17(–19.5) × (5–)5.5–6.5(–7) µm (av. = 15.4 × 6.1 µm, n = 50; L/W = 2.5).

Culture characteristics — Colonies on PDA have fluffy aerial mycelia with an irregular margin, with an appressed mycelial mat that is sparse to moderately dense, a few cottony aerial mycelia reaching to the lid of the Petri dish, smoke grey to iron-grey, covering the dish after 4 d at 25 °C in the dark. Colonies on MEA have fluffy mycelia with an uneven margin, with an appressed mycelial mat that is sparse to moderately dense, smoke grey, covering the dish after 6 d at 25 °C in the dark. Colonies on OA have fluffy aerial mycelia with an uneven margin, with appressed mycelial mat and moderately dense, a few cottony aerial mycelia reaching to the lid of the Petri dish, olivaceous black centre surrounded by a smoke grey margin, covering the dish after 4 d at 25 °C in the dark.

Isolates examined. Australia, Western Australia, Albany, Gull Cove, on *Grevillea* sp., conidiomata induced on PNA medium, 20 Sept. 2015, *P.W. Crous* (CBS H-24114, culture CBS 145971 = CPC 29048). – South Africa, Western Cape province, Stellenbosch, on *Diospyros glabra*, conidiomata induced on PNA medium, 22 May 2008, *F. Roets* (CBS H-24116, culture CBS 123530 = CPC 15186).

Notes — Four recently published species are reduced to synonymy with *Botryosphaeria dothidea* (Fig. 1, S1A–C; parsimony analyses not shown) and two additional species, namely *B. auasmontanum* and *B. minutispermatia*, tentatively retained as separate based on lower sequence similarity values. The latter two species are indicated as possible synonyms of *B. dothidea* above and cluster on longer branches in the *B. dothidea* clade (Fig. 1). Three of the species, namely *B. minutispermatia*, *B. quercus* and *B. sinensis*, were published in the same year. The ex-type culture of *B. dothidea* had the following nucleotide similarities with the sequences of the ex-types of *B. auasmontanum*, *B. minutispermatia*, *B. quercus*, *B. sinensis* and *B. wangensis*. On ITS: 410/415 (98.80 %, including three gaps), 454/457 (99.34 %, including three gaps), 456/456 (100 %), 455/457 (99.56 %, including two gaps; based on CGMCC 3.17723) and 455/457 (99.56 %, including two gaps), respectively. On *tef1*: 223/244 (91.39 %; including one indel of 21 nucleotides), 239/244 (97.95 %, including one gap), no *tef1* available for *B. quercus*, 244/244 (100 %; based on CGMCC 3.17723) and 244/246 (99.59 %, including two gaps). On *tub2*: no *tub2* available for *B. auasmontanum*, *B. minutispermatia* and *B. quercus*, 368/370 (99.46 %, including two gaps) and 383/384 (99.74 %), respectively. A comparison of the ex-type sequences of *B. qinlingensis* (ITS: MK434301, *tef1*: MK425020, *tub2*: MK425022; not included in the phylogenetic trees) revealed that this species is also a synonym of *B. dothidea*: the ITS sequence differed by one nucleotide from several other species (such as *B. 'wangensis'*, *B. 'quercus'*, *B. 'sinensis'* and *B. dothidea*); the *tef1* sequence is identical to *B. 'sinensis'* and *B. dothidea* and differed with two gaps from *B. 'wangensis'* while the *tub2* sequence is identical to *B. qingyuanensis*, *B. fabicerciana*, *B. dothidea* and *B. rosaceae*. Although CBS 123530 clustered apart from the *B. dothidea* clade (Fig. 1), the low number of sequence differences withheld us from introducing a novel species for it: on ITS it differed with

a single nucleotide from *B. dothidea*, *B. fusispora*, *B. kuwatsukai*, *B. minutispermatia*, *B. quercus*, *B. rosaceae*, *B. sinensis* and *B. wangensis*. The Bayesian phylogeny did not resolve it as a new species (Fig. S1A) whereas it formed a unsupported lineage on a short branch in the parsimony phylogeny (data not shown). On *tef1* it differed with a single nucleotide from *B. wangensis* and with two nucleotides from *B. qingyuanensis*. The Bayesian phylogeny placed it closely related to the other species (Fig. S1B), as did the parsimony analysis (data not shown). On *tub2* it is identical to *B. dothidea*, *B. fabicerciana*, *B. qingyuanensis* and *B. rosaceae*. Neither the Bayesian (Fig. S1C) nor the parsimony analyses (data not shown) resolved these species.

Likewise, the clade containing CPC 29048 clustered apart from the *B. dothidea* clade (Fig. 1), but the low number of sequence differences withheld us from introducing a novel species for it: on ITS it differed with a single nucleotide from *B. fabicerciana*, *B. fusispora*, *B. kuwatsukai* and *B. rosaceae*. Both the Bayesian (Fig. S1A) and parsimony (data not shown) analyses placed it in a distinct clade, which also included *B. corticis* on a long branch. On *tef1* it differed with two nucleotides from CBS 123530 and with three nucleotides from *B. wangensis*. It formed a distinct lineage in the Bayesian (Fig. S1B; PP = 1.0) and parsimony (data not shown; 86 % bootstrap support) phylogenies. On *tub2* it differed two nucleotides from *B. dothidea*, *B. fabicerciana*, *B. qingyuanensis* and *B. rosaceae*. It formed a distinct lineage in the Bayesian (Fig. S1C; PP = 1.0) and parsimony (data not shown; 86 % bootstrap support) phylogenies.

Botryosphaeria fabicerciana (S.F. Chen et al.) A.J.L. Phillips & A. Alves, Stud. Mycol. 76: 77. 2013

Basionym. *Fusicoccum fabicercianum* S.F. Chen et al., Pl. Pathol. 60: 746. 2011.

New synonym. *Botryosphaeria fusispora* Boonmee et al., Fungal Diversity 57: 171. 2012.

Notes — *Botryosphaeria fusispora* (Fig. 1, S1A–C; parsimony analyses not shown) is reduced to synonymy with *B. fabicerciana*. The ex-type culture of *B. fabicerciana* has the following nucleotide similarities with the sequences of the ex-type of *B. fusispora*. On ITS, *tef1* and *tub2*, respectively: 455/455 (100 %), 246/246 (100 %) and 383/384 (100 %). It is possible that, when Liu et al. (2012) published *B. fusispora*, the authors were not aware of the existence of *B. fabicerciana* as they did not include this species in their phylogenetic tree, neither did they make any reference to it.

Botryosphaeria kuwatsukai (Hara) G.Y. Sun & E. Tanaka, Fungal Diversity 71: 225. 2014

Basionym. *Macrophoma kuwatsukai* Hara, Practice of Crop Pathology (Tokyo): 482. 1930.

New synonym. *Botryosphaeria rosaceae* Y.P. Zhou & Ying Zhang, Mycosphere 8: 167. 2017.

Notes — *Botryosphaeria rosaceae* is reduced to synonymy with *B. kuwatsukai* (Fig. 1, S1A–C; parsimony analyses not shown). The ex-type culture of *B. kuwatsukai* has the following nucleotide similarities with the sequences of the ex-type of *B. rosaceae*. On ITS and *tef1*, respectively: 455/455 (100 %) and 206/206 (100 %). Zhou et al. (2017) did not include *B. kuwatsukai* in their phylogenetic tree neither did they make any reference to it.

Botryosphaeria ramosa (Pavlic et al.) A.J.L. Phillips & A. Alves, Stud. Mycol. 76: 77. 2013

Basionym. *Fusicoccum ramosum* Pavlic et al., Mycologia 100: 861. 2008.

New synonym. *Botryosphaeria pseudoramosa* G.Q. Li & S.F. Chen, Persoonia 40: 83. 2017 (2018).

Notes — *Botryosphaeria pseudoramosa* is reduced to synonymy with *Botryosphaeria ramosa* (Fig. 1, S1A–C; parsimony analyses not shown). The ex-type culture of *B. ramosa* has

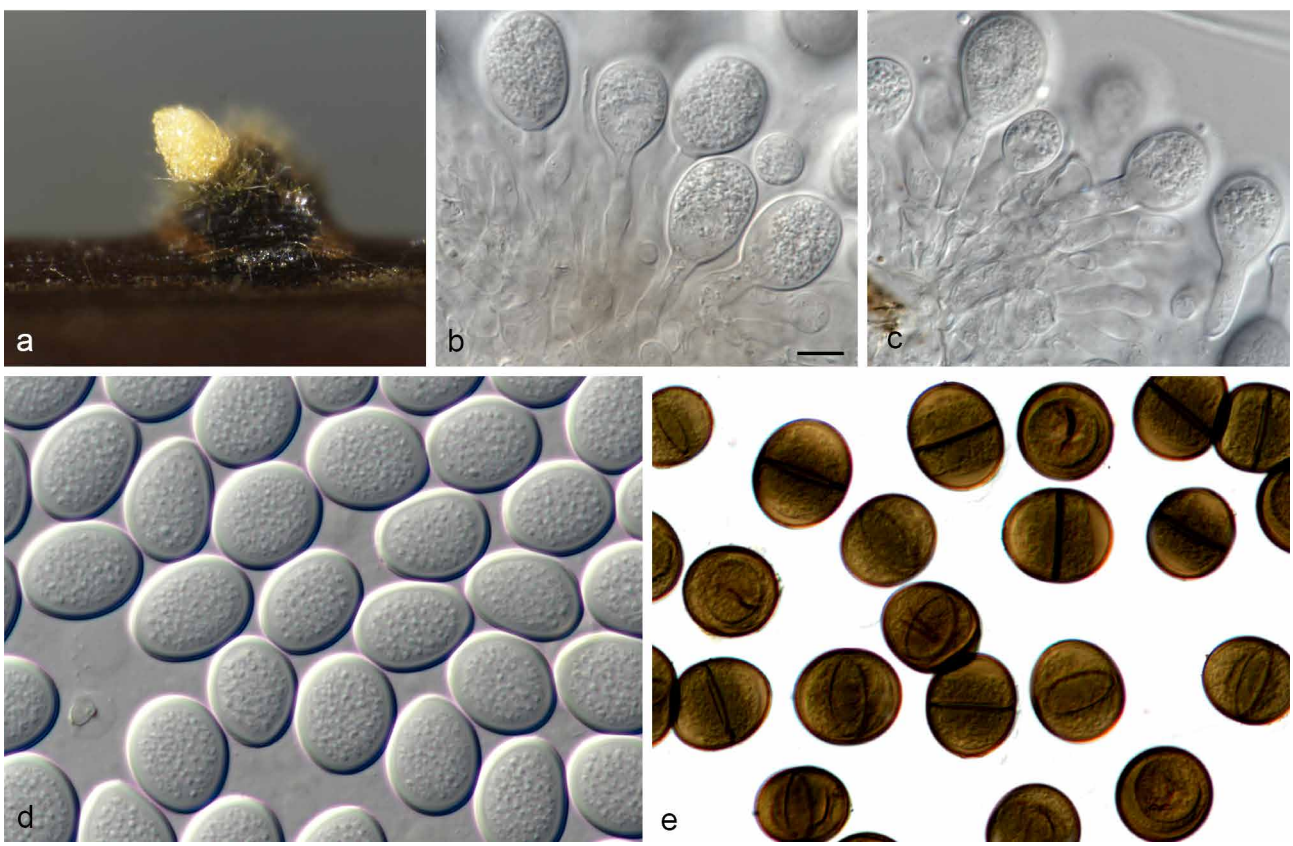

Fig. 13 *Diplodia afrocarpi* (CBS 131681). a. Colony sporulating on PNA; b–c. conidiogenous cells; d. young, hyaline conidia; e. mature, brown 1-septate conidia. — Scale bar: b = 10 µm, scale bar of b applies to b–e.

the following nucleotide similarities with the sequences of the ex-type of *B. pseudoramosa*. On ITS, *tef1* and *tub2*: 451/453 (99.56 %), 246/247 (99.60 %) and 386/386 (100 %), respectively. Li et al. (2018) mentioned that *B. ramosa* and *B. pseudoramosa* were phylogenetically closely related and that they could be distinguished based on the morphology of their conidia.

Diplodia afrocarpi W. Zhang & Crous, *sp. nov*. — MycoBank MB838092; Fig. 13

Etymology. Name refers to *Afrocarpus*, the host genus from which this fungus was collected.

Typus. South Africa, Western Cape province, Knysna, from healthy twigs of *Afrocarpus falcatus*, conidiomata induced on PNA, 5 Feb. 2009, *E.M. Cruywagen* (holotype CBS 131681, preserved as metabolically inactive culture, culture ex-type CBS 131681 = CMW 35506).

Conidiomata pycnidial, produced on PNA, solitary or aggregated, individual conidiomata globose, superficial or semi-immersed, covered with hyphal hairs, uniloculate, thick-walled, exuding conidia in a yellow mucoid mass, up to 1245 µm wide, up to 1100 µm high. *Conidiogenous cells* hyaline, thin-walled, smooth, cylindrical to subcylindrical, discrete, holoblastic with no evidence of annellations, (9–)10–14(–17.5) × (3–)3.5–5(–5.5) µm. *Paraphyses* absent. *Conidia* round to ovoid, both ends broadly rounded, initially hyaline, aseptate, becoming dark brown and 1-septate with age, thick-walled, wall externally smooth, roughened on the inner surface, (20–)22.5–24.5(–26) × (15–)16.5–19(–20) µm (av. = 23.5 × 17.8 µm, n = 50; L/W = 1.3).

Culture characteristics — Colonies on PDA have fluffy aerial mycelia with an irregular margin, with an appressed mycelial mat that is sparse to moderately dense, mouse grey, a few cottony aerial mycelia reaching to the lid of the Petri dish, covering the dish after 6 d at 25 °C in the dark. Colonies on MEA have fluffy aerial mycelia with an uneven margin, with an appressed mycelial mat that is sparse to moderately dense, a few cottony aerial mycelia reaching to the lid of the Petri dish, pale grey to smoke grey, covering the dish after 5 d at 25 °C in the dark. Colonies on OA have fluffy aerial mycelia with an uneven margin, with appressed mycelial mat, white, moderately dense, a few cottony aerial mycelia reaching to the lid of the Petri dish, mouse grey, covering the dish after 5 d at 25 °C in the dark.

Notes — Phylogenetically, *Diplodia afrocarpi* clusters in a separate lineage compared to all other species included in genus *Diplodia* (Fig. 2), representing a new taxon on *Afrocarpus*. Based on ITS sequence data, it differs at eight positions (including two indels) from *D. estuarina* and *D. alatafructa*. It represents a phylogenetically distinct lineage in both the Bayesian (Fig. S2A) and parsimony (data not shown) phylogenies. For the *tef1* data, the best match in the dataset had a 90 % similarity with *D. pterocarpi*. It formed a distinct basal lineage in the Bayesian (Fig. S1B) and parsimony (data not shown) phylogenies. In the *tub2* comparison, the best match in the dataset was a 96 % similarity with *D. corticola*. It formed a distinct basal lineage in the Bayesian (Fig. S1C) and parsimony (data not shown) phylogenies.

Diplodia mutila (Fr.: Fr.) Fr., Summa Veg. Scand. 2: 417. 1849

Basionym. *Sphaeria mutila* Fr.: Fr., Syst. Mycol. (Lundae) 2 (2): 424. 1823.
New synonyms. *Diplodia pyri* Tao Yang & Crous, Fung. Biol. 121: 329. 2016, Nom. illegit., Art. 53.1.
Diplodia magnoliigena Jayasiri et al., Mycosphere 10: 135. 2019.

Notes — *Diplodia pyri* and *D. magnoliigena* are reduced to synonymy with *D. mutila* (Fig. 2, S2A–C; parsimony analyses not shown). The ex-epitype culture of *D. mutila* has the following nucleotide similarities with the sequences of the ex-types of *D. magnoliigena* and *D. pyri*. On ITS: 475/478 (99.37 %, including one gap) and 477/477 (100 %), respectively. On *tef1*: no *tef1* available for *D. magnoliigena* and 249/259 (96.14 %; including one indel of nine nucleotides), respectively. On *tub2*: 343/346 (99.13 %; based on strain MFLUCC 18-1554, GenBank MK412873.1) and 384/385 (99.74 %), respectively.

Diplodia pseudoseriata C.A. Pérez et al., Fungal Diversity 41: 63. 2009 — Fig. 14, 15

New synonyms. *Diplodia alatafructa* Mehl & Slippers, Mycologia 103: 542. 2011.
Diplodia pseudoplatani Wijayaw. et al., Fungal Diversity 77: 108. 2016.
Diplodia insularis Linald. et al., Mycosphere 7: 968. 2016.

Isolate CBS 125527: *Conidiomata* pycnidial, produced on PNA, solitary or aggregated, individual conidiomata globose, superficial or semi-immersed, covered with hyphal hairs, uniloculate, thick-walled, up to 350 µm wide, up to 370 µm high. *Conidiogenous cells* hyaline, smooth, cylindrical, sometimes slightly swollen at the base, holoblastic, proliferating percurrently to form two or three distinct annellations or proliferating internally giving rise to periclinal thickenings, (5–)6–9.5(–11.5) × (2.5–)3–4(–5.5) µm. *Paraphyses* absent. *Conidia* initially hyaline becoming pigmented even while still attached to the conidiogenous cell, dark brown when mature, 0–1-septate, ellipsoid to ovoid, wall finely roughened on inner surface, (19–)21–25.5(–29.5) × (7.5–)8.5–11.5 (–15) µm (av. = 23.2 × 9.8 µm, n = 50; L/W = 2.4).

Culture characteristics — Colonies on PDA have fluffy aerial mycelia with an irregular margin, with an appressed mycelial mat that is sparse to moderately dense, smoke grey to mouse grey surrounded by a white margin, covering the dish after 6 d at 25 °C in the dark. Colonies on MEA have fluffy aerial mycelia with an uneven margin, with an appressed mycelial mat that is sparse to moderately dense, white with a smoke grey centre, covering the dish after 5 d at 25 °C in the dark. Colonies on OA have fluffy aerial mycelia with an uneven margin, with appressed mycelial mat and white, moderately dense, a few cottony aerial mycelia reaching to the lid of the Petri dish, pale grey to smoke grey, covering the dish after 5 d at 25 °C in the dark.

Isolate CBS 124933: *Conidiomata* pycnidial, produced on PNA, solitary or aggregated, individual conidiomata globose, superficial or semi-immersed, covered with hyphal hairs, uniloculate, thick-walled, up to 890 µm wide, up to 840 µm high. *Conidiogenous cells* holoblastic, phialidic, discrete, determinate, doliiform, cylindrical to subcylindrical, hyaline, smooth-walled, (5–)5.5–10(–12.5) × 3–4.5(–5.5) µm. *Paraphyses* absent. *Conidia* ovoid to ellipsoid, apex rounded, base truncate or rounded, aseptate, initially hyaline, becoming brown, thick-walled, wall externally smooth, roughened on the inner surface, (19.5–)23–27 (–30.5) × (8–)10.5–12.5(–14) µm (av. = 25.1 × 11.4 µm, n = 50; L/W = 2.5).

Culture characteristics — Colonies on PDA have fluffy aerial mycelia with an irregular margin, with an appressed mycelial mat that is sparse to moderately dense, vinaceous grey, a few cottony aerial mycelia reaching to the lid of the Petri dish, covering the dish after 5 d at 25 °C in the dark. Colonies on MEA have fluffy aerial mycelia with an uneven margin, with an appressed mycelial mat that is sparse to moderately dense, a few cottony aerial mycelia reaching to the lid of the Petri dish, smoke grey to mouse grey, covering the dish after 4 d at 25 °C in the dark. Colonies on OA have fluffy aerial mycelia with an uneven margin, with appressed mycelial mat, white, moderately dense, a few cottony aerial mycelia reaching to the lid of the Petri dish, greyish sepia to smoke grey, covering the dish after 5 d at 25 °C in the dark.

Isolates examined. South Africa, Mpumalanga province, Buffelskloof Nature Reserve, from *Pterocarpus angolensis*, conidiomata induced on PNA medium, Dec. 2005, *J.W.M. Mehl & J. Roux* (CBS H-24119, culture CBS 124933 = CMW 22721). – Uruguay, Paysandu, Tres Bocas, from *Hexachlamis edulis*, conidiomata induced on PNA medium, 1 Aug. 2006, *C. Perez* (CBS H-24118, culture CBS 125527 = CMW 26742).

Notes — Three species, *D. alatafructa, D. pseudoplatani* and *D. insularis* are reduced to synonymy with *D. pseudoseriata* (Fig. 2, S2A–C; parsimony analyses not shown). The ex-type culture of *D. pseudoseriata* has the following nucleotide similarities with the sequences of the ex-types of *D. alatafructa*, *D. insularis* and *D. pseudoplatani*, respectively. On ITS: 470/473 (99.37 %), 471/473 (99.58 %, including one gap) and 473/474 (99.79 %, including one gap), respectively. On *tef1*: 232/233 (99.57 %, including one gap), 228/230 (99.13 %) and no *tef1* for *D. pseudoplatani*, respectively. On *tub2*: 384/385 (99.74 %), 383/385 (99.48 %; based on strain BL132, GenBank MG015810.1) and no *tub2* for *D. pseudoplatani*, respectively.

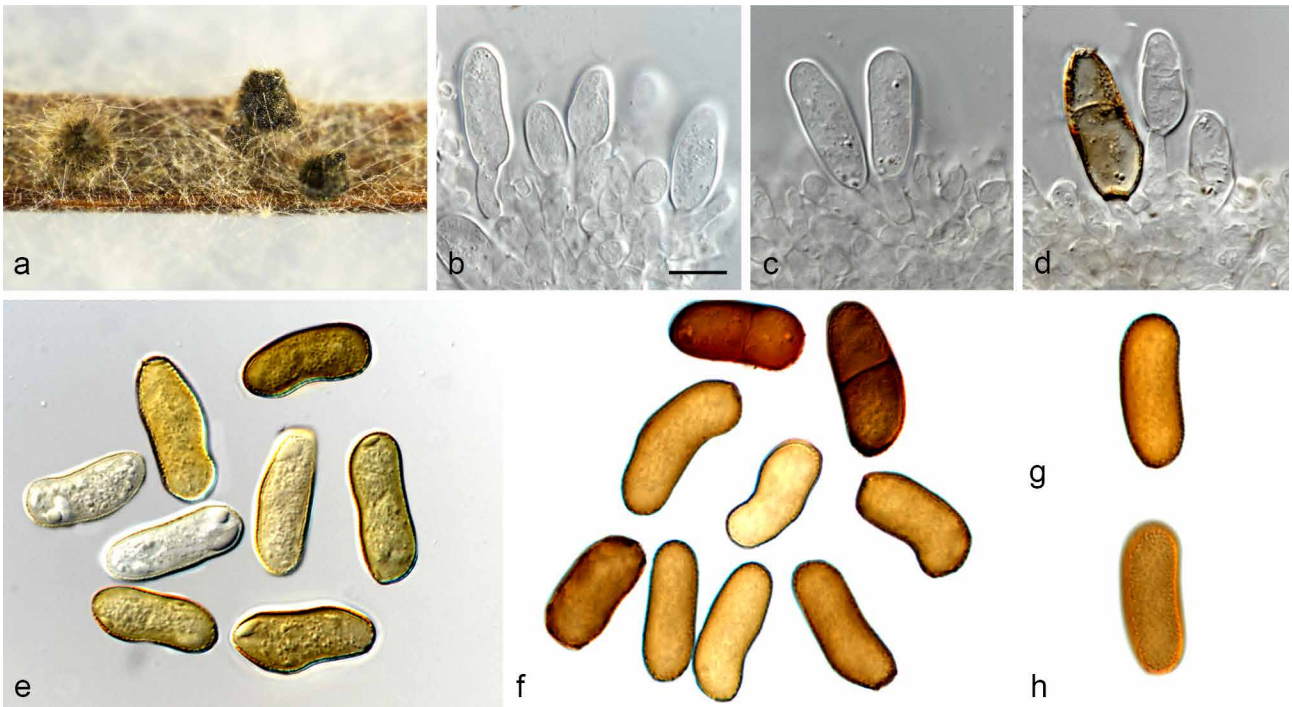

Fig. 14 *Diplodia pseudoseriata* (CBS 125527). a. Colony sporulating on PNA; b–d. conidiogenous cells and developing conidia; e–f. conidia; g–h. brown conidia at two different planes of focus to show the finely verruculose inner surface of the wall. — Scale bar: b = 10 µm, scale bar of b applies to b–h.

Fig. 15 *Diplodia pseudoseriata* (CBS 124933). a. Colony sporulating on PNA; b–c conidiogenous cells; d. young, hyaline conidia intermixed with mature, brown, conidia; e–f. brown conidia at two different planes of focus to show the finely verruculose inner surface of the wall. — Scale bars: b–d = 10 µm, scale bar of d applies to d–f.

Although CBS 125527 clusters basal in the clade, we refrain from introducing a new species for it due to sequence similarity: on ITS it differs three nucleotides from *D. pseudoseriata* and *D. pterocarpi*. The Bayesian (Fig. S2A; PP = 0.93) and parsimony (data not shown; no bootstrap support) phylogenies places it as a sister lineage to *D. alatafructa* inside a larger clade (PP = 1.0; parsimony bootstrap 91 %) containing *D. insularis*, *D. pseudoplatani, D. pseudoseriata* and *D. pterocarpi* at a basal position. On *tef1* it differs three nucleotides from *D. pseudoseriata* and four nucleotides from *D. alatafructa*. It forms a distinct lineage basal to *D. insularis*, *D. pseudoplatani, D. pseudoseriata* and *D. pterocarpi* in the Bayesian (Fig. S2B) and parsimony (data not shown) phylogenies. On *tub2* it differs one nucleotide from *D. pseudoseriata* and two nucleotides from *D. alatafructa*. It forms a distinct lineage in the Bayesian (Fig. S2C; PP = 1.0) and parsimony (data not shown) phylogenies with *D. pseudoseriata* as sister lineage.

Diplodia sapinea (Fr.) Fuckel, Jahrb. Nassauischen Vereins Naturk. 23–24: 393. 1870 [1869–1870]

Basionym. *Sphaeria sapinea* Fr., Syst. Mycol. (Lundae) 2 (2): 491. 1823.
New synonyms. *Diplodia intermedia* A.J.L. Phillips et al., Persoonia 29: 33. 2012.
Diplodia rosacearum S. Giambra et al., Mycosphere 7: 983. 2016.
Diplodia italica Wijayaw. et al., Fungal Diversity 77: 110. 2016.

Notes — Three species, *D. intermedia*, *D. rosacearum* and *D. italica* are reduced to synonymy with *D. sapinea* (Fig. 2, S2A–C; parsimony analyses not shown). The ex-type culture of *D. sapinea* has the following nucleotide similarities with the sequences for the ex-types of *D. intermedia*, *D. italica* and *D. rosacearum*. On ITS: 479/480 (99.79 %, including one gap), 478/481 (99.38 %, including two gaps) and 479/481 (99.58 %, including two gaps), respectively. On *tef1*: 232/234 (99.14 %), no *tef1* available for *D. italica* and 231/234 (98.72 %), respectively. On *tub2*: 382/383 (99.74 %), 384/385 (99.74 %) and 385/385 (100 %), respectively.

Diplodia scrobiculata J. de Wet et al., Mycol. Res. 107: 562. 2003 — Fig. 16

New synonym. *Diplodia guayanensis* Castro-Medina et al., Pl. Dis. 100: 2458. 2016.

Isolate CBS 139796. *Conidiomata* pycnidial, produced on PNA, solitary or aggregated, individual conidiomata globose, superficial or semi-immersed, covered with hyphal hairs, uniloculate, thick-walled, up to 310 µm wide, up to 290 µm high. *Conidiogenous cells* hyaline, thin-walled, smooth, cylindrical to subcylindrical, discrete, holoblastic with no evidence of annellations, (5.5–)9–13(–17) × (2.5–)3–5(–6) µm. *Paraphyses* absent. *Conidia* ovoid to ellipsoid or subcylindrical, apex rounded, base truncate or rounded, 0–3-septate, brown, thick-walled, wall externally smooth, roughened on the inner surface, (27–)29–33.5(–35.5) × (10.5–)11.5–13(–14) µm (av. = 31.3 × 12.3 µm, n = 50; L/W = 2.5).

Culture characteristics — Colonies on PDA have fluffy aerial mycelia with an irregular margin, with an appressed mycelial mat that is sparse to moderately dense, smoke grey with iron-grey edge, covering the dish after 6 d at 25 °C in the dark. Colonies on MEA have fluffy aerial mycelia with an uneven margin, with an appressed mycelial mat that is sparse to moderately dense, mouse grey, covering the dish after 5 d at 25 °C in the dark. Colonies on OA have fluffy aerial mycelia with an uneven margin, with appressed mycelial mat and moderately dense, smoke grey to iron-grey, covering the dish after 5 d at 25 °C in the dark.

Isolate examined. South Africa, Mpumalanga province, Sabie, from twigs of *Pinus patula*, conidiomata induced on PNA medium, 1 Oct. 2008, *W. Bihon* (CBS H-24120, culture CBS 139796 = CMW 30223).

Notes — *Diplodia guayanensis* is reduced to synonymy with *D. scrobiculata* (Fig. 2, S2A–C; parsimony analyses not shown), which is in agreement with the findings of Linaldeddu et al. (2016b). The ex-type culture of *D. scrobiculata* has the following nucleotide similarities with the sequences of the ex-type of *D. guayanensis*. On ITS, *tef1* and *tub2*, respectively: 479/481

Fig. 16 *Diplodia scrobiculata* (CBS 139796). a. Colony sporulating on PNA; b–c. conidiogenous cells; d. mature, brown septate conidia. — Scale bars: b, d = 10 µm, scale bar of b applies to c and scale bar of d applies to e.

(99.58 %), 199/199 (100 %) and 342/344 (99.42 %). Isolate CBS 139796 is phylogenetically (Fig. 2) closely related to *D. scrobiculata*. We refrain from introducing it as a novel species based on sequence similarity: on ITS it differs one nucleotide from *D. guayanensis* and three nucleotides from *D. scrobiculata*. The Bayesian (Fig. S2A) and parsimony (data not shown) phylogenies places it as a distinct clade (PP = 0.95; parsimony bootstrap 63 %) inside a larger clade (PP = 0.91; parsimony bootstrap 86 %) containing *D. guayanensis* and *D. scrobiculata*. On *tef1* it differs two nucleotides from *D. scrobiculata* and three nucleotides from *D. guayanensis*. The Bayesian (Fig. S2B) and parsimony (data not shown) phylogenies places it as a distinct clade (PP = 1.0; parsimony bootstrap 66 %) inside a larger clade (PP = 0.94; parsimony bootstrap 59 %) containing *D. guayanensis* and *D. scrobiculata*. On *tub2* it differs two nucleotides from *D. scrobiculata* and *D. guayanensis*. The Bayesian (Fig. S2C) and parsimony (data not shown) phylogenies places it as a distinct clade (PP = 0.98; parsimony bootstrap 63 %) inside a larger clade (PP = 0.93; parsimony bootstrap 63 %) containing *D. guayanensis* and *D. scrobiculata*.

Diplodia seriata De Not., Microm. Ital. Dec. IV No 6. 1842

New synonym. Diplodia huaxii Wijayaw. et al., Fungal Diversity 77: 108. 2016.

Notes — *Diplodia huaxii* is reduced to synonymy with *D. seriata*. The ITS sequence of the ex-type culture of *D. huaxii* (GUCC 0922-1) is 504/505 (99.80 %) similar to the ex-epitype of *D. seriata* (CBS 112555); no *tef1* or *tub2* sequences are available for the ex-type of *D. huaxii*. A *tef1* sequence of another culture lodged under that species name in GenBank (MF421307.1) is 231/234 (98.72 %) similar to the ex-epitype of *D. seriata* and up to 233/234 (99.57 %) similar to the other *tef1* sequences included under the latter name in the present study.

Dothiorella diospyricola W. Zhang & Crous, *sp. nov.* — MycoBank MB838093; Fig. 17

Etymology. Name refers to *Diospyros*, the host genus from which this fungus was collected.

Typus. South Africa, Kruger National Park, from *Diospyros mespiliformis*, conidiomata induced on PNA medium, 19 Nov. 2010, *P.W. Crous* (holotype CBS H-24124, culture ex-type CBS 145972 = CPC 34653).

Conidiomata produced on PNA, mostly solitary or aggregated, individual conidiomata, superficial or semi-immersed, up to 560 µm wide, up to 2100 µm high and long neck (sometimes branching). *Conidiophores* absent. *Conidiogenous cells* cylindrical to subcylindrical, hyaline, the first conidium produced holoblastically and subsequent conidia enteroblastically, (4–)4.5 × 6.5(–7.5) × (3–)3.5–5(–5.5) µm. *Conidia* ovoid, apices rounded and truncate bases, initially hyaline, aseptate, becoming cinnamon to sepia and 1-septate while still attached to conidiogenous cells, (13.5–)18–21.5(–24) × (6.5–)7.5–9(–10) µm (av. = 19.8 × 8.2 µm, n = 50; L/W =1.5).

Culture characteristics — Colonies on PDA have fluffy aerial mycelia with an uneven margin, with an appressed mycelial mat that is sparse to moderately dense, smoke grey to iron-grey, a few cottony aerial mycelia reaching to the lid of the Petri dish, covering the dish after 6 d at 25 °C in the dark. Colonies on MEA have fluffy aerial mycelia with an irregular margin, with an appressed mycelial mat that is sparse to moderately dense, a few cottony aerial mycelia reaching to the lid of the Petri dish, smoke grey, covering the dish after 5 d at 25 °C in the dark. Colonies on OA have fluffy aerial mycelia with an uneven margin, with appressed mycelial mat and moderately dense, a few cottony aerial mycelia reaching to the lid of the Petri dish, smoke grey to dark mouse grey, covering the dish after 5 d at 25 °C in the dark.

Notes — *Dothiorella diospyricola* is phylogenetically (Fig. 3) closely related to *Do. longicollis* and *Do. brevicollis*. The three species can be distinguished from one another based on

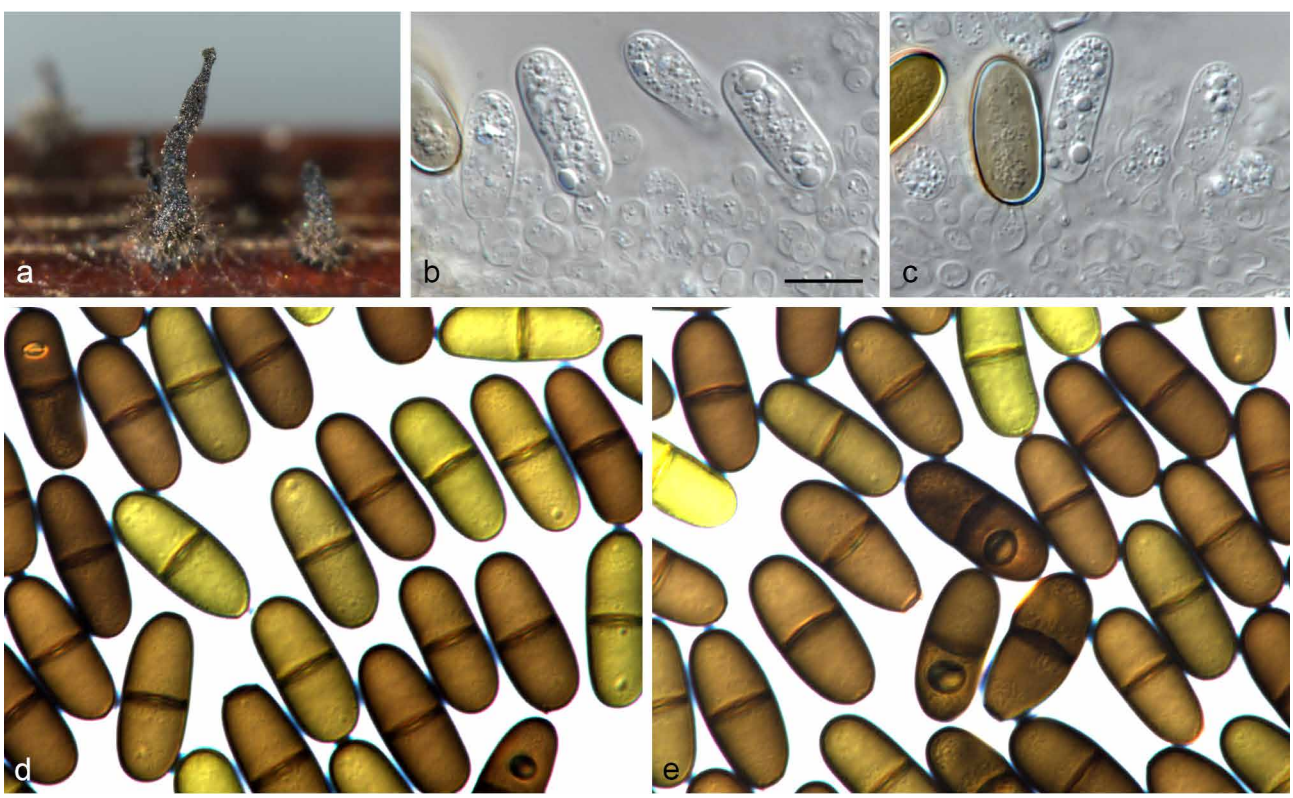

Fig. 17 *Dothiorella diospyricola* (CBS 145972). a. Colony sporulating on PNA; b–c conidiogenous cells and developing conidia; d–e. conidia. — Scale bar: b = 10 µm, scale bar of b applies to b–e.

conidial morphology. Conidia of *Do. diospyricola* (av. = 19.8 × 8.2 µm; L/W = 2.4) are smaller than those of *Do. longicollis* (av. = 20.4 × 8.7 mm; L/W = 2.4) (Pavlic et al. 2008) and *Do. brevicollis* (av. = 23.4 × 10.5 mm; L/W = 2.2) (Jami et al. 2012). On ITS it differs two nucleotides from *Do. brevicollis* and *Do. longicollis*. The Bayesian (Fig. S3A) and parsimony (data not shown) phylogenies do not clearly resolve it from its closest sister species, *Do. longicollis*. On *tef1* it differs five nucleotides from *Do. brevicollis* and *Do. lampangensis* and nine nucleotides from *Do. longicollis*. The Bayesian (Fig. S3B) and parsimony (data not shown) phylogenies place it as a distinct lineage sister to *Do. brevicollis* and *Do. lampangensis*. On *tub2* it differs one nucleotide from *Do. brevicollis* and two nucleotides from *Do. longicollis*. The Bayesian phylogeny (Fig. S3C) places it as a distinct lineage sister to *Do. brevicollis* and *Do. longicollis*, while the parsimony phylogeny (data not shown) do not resolve it well from *Do. brevicollis*. *Dothiorella longicollis* and *Do. brevicollis* can be distinguished from one another based on their lower sequence similarity on *tef1* (97.00 % similar) and *Do. longicollis* and *Do. lampangensis* based on *tub2* (96.60 % similar).

Dothiorella dulcispinae Jami et al., Cryptog. Mycol. 33: 258. 2012

New synonym. Dothiorella oblonga F.J.J. van der Walt et al., Persoonia 33: 163. 2014.

Notes — *Dothiorella oblonga* is reduced to synonymy with *D. dulcispinae* (Fig. 3, S3A–C; parsimony analyses not shown). The ex-type culture of *Do. dulcispinae* has the following nucleotide similarities with the sequences of the ex-type of *Do. oblonga*. On ITS, *tef1* and *tub2*, respectively: 452/453 (99.78 %), 222/225 (98.67 %, including one gap) and 406/406 (100 %). Slippers et al. (2014) did not provide any species notes highlighting the differences between *Do. dulcispinae* and *Do. oblonga*.

Dothiorella eriobotryae Gonz.-Domíng. et al., Pl. Pathol. 66: 86. 2017

New synonym. Dothiorella rhamni Wanas. et al., Fungal Diversity 78: 14. 2016.

Notes — *Dothiorella rhamni* is reduced to synonymy with *Do. eriobotryae* (Fig. 3, S3; parsimony analyses not shown). Only ITS is available for the ex-type culture of *Do. rhamni* and *tef1* sequences available on GenBank (MK078544.1, MF398945.1 and MF398940.1) under that name are most likely not conspecific with this species. The ITS sequences of *Do. eriobotrya* and *Do. rhamni* are identical (495/495 bases). González-Domínguez et al. (2017) did not include *Do. rhamni* in their phylogeny and was probably not aware of the existence of this species when they described *Do. eriobotryae* as new. *Dothiorella eriobotryae* was first published online on 20 May 2016, while *D. rhamni* was first published online on 23 May 2016.

Dothiorella mangifericola (Abdollahz. et al.) Tao Yang & Crous, Fung. Biol. 121: 335. 2016

Basionym. Spencermartinsia mangiferae Abdollahz. et al., Persoonia 32: 9. 2014.

New synonyms. Spencermartinsia rosulata F.J.J. van der Walt et al., Persoonia 33: 164. 2014.

Dothiorella rosulata (F.J.J. van der Walt et al.) Tao Yang & Crous, Fung. Biol. 121: 336. 2016.

Notes — *Dothiorella rosulata* is reduced to synonymy with *Do. mangifericola* (Fig. 3, S3A–C; parsimony analyses not shown). The ex-type culture of *Do. mangifericola* has the following nucleotide similarities with the sequences of the ex-type of *Do. rosulata*. On ITS and *tef1*, respectively: 437/438 (99 %) and 197/197 (100 %). No *tub2* sequence of *Do. mangifericola* was available for comparison.

Dothiorella sarmentorum (Fr.) A.J.L. Phillips et al., Mycologia 97: 522. 2005 — Fig. 18

Basionym. Sphaeria sarmentorum Fr., Kongl. Vetensk. Acad. Handl., ser. 3, 40: 107. 1819.

New synonyms. Dothiorella americana Úrbez-Torr. et al., Fungal Diversity 52: 184. 2012.

Dothiorella italica Dissan. et al., Mycosphere 8: 1166. 2017.

Possible synonyms. Dothiorella iberica A.J.L. Phillips et al., Mycologia 97: 524. 2005.

Dothiorella vidmadera W.M. Pitt et al., Fungal Diversity Res. Ser. 61: 216. 2013.

Dothiorella symphoricarpicola W.J. Li et al. (as '*symphoricarposicola*'), Cryptog. Mycol. 35: 265. 2014.

Dothiorella sempervirentis Abdollahz. et al., Persoonia 32: 6. 2014.

Dothiorella parva Abdollahz. et al., Persoonia 32: 5. 2014.

Dothiorella omnivora Linald. et al., Eur. J. Plant Pathol. 146: 272. 2016.

Dothiorella guttulata Qing Tian et al., Mycol. Progr. 17: 264. 2017.

Dothiorella californica D.P. Lawr. & Trouillas, Fung. Biol. 121: 355. 2017.

Isolate CBS 121001. *Conidiomata* produced on PNA, solitary or aggregated, superficial or semi-immersed, covered with hyphal hairs, uniloculate, thick-walled, non-papillate with a central ostiole, up to 470 µm wide, up to 410 µm high. *Conidiophores* absent. *Conidiogenous cells* lining the pycnidial cavity, hyaline, subcylindrical, proliferating at the same level giving rise to periclinal thickenings, or rarely proliferating percurrently forming one or two indistinct annellations, (4–)7–11(–13) × (2.5–)3.5–4.5(–6) µm. *Conidia* hyaline when young, becoming brown with age, dark brown, often while still attached to the conidiogenous cells, ovoid with a broadly rounded apex and truncate base, brown walled, 1–3-septate, slightly constricted at the septum, (19.5–)22–28(–33.5) × (7.5–)9–11.5(–15.5) µm (av. = 24.9 × 10.3 µm, n = 50; L/W = 2.4).

Culture characteristics — Colonies on PDA have fluffy aerial mycelia with an uneven margin, with an appressed mycelial mat that is sparse to moderately dense, grey dish sepia to iron-grey, covering the dish after 6 d at 25 °C in the dark. Colonies on MEA have fluffy aerial mycelia with an uneven margin, with an appressed mycelial mat that is sparse to moderately dense, smoke grey, covering the dish after 5 d at 25 °C in the dark. Colonies on OA have fluffy aerial mycelia with an uneven margin, with appressed mycelial mat, white, moderately dense, smoke grey to iron-grey, covering the dish after 5 d at 25 °C in the dark.

Isolate examined. USA, California, San Luis Obispo County, from *Vitis vinifera* cv. Zinfandel, conidiomata induced on PNA medium, 2004, *J.R. Úrbez-Torres* (CBS H-24126, culture CBS 121001).

Notes — Eight *Dothiorella* species are considered potential synonyms of *Do. sarmentorum*, with a further two formally reduced to synonymy based on their phylogenetic position in the combined tree (Fig. 3, S3A–C; parsimony analyses not shown). This cluster of species is in need of urgent revision using more genes and a more complete dataset to establish the exact species boundaries, as the genetic differences between many of the species are minute or overlapping, as shown below in the sequence comparisons.

The ex-type culture of *Do. sarmentorum* has the following nucleotide similarities with the sequences of the ex-types of *Do. americana*, *Do. californica*, *Do. guttulata*, *Do. iberica*, *Do. italica*, *Do. omnivora*, *Do. parva*, *Do. sempervirentis*, *Do. symphoricarpicola* and *Do. vidmadera*, respectively. On ITS: 450/453 (99.34 %, including two gaps), 448/451(99.33 %), 442/445 (99.33 %), 449/452 (99.34 %, including one gap), 450/451 (99.78 %, including one gap), 447/451 (99.11 %), 448/451

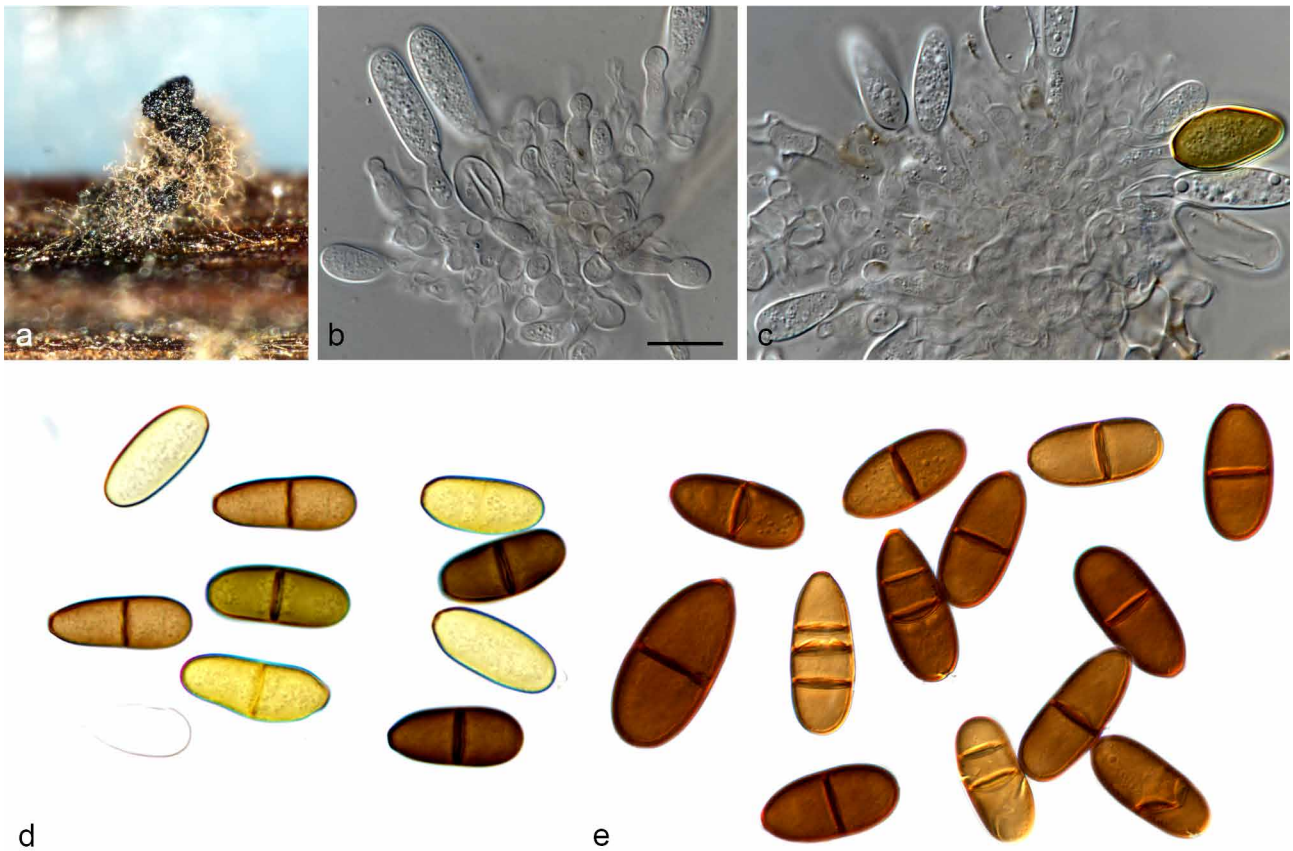

Fig. 18 *Dothiorella sarmentorum* (CBS 121001). a. Colony sporulating on PNA; b–c. conidiogenous cells and developing conidia; d–e. conidia. — Scale bar: b = 10 µm, scale bar of b applies to b–e.

(99.33 %), 447/451 (99.11 %), 448/452 (99.12 %, including two gaps) and 447/451 (99.11 %). On *tef1*: 202/217 (93.09 %, including two gaps and indel of nine nucleotides), 200/216 (92.59 %, including one indel of nine nucleotides), 201/216 (93.48 %, including one indel of nine nucleotides; based on CBS 134886), 203/216 (93.98 %, including one indel of nine nucleotides), 186/186 (100 %), 202/217 (93.09 %, including one gap and indel of nine nucleotides), 202/216 (93.52 %, including one indel of nine nucleotides), 202/218 (92.66 %, including 11 gaps), 201/216 (93.06 %, including one indel of nine nucleotides) and 199/217 (91.71 %, including one gap and indel of nine nucleotides), respectively. On *tub2*: 357/358 (99.72 %), 354/358 (99.88 %), 357/358 (99.72 %; based on CBS 134886), 357/358 (99.72 %), 357/358 (99.72 %; based on CBS 115038), 353/358 (98.60 %; based on CBS 124716), 357/358 (99.72 %), 357/358 (99.72 %), 355/359 (98.89 %, including one gap; based on CBS 135622) and 358/358 (100 %), respectively.

Dothiorella striata A.J.L. Phillips & Abdollahz., Persoonia 32: 7. 2014

New synonym. *Dothiorella neclivora* W.M. Pitt & Úrbez-Torr. (as '*neclivorem*'), Australas. Pl. Pathol. 44: 49. 2015.

Notes — *Dothiorella neclivora* is reduced to synonymy with *Do. striata* (Fig. 3, S3A–C; parsimony analyses not shown). The ex-type culture of *Do. striata* has the following nucleotide similarities with the sequences of the ex-type of *Do. neclivora*. On ITS, *tef1* and *tub2*, respectively: 432/433 (99.77 %), 223/228 (97.80 %, including one gap) and 408/408 (100 %). Pitt et al. (2015) described *Do. neclivora* based on phylogenetic relatedness and non-striate conidia compared to *Do. striata*. However, the authors mentioned that it remained to be seen whether conidial striations were a stable feature, and that the status of *Do. neclivora* should be reviewed in the future.

Dothiorella viticola A.J.L. Phillips & J. Luque, Mycologia 97: 1118. 2006 [2005] — Fig. 19, 20

New synonyms. *Spencermartinsia westralis* W.M. Pitt et al. (as '*westrale*'), Australas. Pl. Path. 44: 48. 2015.

Dothiorella westralis (W.M. Pitt et al.) Tao Yang & Crous, Fung. Biol. 121: 336. 2016.

Isolate CBS 117006. *Conidiomata* produced on PNA, solitary or aggregated, superficial or semi-immersed, covered with hyphal hairs, globose, papillate with a short neck, thick-walled, non-papillate with a central ostiole, up to 560 µm wide, up to 940 µm high. *Conidiophores* absent. *Conidiogenous cells* cylindrical to lageniform, discrete or integrated, holoblastic, indeterminate, proliferating at the same level giving rise to periclinal thickenings, hyaline, thin-walled, smooth, (3.5–)5–8.5(–10) × (2.5–)3–4.5(–5) µm. *Conidia* subcylindrical to ellipsoid or ovoid, brown, 1-septate, occasionally slightly constricted at septum, moderately thick-walled, externally smooth, internally finely verruculose, ends rounded, often with a truncate base, (17.5–)19.5–23(–28.5) × (9–)10.5–12.5(–14) µm (av. = 21.3 × 11.4 µm, n = 50; L/W =1.9).

Culture characteristics — Colonies on PDA have fluffy aerial mycelia with an uneven margin, with an appressed mycelial mat that is sparse to moderately dense, vinaceous grey to fuscous black, a few cottony aerial mycelia reaching to the lid of the Petri dish, covering the dish after 6 d at 25 °C in the dark. Colonies on MEA have fluffy aerial mycelia with an uneven margin, with an appressed mycelial mat that is sparse to moderately dense, a few cottony aerial mycelia reaching to the lid of the Petri dish, iron-grey, covering the dish after 5 d at 25 °C in the dark. Colonies on OA have fluffy aerial mycelia with an irregular margin, with appressed mycelial mat and moderately dense, a few cottony aerial mycelia reaching to the lid of the Petri dish, smoke grey to mouse grey, covering the dish after 5 d at 25 °C in the dark.

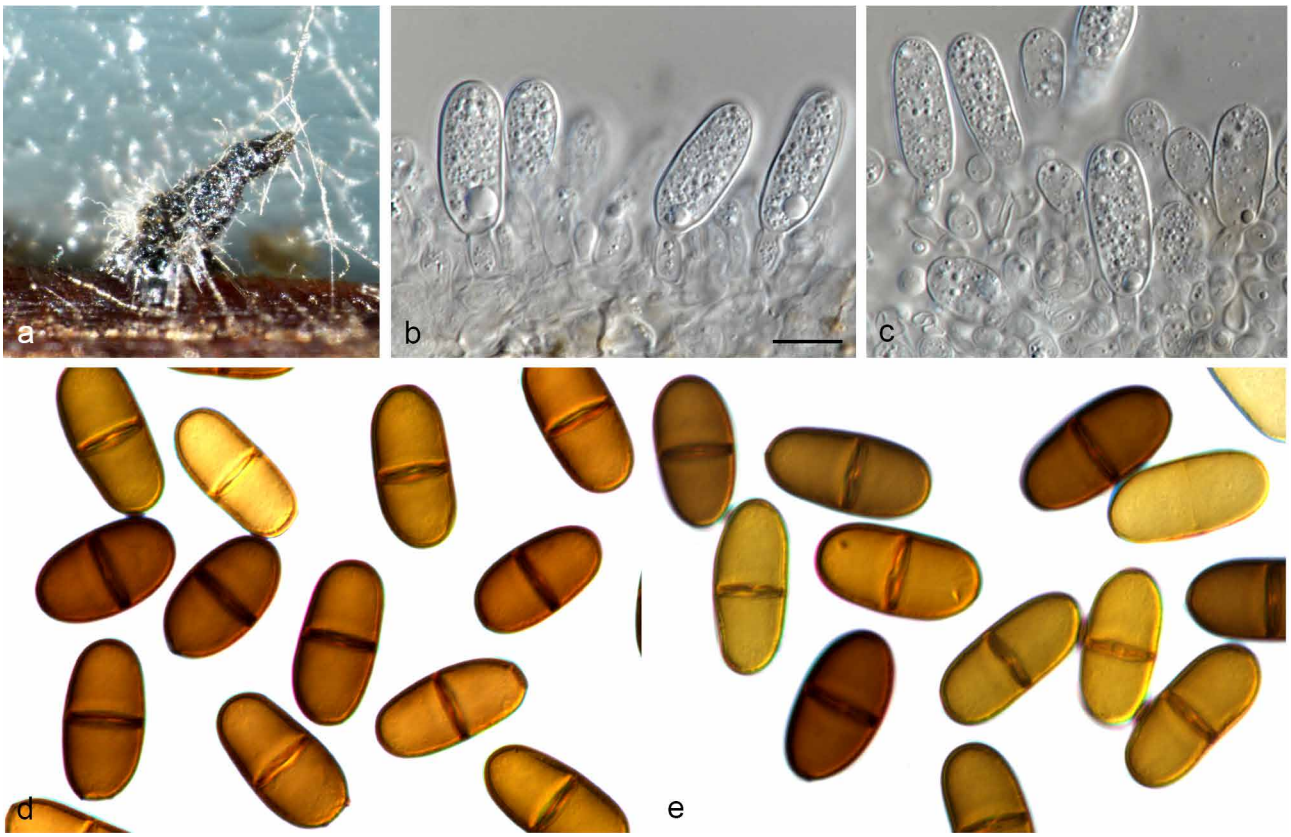

Fig. 19 *Dothiorella viticola* (CBS 117006). a. Colony sporulating on PNA; b–c. conidiogenous cells and developing conidia; d–e. conidia. — Scale bar: b = 10 µm, scale bar of b applies to b–e.

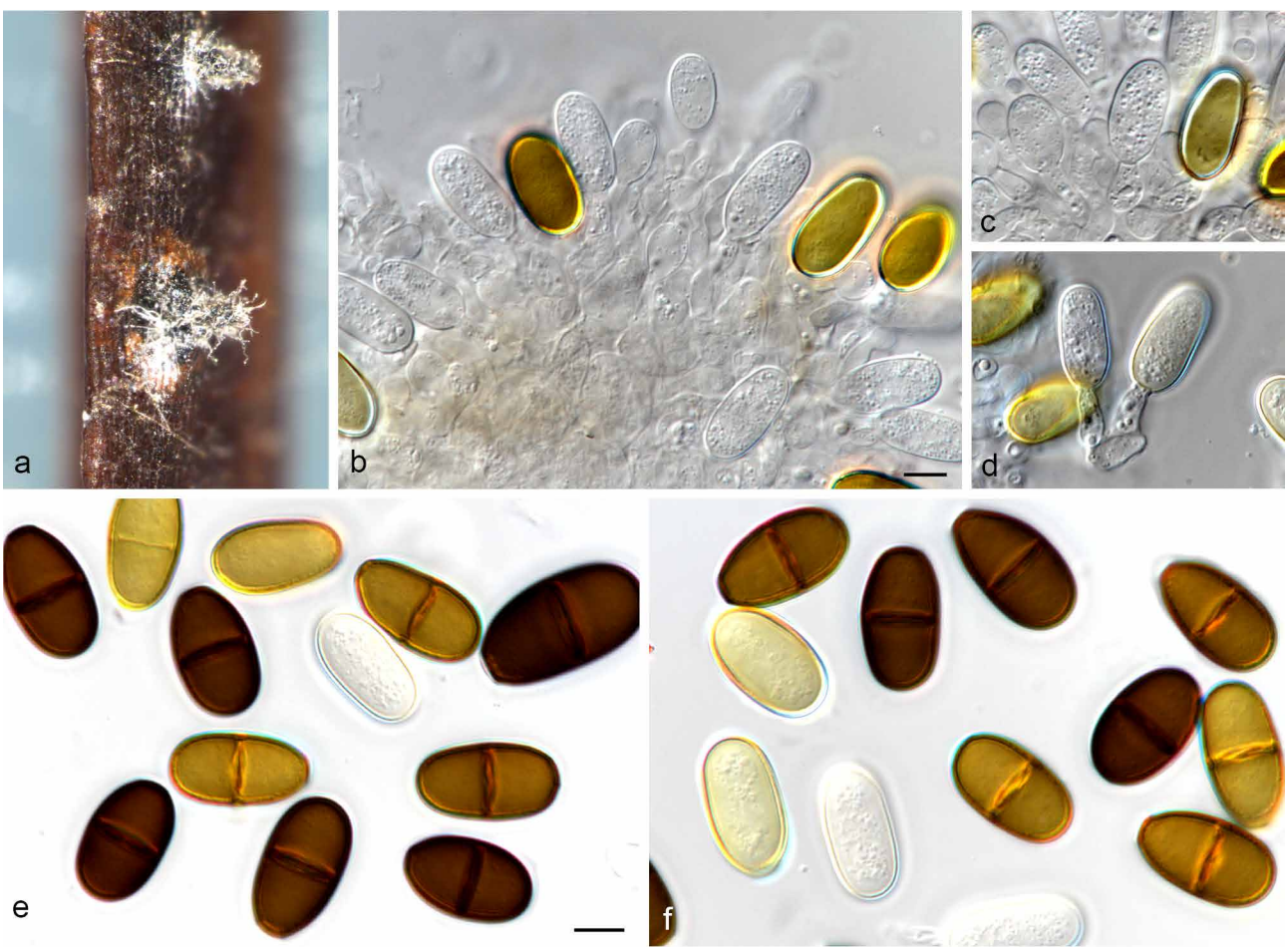

Fig. 20 *Dothiorella viticola* (CBS 112869). a. Colony sporulating on PNA; b–d. conidiogenous cells and developing conidia; e–f. conidia. — Scale bars: b, e = 10 µm, scale bar of b applies to b–d and e applies to e–f.

Isolate CBS 112869. *Conidiomata* pycnidial, produced on PNA, solitary or aggregated, superficial or semi-immersed, covered with hyphal hairs, globose papillate with a short neck, thick-walled, non-papillate with a central ostiole, up to 360 µm wide, up to 630 µm high. *Conidiophores* absent. *Conidiogenous cells* cylindrical to lageniform, discrete or integrated, holoblastic, indeterminate, proliferating at the same level giving rise to periclinal thickenings, hyaline, thin-walled, smooth, (4.5–)5.5–9 (–12.5) × (2.5–)3–4(–5) µm. *Conidia* subcylindrical to ellipsoid or ovoid, brown, 1-septate, occasionally slightly constricted at septum, moderately thick-walled, externally smooth, internally finely verruculose, ends rounded, often with a truncate base, (17.5–)19.5–21.5(–23) × (11–)12–13(–14.5) µm (av. = 20.6 × 12.9 µm, n = 50; L/W = 1.6).

Culture characteristics — Colonies on PDA have fluffy aerial mycelia with an irregular margin, with an appressed mycelial mat that is sparse to moderately dense, iron-grey to fuscous black, covering the dish after 6 d at 25 °C in the dark. Colonies on MEA have fluffy aerial mycelia with an uneven margin, with an appressed mycelial mat that is sparse to moderately dense, smoke grey to greyish sepia, covering the dish after 5 d at 25 °C in the dark. Colonies on OA have fluffy aerial mycelia with an uneven margin, with appressed mycelial mat and moderately dense, iron-grey to fuscous black, covering the dish after 5 d at 25 °C in the dark.

Isolates examined. South Africa, Western Cape province, Stellenbosch, from *Vitis vinifera*, conidiomata induced on PNA medium, 1 July 2001, *J.M. van Niekerk* (CBS H-24125, culture CBS 112869 = STE-U 5048 = CPC 5048). – Spain, Catalonia, Prov. of Tarragona, Vimbodi, from *Vitis vinifera* cv. Garnatxa negra, conidiomata induced on needles of *Pinus* sp. on water agar, 21 June 2003, *J. Luque & R. Mateu* (CBS H-24123, culture CBS 117006).

Notes — *Dothiorella westralis* is reduced to synonymy with *Do. viticola* (Fig. 3, S3A–C; parsimony analyses not shown). The ex-type culture of *Do. viticola* has the following nucleotide similarities with the ITS, *tef1* and *tub2* sequences of the ex-type of *Do. westralis*, respectively: 438/438 (100 %), 196/199 (98.99 %, including two indels caused by extra thymine nucleotides in two strings of thymines) and 410/410 (100 %).

Lasiodiplodia acaciae W. Zhang & Crous, *sp. nov*. — MycoBank MB838094; Fig. 21

Etymology. Name refers to *Acacia*, the host genus from which this fungus was collected.

Typus. Indonesia, on living leaves of *Acacia* sp., conidiomata induced on PNA medium, June 2012, *M.J. Wingfield* (holotype CBS H-24134, culture ex-type CBS 136434 = CPC 20820).

Conidiomata formed on PNA, stromatic under greyish brown mycelia, superficial or rarely semi-immersed, black, solitary, globose with a central ostiole, with or without papilla, up to 370 µm wide, 350 µm high. *Paraphyses* filiform, hyaline, tip rounded, initially aseptate, becoming up to 1–6-septate when mature, rarely branched, extending above the developing conidia layer, up to 69 µm in length, 2–5 µm wide. *Conidiophores* not observed or reduced to a supporting cell. *Conidiogenous cells* hyaline, smooth, cylindrical, slightly swollen at the base, holoblastic, proliferating percurrently to form one or two closely spaced annellations, (9–)11–17.5(–22) × (2.5–)3.5–5(–6) µm. *Conidia* initially hyaline, thick-walled, wall 2–3 µm thick, ellipsoid to ovoid with rounded or slightly tapered apex, turning brown with a median septum and longitudinal striations when mature, (21.5–)25–29.5(–31) × (11–)12–14(–15) µm (av. = 27.3 × 12.9 µm, n = 50, L/W = 2.1).

Culture characteristics — Colonies on PDA have fluffy aerial mycelia with an uneven margin, with an appressed mycelial mat that is sparse to moderately dense, a few cottony aerial mycelia reaching to the lid of the Petri dish, smoke grey, covering the dish after 4 d at 25 °C in the dark. Colonies on MEA have

Fig. 21 *Lasiodiplodia acaciae* (CBS 136434). a. Colony sporulating on PNA; b–c. conidiogenous cells; d. young, hyaline conidia; e. mature, brown, 1-septate conidia; f–g. mature conidia in two different focal planes to show the longitudinal striations. — Scale bar: b = 10 µm, scale bar of b applies to b–g.

fluffy aerial mycelia with an uneven margin, with an appressed mycelial mat that is sparse to moderately dense, a few cottony aerial mycelia reaching to the lid of the Petri dish, pale grey to smoke grey from outside region to the centre, covering the dish after 4 d at 25 °C in the dark. Colonies on OA have fluffy aerial mycelia with an uneven margin, with appressed mycelial mat and moderately dense, a few cottony aerial mycelia reaching to the lid of the Petri dish, smoke grey to mouse grey, covering the dish after 4 d at 25 °C in the dark.

Notes — *Lasiodiplodia acaciae* is phylogenetically (Fig. 4) closely related to *L. swieteniae*, *L. thailandica*, *L. hyalina*, *L. jatrophicola* and *L. iraniensis*, but can be distinguished from these species based on its morphology. Conidia of *L. acaciae* (av. = 27.3 × 12.9 µm) are smaller than those of *L. swieteniae* (av. = 30 × 13 µm) (Jayasiri et al. 2019). Conidia of *L. acaciae* (21.5–31 × 11–15 µm) are larger than these of *L. hyalina* (19–28 × 12–16 µm) (Dou et al. 2017), *L. thailandica* (20–26 × 12–16 µm) (Trakunyingcharoen et al. 2015), *L. jatrophicola* (22–26 × 14–17 µm) (Machado et al. 2014) and *L. iraniensis* (17–23 × 11–14 µm) (Abdollahzadeh et al. 2010). On ITS it is identical to *L. sterculiae* and differs one nucleotide from numerous species such as *L. hyalina*, *L. iraniensis*, *L. jatrophicola*, *L. lignicola*, *L. swieteniae*, *L. tenuiconidia*, *L. thailandica*. The Bayesian (Fig. S4A) and parsimony (data not shown) phylogenies do not resolve it from its closest sister species. On *rpb2* it differs four nucleotides from *L. hyalina* and *L. iraniensis* and *L. microconidia*. The Bayesian (Fig. S4B) and parsimony (data not shown) phylogenies placed it as a lineage distinct from the other species. On *tef1* it differs 10 nucleotides and one indel from *D. theobromae*. The Bayesian (Fig. S4C) and parsimony (data not shown) phylogenies place it as a distinct lineage not closely related to any of the included species. On *tub2* it is identical to numerous species, e.g., *L. cinnamomi*, *L. hyalina*, *L. iraniensis*, *L. pseudotheobromae*, *L. sterculiae*. The Bayesian (Fig. S4D) and parsimony (data not shown) phylogenies do not resolve it from its closest sister species.

Lasiodiplodia crassispora T.I. Burgess & P.A. Barber, Mycologia 98: 425. 2006

New synonym. Lasiodiplodia pyriformis F.J.J. van der Walt et al., Persoonia 33: 163. 2014.

Notes — *Lasiodiplodia pyriformis* is reduced to synonymy with *L. crassispora* (Fig. 4, S4A–D; parsimony analyses not shown). The ex-type culture of *L. crassispora* has the following nucleotide similarities with the sequences of the ex-type of *L. pyriformis*. On ITS, *rpb2*, *tef1* and *tub2*, respectively: 359/360 (99.72 %), 517/520 (99.42 %), 229/234 (97.86 %, including one gap) and 383/383 (100 %).

Lasiodiplodia citricola Abdollahz. et al., Persoonia 25: 4. 2010

New synonyms. *Lasiodiplodia vaccinii* Y. Zhang ter & L. Zhao, Pl. Dis. 103: 2046. 2019.

Lasiodiplodia mitidjana A. Alves et al., PLoS ONE 15 (5): e0232448 (8). 2020.

Notes — *Lasiodiplodia mitidjana* and *L. vaccinii* are reduced to synonymy with *L. citricola* (Fig. 4, S4A–D; parsimony analyses not shown). The ex-type culture of *L. citricola* has the following nucleotide similarities with the ITS, *rpb2*, *tef1* and *tub2* sequences of the ex-type of *L. mitidjana* and *L. vaccinii*, respectively: 358/358 (100 %) and 349/349 (100 %), no *rpb2* for *L. mitidjana* and 520/520 (100 %), 234/237 (98.73 %, including one gap) and 235/237 (99.16 %, including one gap), and no *tub2* for *L. mitidjana* and 356/358 (99.44 %), respectively.

Lasiodiplodia gilanensis Abdollahz. et al., Persoonia 25: 5. 2010

New synonym. Lasiodiplodia missouriana Úrbez-Torr. et al., Fungal Diversity 55: 181. 2012.

Notes — *Lasiodiplodia missouriana* is reduced to synonymy with *L. gilanensis* (Fig. 4, S4A–D; parsimony analyses not shown). The ex-type culture of *L. gilanensis* has the following nucleotide similarities with the ITS, *rpb2*, *tef1* and *tub2* sequences of the ex-type of *L. missouriana*: 355/358 (99.16 %), 518/520 (99.62 %), 241/242 (99.59 %) and 395/399 (99.00 %), respectively.

Lasiodiplodia iraniensis Abdollahz. et al. (as '*iranensis*'), Persoonia 25: 8. 2010

New synonym. Lasiodiplodia jatrophicola A.R. Machado & O.L. Pereira, Fungal Diversity 67: 239. 2014.

Notes — *Lasiodiplodia jatrophicola* is reduced to synonymy with *L. iraniensis* (Fig. 4, S4A–D; parsimony analyses not shown), which is in agreement with the findings of Rodríguez-Gálvez et al. (2017). The ex-type culture of *L. iraniensis* has the following nucleotide similarities with the ITS, *rpb2*, *tef1* and *tub2* sequences of the ex-type of *L. jatrophicola*: 357/358 (99.72 %), 472/474 (99.58 %; based on CBS 111005), 241/242 (99.59 %) and 386/387 (99.74 %), respectively.

Lasiodiplodia lignicola (Ariyaw. et al.) A.J.L. Phillips et al., Stud. Mycol. 76: 120. 2013

Basionym. Auerswaldia lignicola Ariyaw et al., Fungal Diversity 57: 161. 2012.

New synonyms. Lasiodiplodia sterculiae Tao Yang & Crous, Fung. Biol. 121: 336. 2016.

Lasiodiplodia chinensis Z.P. Dou & Y. Zhang ter, Mycosphere 8: 528. 2017.

Lasiodiplodia tenuiconidia Y. Zhang ter & S. Lin, Mycol. Progr. 18: 694. 2019.

Notes — Three *Lasiodiplodia* species are reduced to synonymy with *L. lignicola* (Fig. 4, S4A–D; parsimony analyses not shown). The ex-type culture of *L. lignicola* has the following nucleotide similarities with the sequences of the ex-types of *L. chinensis*, *L. sterculiae* and *L. tenuiconidia*. On ITS: 358/358 (100 %), 358/358 (100 %) and 358/358 (100 %), respectively. On *rpb2*: 512/520 (98.46 %), 517/520 (99.42 %) and 520/520 (100 %), respectively. On *tef1*: 235/236 (99.58 %), 234/235 (99.57 %) and 235/236 (99.58 %), respectively. On *tub2*: 362/362 (100 %), 362/362 (100 %) and no *tub2* for *L. tenuiconidia*, respectively.

Lasiodiplodia mahajangana Begoude et al., Mycol. Progr. 9: 110. 2010 — Fig. 22

New synonyms. Lasiodiplodia exigua Linald. et al., Fungal Diversity 71: 207. 2014.

Lasiodiplodia caatinguensis I.B.L. Cout. et al., Pl. Pathol. 66: 96. 2017.

Lasiodiplodia pandanicola Tibpromma & K.D. Hyde, Fungal Diversity 93: 58. 2018.

Lasiodiplodia irregularis Y. Zhang ter & S. Lin, Mycol. Progr. 18: 690. 2019.

Lasiodiplodia curvata Y. Zhang ter & S. Lin, Mycol. Progr. 18: 689. 2019.

Lasiodiplodia macroconidia Y. Zhang ter & S. Lin (as '*macroconidica*'), Mycol. Progr. 18: 692. 2019.

Isolate CBS 125266. *Conidiomata* formed on PNA, stromatic under greyish brown mycelia, superficial or rarely semi-immersed, black, solitary, globose with a central ostiole, with or without papilla, up to 560 µm wide, 1670 µm high. *Paraphyses* filiform, hyaline, tip rounded, initially aseptate, becoming up to 1–6-septate when mature, rarely branched, extending above

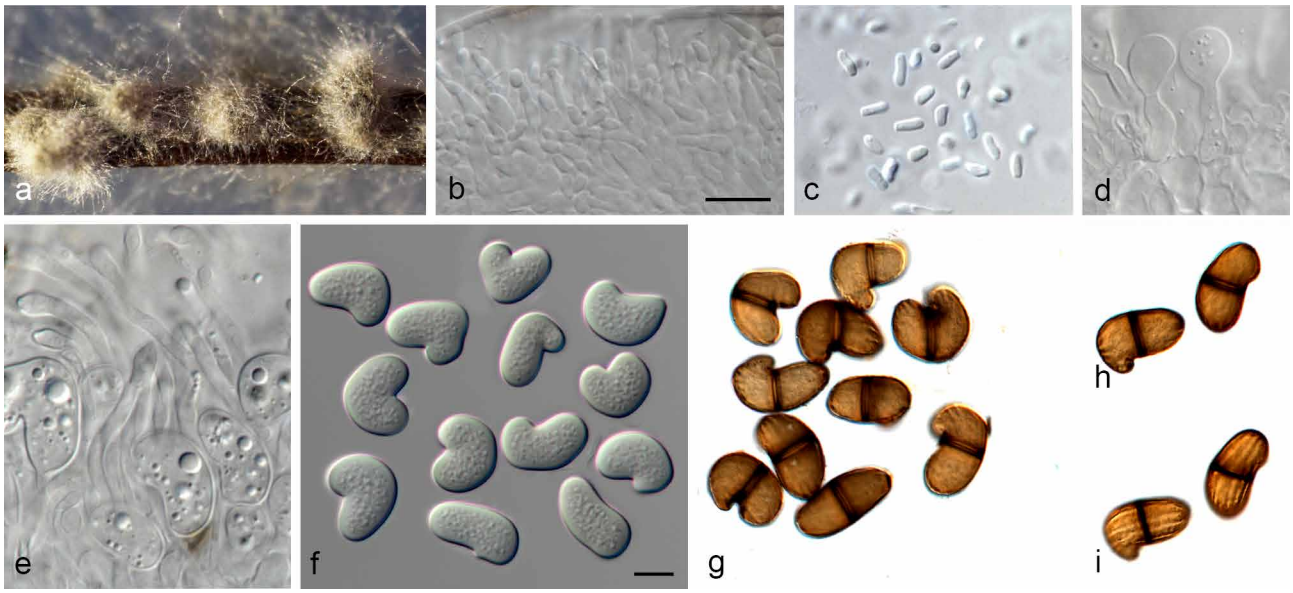

Fig. 22 *Lasiodiplodia mahajangana* (CBS 125266). a. Colony sporulating on PNA; b. spermatogenous cells; c. spermatia; d. conidiogenous cells; e. conidiogenous layer with conidia developing on conidiogenous cells between paraphyses; f. young, hyaline conidia; g. mature, brown, 1-septate conidia; h–i. mature conidia in two different focal planes to show the longitudinal striations. — Scale bars: b, f = 10 µm, scale bar of b applies to b–e and f applies to f–i.

the developing conidia layer, up to 78 µm in length, 2–4 µm wide. *Conidiophores* not observed. *Conidiogenous cells* holoblastic, hyaline, discrete, smooth thin-walled, (8–)9.5–15.5(–18.5) × (2–)2.5–3.5(–4) µm (av. = 12.7 × 2.8 µm). *Conidia* initially hyaline, thin-walled, apex deeply curved, turning brown with a median septum and longitudinal striations when mature, (17.5–)20–23(–25.5) × (10–)11–14(–15.5) µm (av. = 21.5 × 12.5 µm, n = 50; L/W = 1.7). *Spermatogenous cells* discrete or integrated, hyaline, smooth, cylindrical, proliferating via phialides with periclinal thickenings, 7–12 × 1.5–2.5 µm. *Spermatia* hyaline, smooth, aseptate, rod-shaped with rounded ends, 3–4.5 × 1–1.5 µm.

Culture characteristics — Colonies on PDA have fluffy aerial mycelia with an uneven margin, with an appressed mycelial mat that is sparse to moderately dense, a few cottony aerial mycelia reaching to the lid of the Petri dish, greyish sepia, covering the dish after 6 d at 25 °C in the dark. Colonies on MEA have fluffy aerial mycelia with an uneven margin, with an appressed mycelial mat that is sparse to moderately dense, a few cottony aerial mycelia reaching to the lid of the Petri dish, olivaceous grey, covering the dish after 5 d at 25 °C in the dark. Colonies on OA have fluffy aerial mycelia with an uneven margin, with appressed mycelial mat and moderately dense, a few cottony aerial mycelia reaching to the lid of the Petri dish, greyish sepia, covering the dish after 6 d at 25 °C in the dark.

Isolate examined. Tanzania, Ifakara, on *Terminalia sambesiaca*, conidiomata induced on PNA medium, 2010, *J. Roux* (CBS H-24132, culture CBS 125266 = CMW 26709).

Notes — Six species of *Lasiodiplodia* are reduced to synonymy with *L. mahajangana* (Fig. 4, S4A–D; parsimony analyses not shown), which is shown to have straight or curved conidia. The ex-type culture of *L. mahajangana* has the following nucleotide similarities with the sequences of the ex-types of *L. caatinguensis*, *L. curvata*, *L. exigua*, *L. irregularis*, *L. macroconidia* and *L. pandanicola*, respectively. On ITS: 357/358 (99.72 %), 357/357 (100 %), 354/358 (99.88 %), 358/358 (100 %), 353/355 (99.44 %) and 358/358 (100 %), respectively. On *rpb2*: 517/520 (99.42 %; based on CBS 190.73), 517/520 (99.42 %), 517/520 (99.42 %), 517/520 (99.42 %), 515/520 (99.04 %) and no *rpb2* for *L. pandanicola*, respectively. On *tef1*: 216/218 (99.08 %), 234/242 (96.69 %, including one indel of eight nucleotides), 234/234 (100 %), 234/234 (100 %), 216/218 (99.08 %) and 219/219 (100 %), respectively. On *tub2*: 396/399 (99.25 %), 381/384 (99.22 %), 397/399 (99.50 %), 382/384 (99.48 %), 380/384 (98.96 %) and no *tub2* for *L. pandanicola*, respectively.

Lasiodiplodia syzygii C.R. Meng et al., Biodivers. Data J. 9: e60604[7]. 2021 — Fig. 23

Conidiomata formed on PNA, stromatic under greyish brown mycelia, superficial or rarely semi-immersed, black, solitary, globose with a central ostiole, with or without papilla, up to 1070 µm wide, 890 µm high. *Paraphyses* filiform, hyaline, tip rounded, initially aseptate, becoming up to 1–6-septate when mature, rarely branched, extending above the developing conidial layer, up to 78 µm in length, 2–4 µm wide. *Conidiophores* not observed. *Conidiogenous cells* holoblastic, hyaline, discrete, smooth thin-walled, cylindrical to ampulliform, proliferating percurrently, up to (5.5–)8–14.5(–18.5) × 2.5–3.5(–4.5) µm. *Conidia* initially hyaline, thick-walled, wall 2–3 µm thick, ellipsoid to ovoid with rounded or slightly tapered apex, turning brown with a median septum and longitudinal striations when mature, (24.5–)28–32.5(–39.5) × (13–)15–17(–21) µm (av. = 30.2 × 16.1 µm, n = 50; L/W = 1.9).

Culture characteristics — Colonies on PDA have fluffy aerial mycelia with an uneven margin, with an appressed mycelial mat that is sparse to moderately dense, a few cottony aerial mycelia reaching to the lid of the Petri dish, mouse grey, covering the dish after 4 d at 25 °C in the dark. Colonies on MEA have fluffy aerial mycelia with an irregular margin, with an appressed mycelial mat that is sparse to moderately dense, a few cottony aerial mycelia reaching to the lid of the Petri dish, smoke grey, covering the dish after 4 d at 25 °C in the dark. Colonies on OA have fluffy aerial mycelia with an uneven margin, with appressed mycelial mat, white, moderately dense, a few cottony aerial mycelia reaching to the lid of the Petri dish, smoke grey to greyish sepia, covering the dish after 4 d at 25 °C in the dark.

Isolate examined. South Africa, KwaZulu-Natal province, Sodwana Bay, on dead twigs of *Syzygium cordatum*, conidiomata induced on PNA medium, 2010, *M. van Zyl* (CBS H-24136, culture CBS 120512 = CMW 14004 = BOT2619).

Notes — *Lasiodiplodia syzygii* (conidia (27–)30–32(–36) × (13–)15–17(–20) µm) was described for a species causing fruit

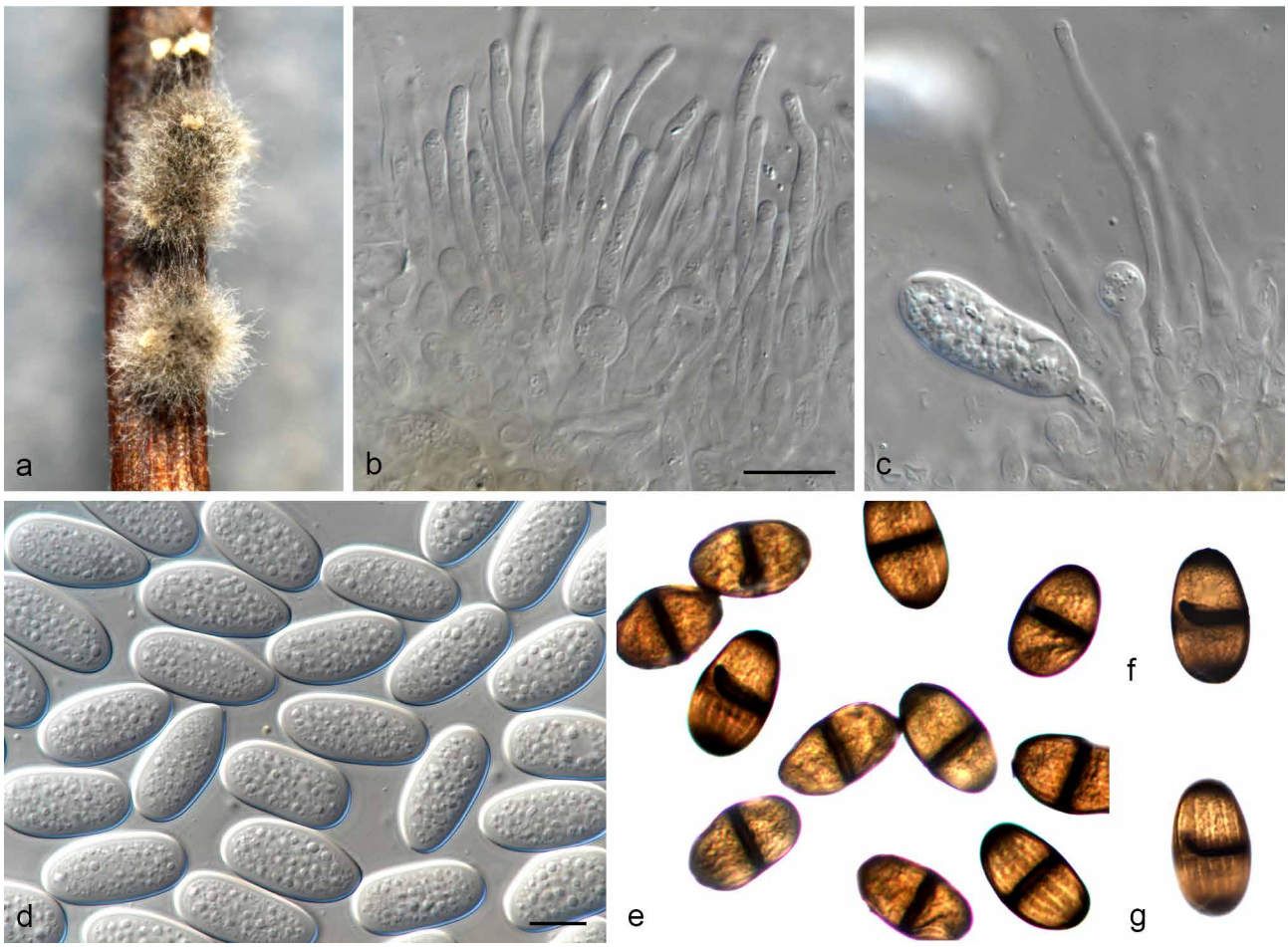

Fig. 23 *Lasiodiplodia syzygii* (CBS 120512). a. Colony sporulating on PNA; b. paraphyses; c. conidiogenous cells between paraphyses; d. young, hyaline conidia; e. mature, brown, 1-septate conidia; f–g. mature conidia in two different focal planes to show the longitudinal striations. — Scale bars: b, d = 10 µm, scale bar of b applies to b–c and d applies to d–g.

rot of *Syzygium samarangense* in Thailand (Meng et al. 2021). Interestingly, the same species was also about to be described as new in the present study, where it was found occurring on branches of *Syzygium cordatum* in South Africa. Further collections will reveal if *L. syzygii* has a wider distribution, and if it is commonly associated with species of *Syzygium*.

Lasiodiplodia syzygii is phylogenetically (Fig. 4) closely related to *L. rubropurpurea* (Burgess et al. 2006), but they can be distinguished based on their morphology. Conidia of *L. syzygii* are larger than those of *L. rubropurpurea* (24–33 × 13–17) (Burgess et al. 2006). On ITS it differs by four nucleotides from *L. rubropurpurea*. The Bayesian (Fig. S4A) and parsimony (data not shown) phylogenies presented the species on a long branch sister to *L. rubropurpurea*. The *rpb2* sequence of *L. syzygii* was not available to compare to other sequences. On *tef1* it is 93 % similar to *L. margaritacea* and *L. venezuelensis*. It represents a distinct species sister to *L. venezuelensis* (Bayesian phylogeny; Fig. S4C) or *L. rubropurpurea* (parsimony phylogeny, data not shown). On *tub2* it differs five nucleotides from *L. rubropurpurea*. The Bayesian (Fig. S4D) and parsimony (data not shown) phylogenies present the species on a long branch sister to *L. rubropurpurea*.

Lasiodiplodia thailandica Trakun. et al., Persoonia 34: 95. 2014

New synonyms. *Lasiodiplodia hyalina* Z.P. Dou & Ying Zhang, Mycosphere 8: 1016. 2017.

Lasiodiplodia swieteniae Jayasiri et al., Mycosphere 10: 143. 2019.

Notes — *Lasiodiplodia hyalina* and *L. swieteniae* are reduced to synonymy with *L. thailandica* (Fig. 4, S4A–D; parsimony analyses not shown). The ex-type culture of *L. thailandica* has the following nucleotide similarities with the sequences of the ex-types of *L. hyalina* and *L. swieteniae*. On ITS: 333/333 (100 %) and 358/358 (100 %, including one gap), respectively. On *rpb2* (based on *L. thailandica* strain BJFU DZP160123-13, GenBank KY676792.1): 520/520 (100 %) and no *rpb2* available for *L. swieteniae*, respectively. On *tef1*: 224/226 (99.12 %) and 250/250 (100 %), respectively. On *tub2* (based on *L. thailandica* strain BJFU DZP160123-13, GenBank KY676795.1): 383/384 (99.74 %) and no *tub2* available for *L. swieteniae*, respectively.

Lasiodiplodia theobromae (Pat.) Griffon & Maubl., Bull. Soc. Mycol. France 25: 57. 1909

Basionym. *Botryodiplodia theobromae* Pat., Bull. Soc. Mycol. France 8 (3): 136. 1892.

New synonym. *Lasiodiplodia laosensis* Y. Zhang ter & S. Lin, Mycol. Progr. 18: 691. 2019.

Notes — *Lasiodiplodia laosensis* is reduced to synonymy with *L. theobromae* (Fig. 4, S4A–D; parsimony analyses not shown). The ex-type culture of *L. theobromae* has the following nucleotide similarities with the sequences of the ex-type of *L. laosensis*. On ITS: 357/358 (99.72 %, including one gap), on *rpb2*: 520/520 (100 %), on *tef1*: 241/242 (99.59 %) and on *tub2*: 364/364 (100 %).

Neofusicoccum arbuti (D.F. Farr & M. Elliott) Crous et al., Stud. Mycol. 55: 248. 2006

Basionym. *Fusicoccum arbuti* D.F. Farr & M. Elliott, Mycologia 97: 731. 2005.

New synonyms. *Fusicoccum andinum* Mohali et al., Mycol. Res. 110: 408. 2006.

Neofusicoccum andinum (Mohali et al.) Mohali et al., Stud. Mycol. 55: 247. 2006.

Notes — *Neofusicoccum andinum* is reduced to synonymy with *N. arbuti* (Fig. 5, S5A–D; parsimony analyses not shown). The ex-type culture of *N. arbuti* has the following nucleotide similarities with the sequences of the ex-type of *N. andinum*. On ITS, *rpb2*, *tef1* and *tub2*: 466/471 (98.94 %), 536/537 (99.81 %), 240/241 (99.59 %) and 376/376 (100 %), respectively. *Fusicoccum arbuti* was not included in the phylogenetic tree presented by Mohali et al. (2006) and it is possible that sequences for the species were not available at that time.

Neofusicoccum luteum (Pennycook & Samuels) Crous et al., Stud. Mycol. 55: 248. 2006

Basionym. *Fusicoccum luteum* Pennycook & Samuels, Mycotaxon 24: 456. 1985.

New synonym. *Neofusicoccum mangroviorum* J.A. Osorio et al., Fung. Biol. 121: 378. 2016.

Notes — *Neofusicoccum mangroviorum* is reduced to synonymy with *N. luteum* (Fig. 5, S5A–D; parsimony analyses not shown). The ex-type culture of *N. luteum* has the following nucleotide similarities with the sequences of the ex-type of *N. mangroviorum*. On ITS, *rpb2*, *tef1* and *tub2*: 472/473 (99.79 %), 534/537 (99.44 %), 240/244 (98.36 %, including one gap) and 316/317 (99 %), respectively.

Neofusicoccum mediterraneum Crous et al., Fung. Planet, no. 11–21: 19: [2]. 2007

New synonyms. *Neofusicoccum pistaciarum* Tao Yang & Crous, Fung. Biol. 121: 338. 2016.

Neofusicoccum pistaciicola Crous, Stud. Mycol. 86: 171. 2017.

Notes — *Neofusicoccum pistaciarum* and *N. pistaciicola* are reduced to synonymy with *Neofusicoccum mediterraneum* (Fig. 5, S5A–D; parsimony analyses not shown). The ex-type culture of *N. mediterraneum* has the following nucleotide similarities with the sequences of the ex-types of *N. pistaciarum* and *N. pistaciicola*. On ITS: 468/470 (99.57 %) and 470/473 (99.37 %), respectively. On *rpb2*: 537/537 (100 %) and 537/537 (100 %), respectively. On *tef1*: 242/242 (100 %) and 242/242 (100 %), respectively. On *tub2*: 375/376 (99.73 %) and 375/376 (99.73 %), respectively.

Neofusicoccum parvum (Pennycook & Samuels) Crous et al., Stud. Mycol. 55: 248. 2006 — Fig. 24, 25

Basionym. *Fusicoccum parvum* Pennycook & Samuels, Mycotaxon 24: 455. 1985.

New synonyms. *Neofusicoccum algeriense* Berraf-Tebbel & A.J.L. Phillips, Fungal Diversity 53: 423. 2014.

Neofusicoccum italicum Dissan. & K.D. Hyde, Stud. Mycol. 86: 170. 2017.

Neofusicoccum pandanicola Tibpromma & K.D. Hyde, Fungal Diversity 93: 60. 2018.

Fig. 24 *Neofusicoccum parvum* (CBS 145997). a. Colony sporulating on PNA; b–d. conidiogenous cells and developing conidia; e–f. conidia. — Scale bar: b = 10 µm, scale bar of b applies to b–f.

Isolate CPC 35861. *Conidiomata* pycnidial, produced on PNA, solitary, globose to ovoid, dark brown to black, up to 750 µm wide, up to 690 µm high, embedded in needle tissue, semi-immersed to superficial, unilocular, with a central ostiole. *Conidiophores* reduced to conidiogenous cells. *Conidiogenous cells* holoblastic, discrete, hyaline, cylindrical, phialidic with periclinal thickening, (4.5–)5.5–11.5(–16) × (2–)2.5–3.5(–4.5) µm. *Paraphyses* not seen. *Conidia* hyaline, thin-walled, smooth with granular contents, unicellular, aseptate narrowly fusoid, base subtruncate to bluntly rounded, (11–)14–17(–20.5) × (4–)5–6(–8) µm (av. = 15.6 × 5.9 µm, n = 50; L/W = 2.6). *Spermatogenous cells* discrete or integrated, hyaline, smooth, cylindrical, producing spermatia on their tips, holoblastic or proliferating via phialides with periclinal thickening, 4–9.5 × 3.5–5.5 µm. *Spermatia* aseptate, hyaline, thin-walled, allantoid to rod-shaped, 3.5–8 × 2–4 µm, L/W = 1.9.

Culture characteristics — Colonies on PDA have fluffy aerial mycelia with an uneven margin, with an appressed mycelial mat that is sparse to moderately dense, smoke grey, a few cottony aerial mycelia reaching to the lid of the Petri dish, covering the dish after 6 d at 25 °C in the dark. Colonies on MEA have fluffy aerial mycelia with an uneven margin, with an appressed mycelial mat that is sparse to moderately dense, a few cottony aerial mycelia reaching to the lid of the Petri dish, smoke grey to greyish sepia, covering the dish after 5 d at 25 °C in the dark. Colonies on OA have fluffy aerial mycelia with an uneven margin, with appressed mycelial mat and moderately dense, a few cottony aerial mycelia reaching to the lid of the Petri dish, greyish sepia to olivaceous, covering the dish after 5 d at 25 °C in the dark.

Isolate CBS 133503. *Conidiomata* pycnidial, produced on PNA, solitary, globose to ovoid, dark brown to black, up to 390 µm wide, up to 350 µm high, embedded in needle tissue, semi-immersed to superficial, unilocular, with a central ostiole. *Conidiophores* reduced to conidiogenous cells. *Conidiogenous cells* holoblastic, discrete, hyaline, cylindrical, phialidic with periclinal thickening, (4.5–)5–7.5(–9) × (2–)2.5–3.5(–4) µm. *Paraphyses* not seen. *Conidia* hyaline, thin-walled, smooth with granular contents, aseptate, narrowly fusoid, base subtruncate to bluntly rounded, (12–)13–16(–17.5) × (4–)4.5–6.5 µm (av. = 14.5 × 5.9 µm, n = 50; L/W = 2.5).

Culture characteristics — Colonies on PDA have fluffy aerial mycelia with an irregular margin, with an appressed mycelial mat that is sparse to moderately dense, fuscous black centre surround with pale smoke grey, a few cottony aerial mycelia reaching to the lid of the Petri dish, covering the dish after 6 d at 25 °C in the dark. Colonies on MEA have fluffy aerial mycelia with an uneven margin, with an appressed mycelial mat that is sparse to moderately dense, a few cottony aerial mycelia reaching to the lid of the Petri dish, smoke to iron-grey, covering the dish after 5 d at 25 °C in the dark. Colonies on OA have fluffy aerial mycelia with an uneven margin, with appressed mycelial mat, white, moderately dense, a few cottony aerial mycelia reaching to the lid of the Petri dish, olivaceous black centre surrounded with white, covering the dish after 5 d at 25 °C in the dark.

Isolates examined. South Africa, Gauteng province, Pretoria, University of Pretoria campus, from leaves of *Aloe* sp., conidiomata induced on PNA medium, 20 June 2010, *P.W. Crous* (CBS H-24138, culture CBS 145997 = CPC 35861 = HPC 2461). – USA, California, from branch of *Persea americana*, conidiomata induced on PNA medium, 2010, *A. Eskalen* (CBS H-24142, culture CBS 133503 = UCR295).

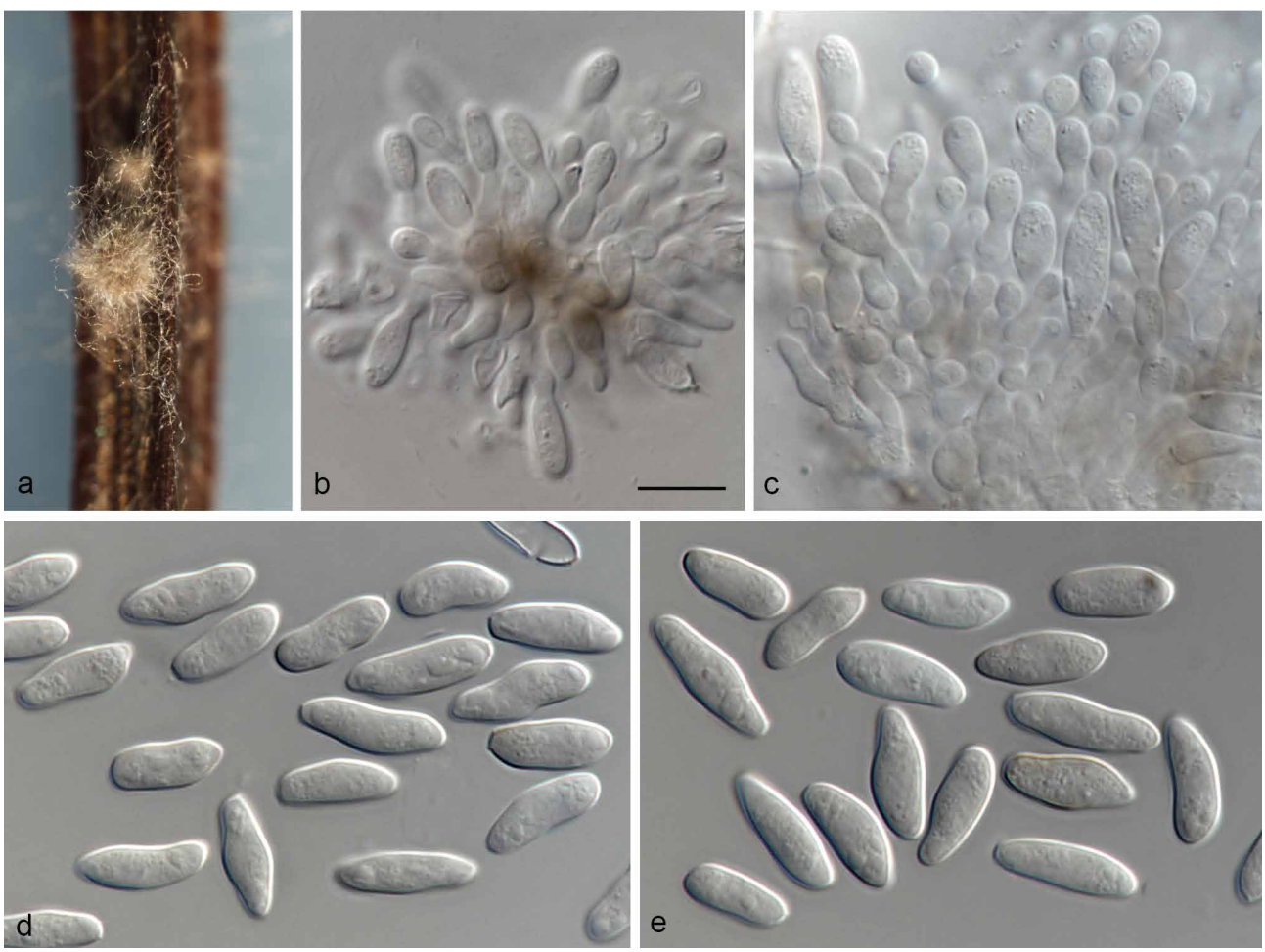

Fig. 25 *Neofusicoccum parvum* (CBS 133503). a. Colony sporulating on PNA; b–c. conidiogenous cells and developing conidia; d–e. conidia. — Scale bar: b = 10 µm, scale bar of b applies to b–e.

Notes — *Neofusicoccum algeriense, N. italicum* and *N. pandanicola* are reduced to synonymy with *N. parvum* (Fig. 6, S6A–D; parsimony analyses not shown). The synonymy of *N. algeriense* with *N. parva* was also previously suggested by Lopes et al. (2017). The ex-type culture of *N. parvum* has the following nucleotide similarities with the sequences of the ex-types of *N. algeriense*, *N. italicum* and *N. pandanicola*. On ITS: 466/470 (99.15 %), 467/470 (99.36 %) and 470/470 (100 %), respectively. On *rpb2*: 535/535 (100 %; based on CBS 117923), 535/535 (100 %; based on CBS 119937) and 535/535 (100 %; based on CBS 118832), respectively. On *tef1*: 188/191 (98.43 %), 220/220 (100 %) and 255/256 (99.61 %; based on CBS 118832), respectively. On *tub2*: 389/389 (100 %), 389/389 (100 %; based on CBS 119937) and 389/389 (100 %; based on CBS 118832), respectively. We refrain from establishing a new species for the clade (Fig. 6) containing strain CPC 35861 due to the high genetic similarity to *N. parvum*. On ITS it is identical to, or differs one nucleotide from *N. parvum,* and it differs one nucleotide from *N. pandanicola*, *N. perseae* and *N. sinoeucalypti*. On *rpb2* it is identical to *N. algeriense*, *N. italicum*, *N. pandanicola*, *N. parvum* and *N. perseae*. On *tef1* it is identical to *N. algeriense*, *N. italicum* and *N. parvum*. On *tub2* it differs one nucleotide from *N. hongkongense* and two nucleotides from *N. algeriense*. The Bayesian (Fig. S5A–D, S6A–D) and parsimony (data not shown) phylogenies do not resolve this species from the closest sister species.

Neofusicoccum podocarpi W. Zhang & Crous, *sp. nov*. — MycoBank MB838096; Fig. 26

Etymology. Name refers to *Podocarpus*, the host genus from which this fungus was collected.

Typus. South Africa, Mpumalanga province, Tweefontein, diseased twigs of *Podocarpus henkelii*, conidiomata induced on PNA medium, 8 Apr. 2008, *J. Roux & M.L. Ndove* (holotype CBS H-24140, culture ex-type CBS 131677 = CMW 35494).

Sexual morph not observed. *Conidiomata* pycnidial, produced PNA, solitary, globose to ovoid, dark brown to black, up to 890 µm wide, up to 780 µm high, embedded in needle tissue, semi-immersed to superficial, unilocular, with a central ostiole. *Conidiophores* reduced to conidiogenous cells, or forming a supporting cell. *Conidiogenous cells* holoblastic, discrete, hyaline, cylindrical, phialidic with periclinal thickening, (5–)6.5–13(–18) × (2–)2.5–4(–5) µm (av. = 9.6 × 3.2 µm). *Paraphyses* not seen. *Conidia* hyaline, thin-walled, smooth with granular contents, aseptate, aseptate narrowly fusoid, base subtruncate to bluntly rounded, (14–)17–24.5(–31) × (5–)6–6.5(–7.5) µm (av. = 20.6 × 6.2 µm, n = 50; L/W = 3.3).

Culture characteristics — Colonies on PDA have fluffy aerial mycelia with an uneven margin, with an appressed mycelial mat that is sparse to moderately dense, iron-grey, a few cottony aerial mycelia reaching to the lid of the Petri dish, covering the dish after 6 d at 25 °C in the dark. Colonies on MEA have fluffy aerial mycelia with an uneven margin, with an appressed mycelial mat that is sparse to moderately dense, a few cottony aerial mycelia reaching to the lid of the Petri dish, mouse grey to iron-grey, covering the dish after 5 d at 25 °C in the dark. Colonies on OA have fluffy aerial mycelia with an uneven margin, with appressed mycelial mat and white, moderately dense, a few cottony aerial mycelia reaching to the lid of the Petri dish, smoke grey to mouse grey, covering the dish after 5 d at 25 °C in the dark.

Fig. 26 *Neofusicoccum podocarpi* (CBS 131677). a. Colony sporulating on PNA; b–c. conidiogenous cells and developing conidia; d–e. conidia. — Scale bar: b = 10 µm, scale bar of b applies to b–e.

Notes — Based on phylogenetic analyses (Fig. 5, 6), *N. podocarpi* clusters in the *N. parvum* species complex. *Neofusicoccum podocarpi* clusters in a separate lineage compared to all other species included in the *N. parvum* species complex. On ITS it differs one nucleotide from *N. illicii*, *N. parvum* and *N. sinoeucalypti*. The Bayesian (Fig. S5A, S6A) and parsimony (data not shown) phylogenies places it in the same clade with *N. illicii* with slight separation in the parsimony analyses. On *rpb2* it differs two nucleotides from *N. batangarum* and *N. ribis*, but is identical to the *rpb2* sequence of *N. parvum* strain NpAaBR. The Bayesian (Fig. S5B, S6B) and parsimony (data not shown) phylogenies place this species separate from other species, but with the inclusion of *N. parvum* strain NpAaBR in the clade. On *tef1* it differs with one nucleotide from *N. algeriense*, *N. hongkongense*, *N. italicum* and *N. parvum*. The Bayesian (Fig. S5C, S6C) and parsimony (data not shown) phylogenies do not resolve this species from the closest sister species. On *tub2* it differs two nucleotides from *N. hongkongense*, but it is identical to the *tub2* sequence of *N. parvum* strain NpAaBR. The Bayesian (Fig. S5D, S6D) and parsimony (data not shown) phylogenies place this species separate from other species, but with the inclusion of *N. parvum* strain NpAaBR in the clade.

Neofusicoccum rapaneae W. Zhang & Crous, *sp. nov*. — MycoBank MB838097; Fig. 27

Etymology. Name refers to *Rapanea*, the host genus from which this fungus was collected.

Typus. South Africa, Eastern Cape province, Amathole, from living leaves of *Rapanea melanophloeos*, conidiomata induced on PNA medium, 25 Sept. 2017, *M.J. Wingfield* (holotype CBS H-24143, culture ex-type CBS 145973 = CPC 35287).

Sexual morph not observed. *Conidiomata* pycnidial, produced on PNA, solitary, globose to ovoid, dark brown to black, exuding conidia in a white mucoid mass, up to 370 µm wide, up to 340 µm high, embedded in needle tissue, semi-immersed to superficial, unilocular, with a central ostiole. *Conidiophores* reduced to conidiogenous cells. *Conidiogenous cells* holoblastic, discrete, hyaline, cylindrical, phialidic with periclinal thickening, (5–)7–12(–16.5) × (2.5–)3–4.5(–5.5) µm (av. = 9.4 × 3.8 µm). *Paraphyses* not seen. *Conidia* hyaline, thin-walled, smooth with granular contents, aseptate, narrowly fusoid, base subtruncate to bluntly rounded, (18–)21.5–25.5(–29) × (5–)6–7(–8) µm (av. = 23.4 × 6.5 µm, n = 50; L/W = 3.6).

Culture characteristics — Colonies on PDA have fluffy aerial mycelia with an uneven margin, with an appressed mycelial mat that is sparse to moderately dense, iron-grey to fuscous black, a few cottony aerial mycelia reaching to the lid of the Petri dish, covering the dish after 6 d at 25 °C in the dark. Colonies on MEA have fluffy aerial mycelia with an uneven margin, with an appressed mycelial mat that is sparse to moderately dense, a few cottony aerial mycelia reaching to the lid of the Petri dish, smoke grey, covering the dish after 5 d at 25 °C in the dark. Colonies on OA have fluffy aerial mycelia with an uneven margin, with appressed mycelial mat, white, moderately dense, a few cottony aerial mycelia reaching to the lid of the Petri dish, smoke grey, covering the dish after 5 d at 25 °C in the dark.

Additional isolates examined. South Africa, Eastern Cape province, Amathole, from living leaves of *Rapanea melanophloeos*, 25 Sept. 2017, *M.J. Wingfield* (culture CPC 35288); Eastern Cape province, Amathole, from leaves of *Rapanea* sp., 24 Sept. 2016, *M.J. Wingfield* (culture CPC 32578).

Notes — *Neofusicoccum rapanea* is phylogenetically (Fig. 5) closely related to *N. lumnitzerae* and *N. variabile*. The three

Fig. 27 *Neofusicoccum rapaneae* (CBS 145973). a. Colony sporulating on PNA; b–c. conidiogenous cells and developing conidia; d–e. conidia. — Scale bar: b = 10 µm, scale bar of b applies to b–e.

species can be distinguished from each other based on their conidial morphology. Conidia of *N. rapanea* (18–)21.5–25.5(–29) × (5–)6–7(–8) are larger than those of *N. lumnitzerae* (13–)17–18(–21) × (5–)6.5–7(–8.5) (Osorio et al. 2017) and *N. variabile* (14.5–24.5 × 4.5–8) (Jami et al. 2018). On ITS it differs one nucleotide from *N. stellenboschiana*, and one nucleotide and one indel from *N. luteum*. The Bayesian (Fig. S5A) and parsimony (data not shown) phylogenies support it as a distinct clade. On *rpb2* it differs four nucleotides from *N. lumnitzerae* and five nucleotides from *N. stellenboschiana*. The Bayesian (Fig. S5B) and parsimony (data not shown) phylogenies group this species as a distinct sister lineage to *N. lumnitzerae* (PP = 0.94; parsimony bootstrap 71 %). On *tef1* it differs with two nucleotides from *N. stellenboschiana* and three nucleotides from *N. australe*. The Bayesian (Fig. S5C) and parsimony (data not shown) phylogenies resolved it as distinct from its closest sister species. On *tub2* it differs three nucleotides from *N. lumnitzerae* and five nucleotides from *N. stellenboschiana*. The Bayesian (Fig. S5D) and parsimony (data not shown) phylogenies resolve it as distinct from its closest sister species, *N. lumnitzerae* and *N. variabile*.

Neofusicoccum ribis (Slippers et al.) Crous et al., Stud. Mycol. 55: 249. 2006 — Fig. 28, 29

Basionym. *Fusicoccum ribis* Slippers et al., Mycologia 96: 96. 2004.
New synonyms. *Neofusicoccum umdonicola* Pavlic et al., Mycologia 100: 644. 2008.
Neofusicoccum batangarum Begoude et al., Stud. Mycol. 76: 137. 2013.

Isolate CBS 117915. *Conidiomata* pycnidial, produced on PNA, solitary, globose to ovoid, dark brown to black, up to 350 µm wide, up to 290 µm high, embedded in needle tissue, semi-immersed to superficial, unilocular, with a central ostiole. *Conidiophores* reduced to conidiogenous cells. *Conidiogenous cells* holoblastic, discrete, hyaline, cylindrical, phialidic with periclinal thickening, (9–)10.5–15.5(–17.5) × (2–)2.5–3.5(–4.5) µm. *Paraphyses* not seen. *Conidia* hyaline, thin-walled, smooth with granular contents, aseptate, narrowly fusoid, base subtruncate to bluntly rounded, becoming 2-septate and brown before germination, (15–)16.5–19(–20) × (5–)5.5–6.5(–7) µm (av. = 17.5 × 5.9 µm, n = 50; L/W = 2.9).

Culture characteristics — Colonies on PDA have fluffy aerial mycelia with an uneven margin, with an appressed mycelial mat that is sparse to moderately dense, mouse grey to iron-grey, a few cottony aerial mycelia reaching to the lid of the Petri dish, covering the dish after 6 d at 25 °C in the dark. Colonies on MEA have fluffy aerial mycelia with an uneven margin, with an appressed mycelial mat that is sparse to moderately dense, a few cottony aerial mycelia reaching to the lid of the Petri dish, smoke grey, covering the dish after 5 d at 25 °C in the dark. Colonies on OA have fluffy aerial mycelia with an irregular margin, with appressed mycelial mat and moderately dense, a few cottony aerial mycelia reaching to the lid of the Petri dish, mouse grey, covering the dish after 5 d at 25 °C in the dark.

Isolate CBS 122553. *Conidiomata* pycnidial, produced on PNA, solitary, globose to ovoid, covered with hyphal hairs, dark brown to black, up to 350 µm wide, up to 290 µm high, embedded in needle tissue, semi-immersed to superficial, unilocular, with a central ostiole. *Conidiophores* reduced to conidiogenous cells. *Conidiogenous cells* holoblastic, discrete, hyaline, cylindrical, phialidic with periclinal thickening, (4–)5–8(–10) × 2–3(–3.5) µm. *Paraphyses* not seen. *Conidia* hyaline, thin-walled, smooth with

Fig. 28 *Neofusicoccum ribis* (CBS 117915). a. Colony sporulating on PNA; b–c. conidiogenous cells and developing conidia; d–e. conidia; f. mature conidia with 1–2 septa. — Scale bar: b = 10 µm, scale bar of b applies to b–f.

granular contents, aseptate, narrowly fusoid, base subtruncate to bluntly rounded, (15.5–)17–20(–21.5) × (4–)4.5–5(–5.5) µm (av. = 18.5 × 4.7 µm, n = 50; L/W = 3.3). *Spermatogenous cells* discrete or integrated, hyaline, smooth, cylindrical, producing spermatia on their tips, holoblastic or proliferating via phialides with periclinal thickenings, 4.5–8 × 1.5–2.5 µm. *Spermatia* unicellular, aseptate, hyaline, thin-walled, allantoid to rod-shaped, 5–8 × 2–3 µm, L/W = 2.5.

Culture characteristics — Colonies on PDA have fluffy aerial mycelia with an uneven margin, with an appressed mycelial mat that is sparse to moderately dense, mouse grey to olivaceous black, a few cottony aerial mycelia reaching to the lid of the Petri dish, covering the dish after 6 d at 25 °C in the dark. Colonies on MEA have fluffy aerial mycelia with an uneven margin, with an appressed mycelial mat that is sparse to moderately dense, a few cottony aerial mycelia reaching to the lid of the Petri dish, mouse grey to iron-grey, covering the dish after 5 d at 25 °C in the dark. Colonies on OA have fluffy aerial mycelia with an uneven margin, with appressed mycelial mat and white, moderately dense, a few cottony aerial mycelia reaching to the lid of the Petri dish, iron-grey to dark slate blue, covering the dish after 5 d at 25 °C in the dark.

Isolates examined. Panama, Colon, Bocas del Toro, from leaves *Theobroma cacao*, conidiomata induced on PNA medium, 2008, *E. Rojas* (CBS H-24141, culture CBS 122553 = PI 006). – Venezuela, Portuguesa, from *Eucalyptus urophylla*, conidiomata induced on PNA medium, 2010, *S. Mohali* (CBS H-24139, culture CBS 117915 = CMW 13355).

Notes — *Neofusicoccum batangarum* and *N. umdonicola* are reduced to synonymy with *N. ribis* (Fig. 6, S6A–D; parsimony analyses not shown). The ex-type culture of *N. ribis* has the following nucleotide similarities with the sequences of the ex-types of *N. batangarum* and *N. umdonicola*. On ITS: 469/472 (99.36 %, including one gap) and 470/471 (99.79 %), respectively. On *rpb2*: 535/535 (100 %) and 533/535 (99.63 %), respectively. On *tef1*: 254/271 (93.73 %, including an indel of 14 nt) and 253/270 (93.70 %, including an indel of 14 nt), respectively. On *tub2*: 388/389 (99.74 %) and 387/389 (99.49 %), respectively. *Neofusicoccum sinense* is a potential synonym of *N. ribis*, but as the species is at this moment based on sequences from only a single strain, we prefer to keep it separate pending the availability of sequences from more isolates. Compared to *N. ribis* similarity of ITS, *tef1* and *tub2* are: 464/473 (98.10 %, including two gaps), 251/270 (92.96 %, including an indel of 14 nt) and 386/390 (98.97 %, including one gap), respectively.

Neofusicoccum vitifusiforme (Van Niekerk & Crous) Crous et al., Stud. Mycol. 55: 249. 2006

Basionym. *Fusicoccum vitifusiforme* Van Niekerk & Crous, Mycologia 96: 793. 2004.

New synonyms. *Neofusicoccum pruni* Crous, Stud. Mycol. 86: 171. 2017.
Neofusicoccum corticosae Crous & Summerell, Stud. Mycol. 94: 197. 2019.

Notes — *Neofusicoccum corticosae* and *N. pruni* are reduced to synonymy with *N. vitifusiforme* (Fig. 5, S5A–D; parsimony analyses not shown). The ex-type culture of *N. vitifusiforme* has the following nucleotide similarities with the sequences of the ex-types of *N. corticosae* and *N. pruni*. On ITS: 472/477 (98.95 %, including an indel of four nucleotides) and 471/473 (99.58 %, including one gap), respectively. On *rpb2*: 533/537 (99.26 %) and 533/537 (99.26 %), respectively. On *tef1*: 240/240 (100 %) and no *tef1* available for *N. pruni*, respectively.

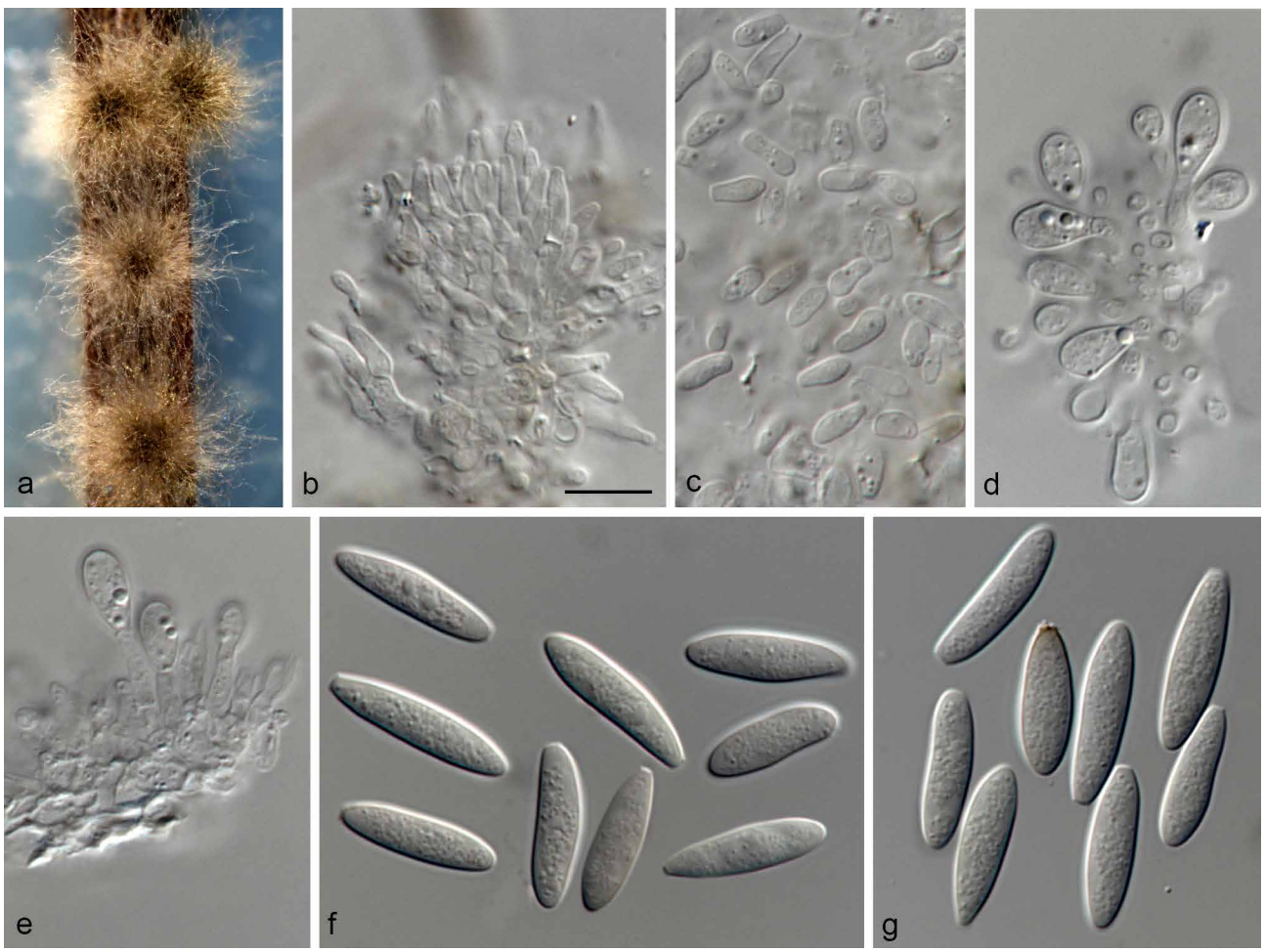

Fig. 29 *Neofusicoccum ribis* (CBS 122553). a. Colony sporulating on PNA; b. spermatogenous cells; c. spermatia; d–e. conidiogenous cells and developing conidia; f–g. conidia. — Scale bar: b = 10 µm, scale bar of b applies to b–g.

On *tub2*: 376/376 (100 %) and 374/376 (99.47 %, including one indel of two nucleotides), respectively.

Neoscytalidium dimidiatum (Penz.) Crous & Slippers, Stud. Mycol. 55: 244. 2006 — Fig. 30, 31

Basionym. *Torula dimidiata* Penz., in Saccardo, Michelia 2 (8): 466. 1887.
New synonyms. *Neoscytalidium novaehollandiae* Pavlic et al., Mycologia 100: 862. 2008.

Neoscytalidium orchidacearum S.K. Huang et al., Mycobiology 44: 83. 2016.

Isolate CBS 312.90. *Conidiomata* produced on PNA, semi-immersed or superficial, solitary or in multilocular stromata, black, with globose base, up to 430 µm wide, up to 530 µm high. *Conidiogenous cells* holoblastic, cylindrical to subcylindrical, hyaline, the first conidium produced holoblastically and subsequent conidia enteroblastically, (6.5–)7–10(–11.5) × 3–4 µm.

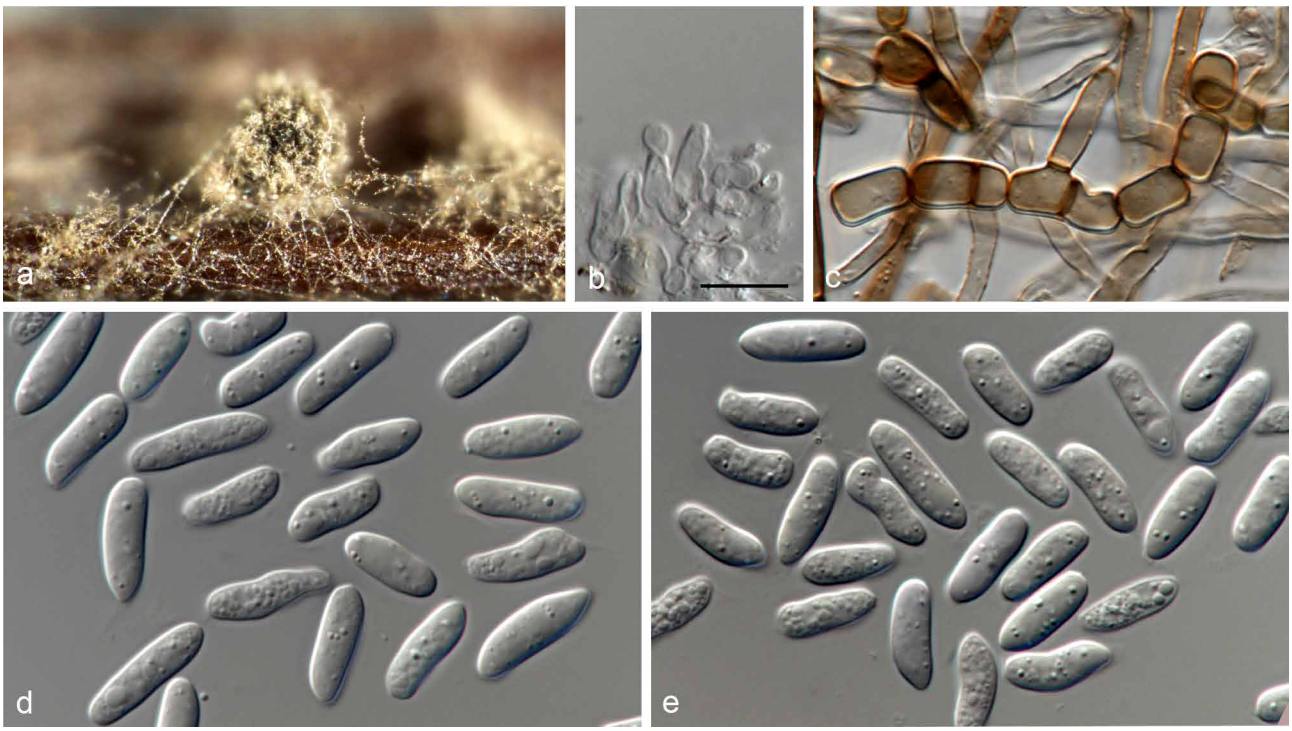

Fig. 30 *Neoscytalidium dimidiatum* (CBS 312.90). a. Colony sporulating on PNA; b. conidiogenous cells; c. scytalidium-like anamorph showing various shapes and maturity stages of arthroconidia segmenting from hyphae; d–e. fusicoccum-like pycnidial conidia. — Scale bar: b = 10 µm, scale bar of b applies to b–e.

Fig. 31 *Neoscytalidium dimidiatum* (CBS 125610). a. Colony sporulating on PNA; b. scytalidium-like asexual morph showing various shapes and maturity stages of arthroconidia segmenting from hyphae; c–d. conidiogenous cells; e–f. fusicoccum-like pycnidial conidia. — Scale bar: b = 10 µm, scale bar of b applies to b–f.

Conidia ellipsoidal to oval, apices rounded, initially hyaline, aseptate, (10.5–)12–14(–15) × (3.5–)4–5(–5.5) µm (av. = 13.1 × 4.4 µm, n = 50; L/W = 3.0). Aerial mycelium forms chains of *arthroconidia*, (3.5–)5–8(–10.5) × (2.5–)3.5–5(–6.5) µm (av. = 6.4 × 4.2 µm, n = 50; L/W = 1.5), unicellular, powdery to the touch, disarticulating, cylindrical, oblong to obtuse to doliiform, thick-walled, initially hyaline becoming cinnamon to sepia and 0–1-septate.

Culture characteristics — Colonies on PDA have fluffy aerial mycelia with entire edge, colourless to pale brown, reaching 70–75 mm diam after 7 d at 25 °C in the dark. Colonies on MEA flat with undulate edge, colourless to pale brown, reaching 70–80 mm diam after 7 d at 25 °C in the dark. Colonies on OA have fluffy aerial mycelia with an uneven margin, with appressed mycelial mat, white, moderately dense, a few cottony aerial mycelia reaching to the lid of the Petri dish, smoke grey to mouse grey, reaching the edge of the 90 mm plates after 5 d at 25 °C in the dark.

Isolate CBS 125610. *Conidiomata* produced on PNA, semi-immersed or superficial, solitary or in multilocular stromata, black, with globose base, up to 430 µm wide, up to 430 µm high. *Conidiogenous cells* holoblastic, cylindrical to subcylindrical, hyaline, the first conidium produced holoblastically and subsequent conidia enteroblastically, 8–10(–11.5) × 3–4(–4.5) µm. *Conidia* ellipsoidal to oval, apices rounded, hyaline, aseptate, (8–)10–12(–12.5) × (3.5–)4–4.5(–5) µm (av. = 11 × 4.1 µm, n = 50; L/W = 2.7). Aerial mycelium forming chains of *arthroconidia*, (4.5–)5.5–7.5(–9) × (2.5–)3–4.5(–5) µm (av. = 6.5 × 3.8 µm, n = 50; L/W = 1.7), unicellular, powdery to the touch, disarticulating, cylindrical, oblong to obtuse to doliiform, thick-walled, initially hyaline becoming cinnamon to sepia, 0–1-septate.

Culture characteristics — Colonies on PDA have fluffy aerial mycelia with an entire margin, greyish sepia to fuscous black, covering the dish after 6 d at 25 °C in the dark. Colonies on MEA have fluffy aerial mycelia with an uneven margin, with an appressed mycelial mat that is sparse to moderately dense, a few cottony aerial mycelia reaching to the lid of the Petri dish, mouse grey to iron-grey, covering the dish after 5 d at 25 °C in the dark. Colonies on OA have fluffy aerial mycelia with an uneven margin, a few cottony aerial mycelia reaching to the lid of the Petri dish, smoke grey to mouse grey, covering the dish after 5 d at 25 °C in the dark.

Isolates examined. Gabon, from human tissue, collection date unknown, *M. Kombila* (CBS H-24144, culture CBS 125610). – Netherlands, Utrecht, Wilhelmina Kinderziekenhuis, from a human blood culture of leucopene patient, conidiomata induced on PNA medium, collection date unknown, *R. Benne* (CBS H-24145, culture CBS 312.90).

Notes — *Neoscytalidium novaehollandiae* and *Ne. orchidacearum* are reduced to synonymy with *Ne. dimidiatum* (Fig. 7, S7A–D; parsimony analyses not shown). The ex-type culture of *Ne. dimidiatum* has the following nucleotide similarities with the sequences of the ex-types of *Ne. novaehollandiae* and *Ne. orchidacearum*. On ITS: 489/492 (99.39 %) and 486/492 (98.78 %), respectively. On *tef1*: 185/187 (98.93 %) and no *tef1* available for *Ne. orchidacearum*, respectively. On *tub2*: 358/358 (100 %) and no *tub2* available for *Ne. orchidacearum*, respectively.

Phaeobotryon ulmi W. Zhang & Crous, *sp. nov.* — MycoBank MB838098; Fig. 32

Etymology. Name refers to *Ulmus*, the host genus from which this fungus was collected.

Typus. Germany, near Berlin, on dead twigs of *Ulmus leavis*, 15 Feb. 2014, *R.K. Schumacher* (holotype CBS H-24146, culture ex-type CBS 138854 = CPC 24264).

Conidiomata pycnidial, produced on PNA, solitary, globose to ovoid, dark brown to black, up to 660 µm wide, up to 620 µm high, embedded in needle tissue, semi-immersed to superficial, unilocular, with a central ostiole. *Paraphyses* present, numerous, filiform, up to 55 × 2 µm (but absent when studied on PNA in culture). *Conidiogenous cells* formed from the cells lining the inner walls of the locules, hyaline, smooth, subcylindrical, (5.5–)6.5–11.5(–17) × (3–)3.5–5(–5.5) µm. *Conidia* ellipsoid to oblong, smooth to verruculose, moderately thick-walled, guttulate, ends rounded, initial hyaline with mucoid sheath, aseptate, becoming brown, 1-septate when mature, (26–)28.5–32.5(–34.5) × (15–)16.5–18.5(–20) (av. = 30.4 × 17.5 µm, n = 50, L/W = 1.7).

Culture characteristics — Colonies on PDA have fluffy aerial mycelia with an uneven margin, with an appressed mycelial mat that is sparse to moderately dense, a few cottony aerial mycelia reaching to the lid of the Petri dish, olivaceous black centre, surround with pale smoke grey, covering the dish after 4 d at 25 °C in the dark. Colonies on MEA have fluffy aerial mycelia with an uneven margin, with an appressed mycelial mat that is sparse to moderately dense, a few cottony aerial mycelia reaching to the lid of the Petri dish, smoke grey to pale grey from centre to outside region, covering the dish after 4 d at 25 °C in the dark. Colonies on OA have fluffy aerial mycelia with an uneven margin, with appressed mycelial mat, white, moderately dense, a few cottony aerial mycelia reaching to the lid of the Petri dish, iron-grey to mouse grey from centre to outside region, covering the dish after 4 d at 25 °C in the dark.

Notes — Fuckel (1870) published a treatment of the genus *Cryptospora* and amended its circumscription. Under the genus name, he emphasized that he believed he was merging fungi (asexual and sexual morphs) that belong together. Fuckel (1870) introduced the combination *Cryptospora hypodermia* and erroneously associated this name with an asexual morph that does not pertain to the lifecycle of that species. Later, Saccardo (1877) introduced the new genus *Cryptosporella* and the new combination *C. hypodermia*, also listed in Saccardo (1882: 466). However, the association with an asexual morph as proposed by Fuckel (1870) was neither cited nor included in Saccardo (1877). He did not recognize this sexual/asexual link, which is relevant regarding his later conclusion published in Saccardo (1884: 724). In the latter work, Saccardo introduced the name *Myxosporium hypodermium*, which is not a combination based on *Sphaeria hypodermia* as previously and incorrectly assumed. Rather, it constitutes and was intended to be a new species name explicitly for the asexual morph erroneously associated with *Sphaeria hypodermia* by Fuckel (1870), i.e., the latter name was not cited as 'basionym', neither directly nor indirectly. Fuckel's collections of this asexual morph, including Fungi Rhen 2002, represents syntype material, designated here as lectotype.

Botryodiplodia hypodermia (Sacc.) Petr., Repert. Spec. Nov. Regni Veg. Beih. 42: 155. 1927

Basionym. *Myxosporium hypodermium* Sacc., Syll. Fung. 3: 724. 1884.
Synonyms. *Botryosphaerostroma hypodermia* (Sacc.) Petr., Ann. Mycol. 19 (3–4): 213. 1921.
Botryodiplodia hypodermia (Sacc.) Petr., Ann. Mycol. 21 (3/4): 334. 1923.
Macrophoma ulmicola Dearn., Mycologia 9: 353. 1917. Nom. illegit., Art. 53.1.

Typus. Germany, on twigs of *Ulmus minor* (= *U. campestre*), labelled as *Myxosporium hypodermium* Sacc., lectotype designated here, MBT394966, Fuckel's exsiccatae, Fungi Rhen. 2002 (Hal).

Conidiomata immersed in the bark of slender twigs, later somewhat erumpent, diameter on average 500 µm. Stromatic base and wall composed of cells rounded to somewhat angular-irregular in outline, 6–24 µm diam, brown. *Conidiogenous cells*

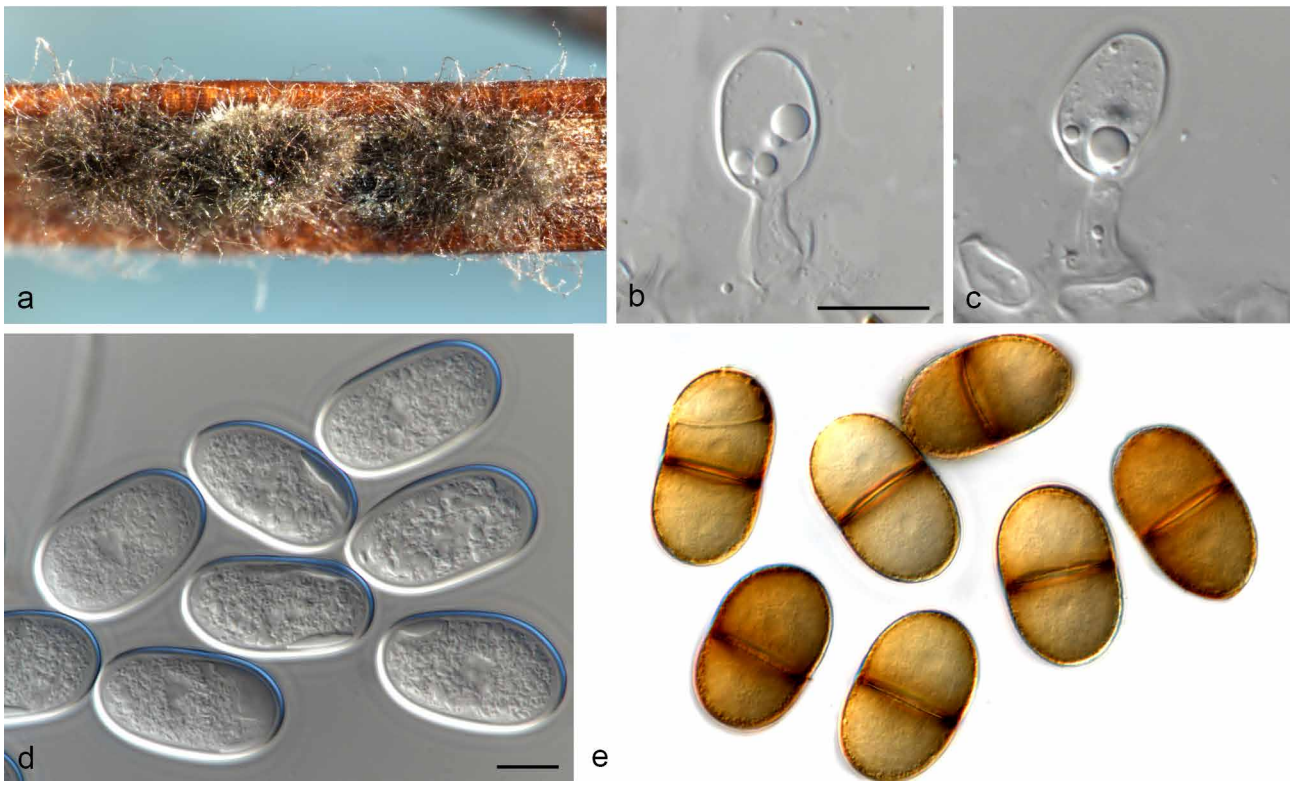

Fig. 32 *Phaeobotryon ulmi* (CBS 138854). a. Colony sporulating on PNA; b–c. conidiogenous cells; d. conidia; e. mature, brown and 1-septate conidia. — Scale bars: b, d = 10 µm, scale bar of b applies to b–c and d applies to d–e.

not maintained (not discernible), but conidiomata not formed as closed pycnidia with terminal ostiolum, erumpent conidiomata rupturing the bark, opening with a sub-circular to irregular ostiolum-like spitting, about 30–60 µm diam. *Conidia* subglobose to broad ellipsoid or ellipsoid-ovoid, end rounded, 15–28 × 10–20 µm (av. 20.3 × 15.3 µm), length/width ratio 1.0–2.2, on average 1.4, wall to 1.5 µm thick, hyaline, smooth, content mostly yellowish, greenish to faintly olivaceous.

The interpretation and application of the nomenclature of *Myxosporium hypodermium* by Petrak & Sydow (1927) is correct and should be followed. Further collections are needed, however, to determine to which genus this species should be allocated.

Botryodiplodia hypodermia (as *Myxosporium hypodermium*) was originally described from *Ulmus* twigs collected in Germany. The fungus has commonly been referred to as *Botryodiplodia hypodermia*, being associated with cankers on elm trees (Krupinsky 1981). Isolate CBS 123.30, originating from *Ulmus* in Cambridge, Massachusetts, was treated by Yang et al. (2017) as '*Phaeobotryon* sp.', but its taxonomy was not resolved. The isolate was collected in April 1930 in the USA by Christine J. Buisman, and later preserved as '*Diplodia mutila*' in the CBS culture collection. Further investigation revealed that Buisman (who studied Dutch elm disease in Europe), received a fellowship from the Radcliffe College in Cambridge, Massachusetts, allowing her to study die-back diseases of elms in the USA. In the paper that resulted from that study, Buisman (1931) isolated three species associated with different canker diseases of elms, which she identified as *Botryodiplodia malorum, B. ulmicola* and *B. hypodermia*, the latter of which caused the most prominent cankers in her inoculation experiments.

A fungus identified as *B. hypodermia* was reported as a primary pathogen of elms from North America (Krupinsky & Cunningham 1993). Bartnik et al. (2019) reported two phylogenetic lineages associated with cankers on elms, namely an American lineage (*Sphaeropsis ulmicola sensu* Zhou & Stanosz (2001), treated as *Botryodiplodia ulmicola* (conidia 15–28 × 10–20 µm) by Buisman (1931), and is possibly the fungus described as *Macrophoma ulmicola* (conidia 18–30 × 15–18 µm), nom. illegit.). Bartnik et al. (2019) also identified a European lineage, which occurs in both Europe and the USA, to which we apply the name *Phaeobotryon ulmi*.

Morphologically, *Phaeobotryon ulmi* has the largest conidia (26–34.5 × 15–20 µm) when compared to other known species of *Phaeobotryon* (Fan et al. 2015, Daranagama et al. 2016, Zhu et al. 2018). Phylogenetically (Fig. 8), *Phaeobotryon ulmi* also clustered in a separate lineage (ML bootstrap/PP = 100 %/1) to other species presently known in the genus. On ITS and LSU it clustered separate from other species of *Phaeobotryon* on a long branch in the Bayesian (Fig. S8A, S8B) and parsimony (data not shown) phylogenies. On *tef1*, it clustered as a distinct lineage amongst other species of *Phaeobotryon* in the Bayesian (Fig. S8C) and parsimony (data not shown) phylogenies.

Pseudofusicoccum kimberleyense Pavlic et al., Mycologia 100: 857. 2008 — Fig. 33

Isolate CPC 29627. *Conidiomata* pycnidial, produced on PNA, semi-immersed, solitary to aggregated, mostly aggregated, dark brown, unilocular, rarely multilocular, with globose base, up to 890 µm wide, up to 970 µm high, covered by pale brown, septate hyphal hairs, that turn dark brown with age; outer layers composed of dark brown *textura angularis*, becoming thin-walled and hyaline toward the inner region, 5–6 cells thick. *Ostiole* central, circular. *Conidiogenous cells* holoblastic, smooth, cylindrical, hyaline, the first conidium produced holoblastically and subsequent conidia enteroblastically, (4–)5–9(–10) × 3–4(–4.5) µm. *Conidia* ellipsoid to subcylindrical, straight or slightly bent, apices rounded, smooth, with fine granular content, hyaline, thin-walled, covered with a persistent mucoid sheath, aseptate, (25–)28–34.5(–37) × (6.5–)7.5–8.5(–9) µm (av. = 31.2 × 7.9 µm, n = 50; L/W = 4.0).

Culture characteristics — Colonies on PDA have fluffy aerial mycelia with an uneven margin, with appressed mycelial mat,

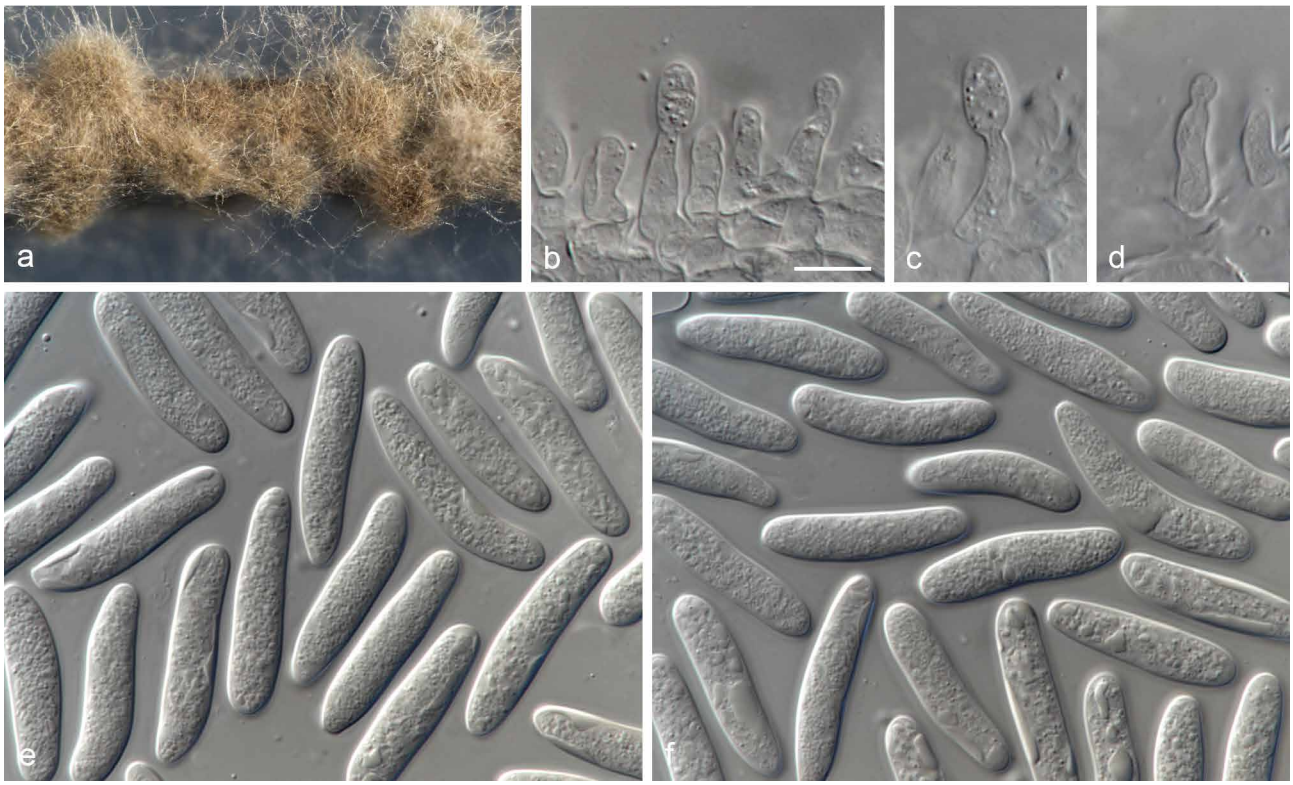

Fig. 33 *Pseudofusicoccum kimberleyense* (CBS 145974). a. Colony sporulating on PNA; b–d. conidiogenous cells; e–f. conidia (arrows denote mucoid sheaths). — Scale bar: b = 10 µm, scale bar of b applies to b–f.

white, moderately dense, a few cottony aerial mycelia reaching to the lid of the Petri dish, hazel to pale smoke grey, covering the dish after 4 d at 25 °C in the dark. Colonies on MEA have fluffy aerial mycelia with an uneven margin, with an appressed mycelial mat that is sparse to moderately dense, smoke grey in the centre, white towards the margin, covering the dish after 5 d at 25 °C in the dark. Colonies on OA have fluffy aerial mycelia with an entire edge, with appressed mycelial mat, white, moderately dense, hazel to pale smoke grey, covering the dish after 5 d at 25 °C in the dark.

Isolate examined. USA, Florida, on fruit of *Persea americana*, 16 Sept. 2015, *S. Rooney Latham* (CBS H-24147, culture CBS 145974 = CPC 29627).

Notes — *Pseudofusicoccum kimberleyense* is phylogenetically (Fig. 9) closely related to *P. calophylli*. Conidia of CPC 29627 (25–37 × 6–9 µm) are longer than those originally reported for *P. kimberleyense* (24–34 × 6.5–8.5 µm) (Pavlic et al. 2008), and longer and wider than those of *P. calophylli* (14–17 × 4–5 µm) (Jayasiri et al. 2019). On ITS CPC 29627 is identical to *P. kimberleyense* and *P. violaceum*. The Bayesian (Fig. S9A) and parsimony (data not shown) phylogenies did not resolve it from the closest sister species. On *tef1* it differs with two to three nucleotides from *P. ardesiacum*, *P. calophylli* and *P. kimberleyense*. The Bayesian phylogeny (Fig. S9B) did not resolve it well from its sister species whereas the parsimony phylogeny (data not shown) places it as a basal lineage in a clade containing *P. calophylli* and *P. kimberleyense*. On *tub2* it is identical to, or differs one nucleotide from *P. violaceum,* and it differs three nucleotides from *P. kimberleyense*. The Bayesian (Fig. S9C) and parsimony (data not shown) phylogenies do not resolve it from *P. violaceum*.

Saccharata grevilleae W. Zhang & Crous, *sp. nov*. — MycoBank MB838099; Fig. 34

Etymology. Name refers to *Grevillea*, the host genus from which this fungus was collected.

Typus. Australia, Western Australia, Kalgan, Gull Rock National Park, on living leaves of *Grevillea tripartita*, conidiomata induced on PNA medium, 22 Sept. 2015, *P.W. Crous* (holotype CBS H-24148, culture ex-type CBS 145998 = CPC 29088).

Conidiomata pycnidial, produced on PNA, solitary, globose to ovoid, dark brown to black, up to 320 µm wide, up to 410 µm high, embedded in needle tissue, semi-immersed to superficial, unilocular, with a central ostiole. *Conidiophores* hyaline, smooth, branched, below or not, subcylindrical, 1–2-septate, formed from the inner layer of the locule, 10–25 × 2.5–3.5 µm, intermingled with hyaline, aseptate paraphyses up to 50 µm long. *Conidiogenous cells* phialidic, discrete or integrated, hyaline, smooth, cylindrical, enteroblastic, proliferating percurrently with several apical annellations, (6–)7.5–12.5(–13.5) × 2.5–4 (–4.5) µm. *Conidia* hyaline, thin-walled, guttulate, aseptate, smooth, fusoid, widest in the middle of the conidium, frequently constricted at septum, with a subobtuse apex, and a truncate base, 2–3 µm diam, (18–)20.5–25(–29) × 3.5–4.5(–5) µm (av. = 22.6 × 4.0 µm, n = 50; L/W = 5.7).

Culture characteristics — Colonies on PDA flat with entire edge, pale greenish grey, with white centre, reaching 80–85 mm diam after 7 d at 25 °C in the dark. Colonies on MEA flat with ruffled lines on surface, erose or dentate edge, white, reaching 70–75 mm diam after 7 d at 25 °C in the dark. Colonies on PDA flat with fimbriate edge, colourless, reaching 42–45 mm diam after 7 d at 25 °C in the dark.

Additional isolates examined. Australia, Western Australia, Kalgan, Gull Rock National Park, on *Petrophile fastigiata*, 22 Sept. 2015, *P.W. Crous*, culture CPC 29228; idem., on *P. longifolia*, 22 Sept. 2015, *P.W. Crous*, culture CPC 29521.

Notes — *Saccharata grevilleae* is phylogenetically (Fig. 10) closely related to *S. lambertiae*, but can be distinguished based on its conidial dimensions. Conidia of *S. grevilleae* (18–29 × 3.5–5 µm) are longer and narrower than those of *S. lambertiae* (9–25 × 4–7 µm) (Crous et al. 2016). On ITS it differs with six nucleotides from *S. petrophiles* and nine nucleotides from

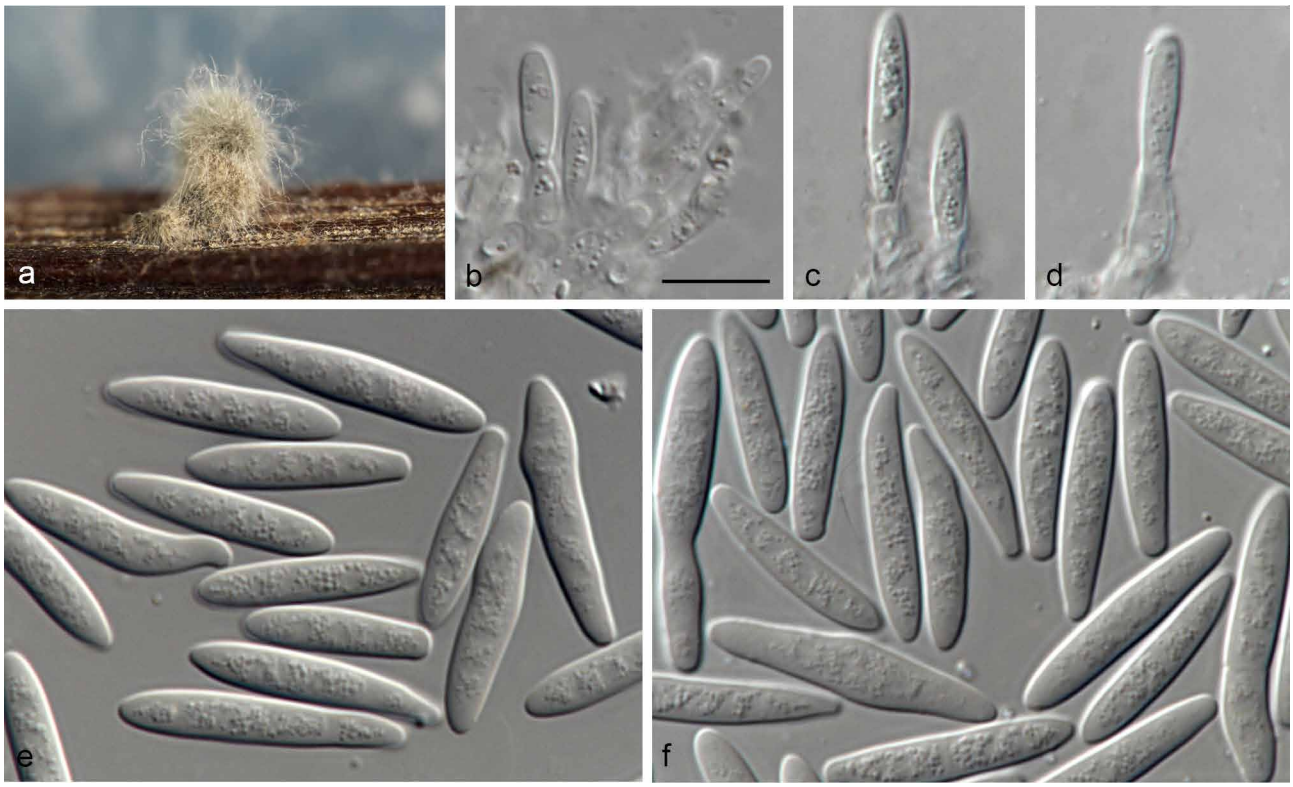

Fig. 34 *Saccharata grevilleae* (CBS 145998). a. Colony sporulating on PNA; b–d. conidiogenous cells; e–f. conidia. — Scale bar: b = 10 µm, scale bar of b applies to b–f.

S. epacridis. The Bayesian (Fig. S10A) and parsimony (data not shown) phylogenies resolve it as distinct from its closest sister species. On *rpb2* it differs eight nucleotides from *S. lambertiae* and *S. banksiae* and seven nucleotides from *S. petrophiles*. The Bayesian (Fig. S10B) and parsimony (data not shown) phylogenies resolve *S. grevilleae* as a distinct sister lineage to *S. lambertiae*. On *tef1* it differs 10 nucleotides from *S. lambertiae* and 14 nucleotides from *S. petrophiles*. The Bayesian (Fig. S10C) and parsimony (data not shown) phylogenies resolve *S. grevilleae* as a distinct sister lineage to *S. lambertiae*.

Saccharata hakeiphila W. Zhang & Crous, *sp. nov*. — MycoBank MB838100; Fig. 35

Etymology. Name refers to *Hakea*, the host genus from which this fungus was collected.

Typus. Australia, Western Australia, Albany, Stirling Range National Park, Mt Hassell walk, on living leaves of *Hakea* sp., conidiomata induced on MEA medium, 19 Sept. 2015, *P.W. Crous* (holotype CBS H-24149, culture ex-type CBS 142169 = CPC 29704).

Conidiomata on PNA pycnidial, eustromatic, up to 200–300 µm diam, immersed, subepidermal, erumpent in culture, separate, or aggregated, dark brown, unilocular, walls consisting of 6–8 layers of dark brown *textura angularis*, ostiolate. *Conidiophores* hyaline, smooth, branched, below or not, subcylindrical, 0–1-septate, formed from the inner layer of the locule, 10–25 × 2.5–3.5 µm. *Conidiogenous cells* phialidic, discrete or integrated, hyaline, smooth, cylindrical, enteroblastic, proliferating percurrently with several apical annellations, (7–)15.5–19(–25) × 3.5–5 µm. *Conidia* hyaline, thick-walled, aseptate, smooth, fusoid, widest in the middle of the conidium, with a subobtuse apex, and a truncate base, 3–4 µm diam, (26.5–)36.5–45.5(–47) × (7–)8–9.5(–10.5) µm (av. = 40.1 × 8.7 µm, n = 50; L/W = 4.6).

Culture characteristics — Colonies on PDA flat with undulate edge, dark brown, with grey margin, reaching 38–43 mm diam after 4 wk at 25 °C in the dark. Colonies on MEA flat with ruffle lines on surface, undulate edge, white, reaching 32–36 mm diam after 4 wk at 25 °C in the dark. Colonies on PDA flat with undulate edge, white with black margin, reaching 42–45 mm diam after 4 wk at 25 °C in the dark.

Notes — Isolate CBS 142169 was treated as *S. hakeae* in Crous et al. (2016). However, in the present study (Fig. 10), the combined sequence dataset (ITS, *tef1* and *rpb2*), revealed several isolates from *Hakea* closely related to *S. acaciae* (Crous et al. 2017), which was described from leaves of an *Acacia* sp. in the Morton National Park in New South Wales. *Saccharata hakeiphila* was distinguished from *S. hakeae* and *S. acaciae* based on its conidial dimensions. Conidia of *S. hakeiphila* (26.5–47 × 7–10.5 µm) are larger than those of *S. hakeae* (24–33 × 6.5–8 µm) (Crous et al. 2016) and *S. acaciae* (25–42 × 6.5–9 µm) (Crous et al. 2017). On ITS it differs in five nucleotides from *S. acaciae* and *S. hakeae*. The Bayesian (Fig. S10A) and parsimony (data not shown) phylogenies place *S. hakeiphila* on a long branch in a clade containing unresolved *S. acaciae* and *S. hakeae* sequences. On *rpb2* it differs 9–12 nucleotides from *S. acaciae* and 14–16 nucleotides from *S. hakeae*. The Bayesian (Fig. S10B) and parsimony (data not shown) phylogenies resolve it as a lineage distinct from its closest sister species. On *tef1* it is only 94 % similar to *S. acaciae* and *S. hakeae*. The Bayesian (Fig. S10C) and parsimony (data not shown) phylogenies resolve it as a lineage distinct from its closest sister species.

Saccharata hawaiiensis Tao Yang & Crous, Fung. Biol. 121: 340. 2016

New synonym. *Saccharata protearum* Crous, Stud. Mycol. 86: 197. 2017.

Notes — *Saccharata protearum* is reduced to synonymy with *S. hawaiiensis* (Fig. 10, S10A–C; parsimony analyses not shown). The ex-type culture of *S. hawaiiensis* has the following nucleotide similarities with the sequences of the ex-types of *S. protearum*. On ITS, *rpb2* and *tef1*: 505/505 (100 %), 625/627

Fig. 35 *Saccharata hakeiphila* (CBS 142169). a. Colony sporulating on PDA; b–c. conidiogenous cells; d–e. conidia. — Scale bar: b = 10 µm, scale bar of b applies to b–e.

(99 %) and 291/295 (99 %, including one indel of four nucleotides), respectively.

DISCUSSION

The *Botryosphaeriales* has recently undergone extensive revision based on the phylogenetic relationships between its various families and genera (Liu et al. 2012, Phillips et al. 2013, 2019, Slippers et al. 2013, 2017, Crous et al. 2015, Yang et al. 2017). Yet, the identity and taxonomic position of many isolates available in the CBS collection has remained unresolved. In this study, 895 isolates from the collection were incorporated into the existing multigene phylogenies for *Botryosphaeriales*. These isolates were found to reside in 13 genera isolated from 164 different hosts or substrates. Many species of *Botryosphaeriales* have in the past been described based on single strains, or supported with data for only single DNA loci. This has led to a rapid inflation of species names in the various genera of the order. Because many of the isolates treated in previous studies were deposited in the CBS collection, we were provided with a unique opportunity to reconsider their species boundaries more broadly. This was achieved by considering a larger number of isolates, and/or generating more complete multigene datasets for the various genera studied.

This study resulted in the recognition of eight new species and reduced 58 species to synonymy with existing taxa distributed across nine genera. Overall, these results emphasise the importance and impact that multigene DNA sequence data have on improving the appropriate identification of these ecologically and in some cases, commercially important fungi. The results also highlight the value of re-assessing older acquisitions in culture collections using the latest available methods and taxonomic frameworks. Importantly, critically looking at the phylogenetic trees and especially the underlying nucleotide diversity, also sets an important precedence in stabilising the taxonomy of species in *Botryosphaeriales*.

The genus *Botryosphaeria*, based on the type species *B. dothidea*, typically has ascospores that are hyaline and aseptate, but can become pale brown and septate with age, and *Fusicoccum* asexual morphs (Alves et al. 2004, Phillips et al. 2005). Given the new synonymies proposed in the present study, this genus currently includes eight accepted species (Slippers et al. 2014, Xu et al. 2015, Wijayawardene et al. 2016, Zhou et al. 2016, 2017, Liang et al. 2019) (Table 3), but many older names remain either untreated, or insufficiently known.

Diplodia, based on *D. mutila*, is probably best known for the pine-infesting species *D. sapinea*, which has a global distribution, and for which several new synonymies are introduced here. Although there are more than 1 000 names listed for this genus in databases such as Index Fungorum and MycoBank, presently 25 species are recognised based on their DNA sequence data. *Dothiorella*, based on *D. pyrenophora*, includes approximately 30 accepted species (Slippers et al. 2017), many of which have been reduced to synonymy in this study, especially those with *D. sarmentorum* and *D. viticola*. This has resulted in 25 accepted species of *Diplodia* and 29 in *Dothiorella* (Table 3).

Lasiodiplodia, based on *L. theobromae*, is a genus commonly associated with diseases of agricultural and forestry crops, and has a wide global distribution, commonly causing problems in more arid climates. Although Slippers et al. (2017) recognised more than 30 species, we have reduced several to synonymy. These are especially those with a morphology similar to *L. mahajangana, L. plurivora* and *L. theobromae*, resulting in 34 accepted species (Table 3). However, further research incorporating more informative markers remains to be conducted on *Lasiodiplodia*, which could likely lead to more additional synonymies in the future.

Neofusicoccum, based on *N. parvum*, accommodates pathogens of woody plants, many of which have an endophytic life stage (Phillips et al. 2013) and were previously accommodated in *Botryosphaeria* (Crous et al. 2006). Species of *Neofusicoccum* are morphologically similar and difficult to differentiate

Table 3 Species and their synonyms recognized in the genera treated in this study.

Barriopsis
- *Barriopsis archontophoenicis*
- *Barriopsis iraniana*
- *Barriopsis stevensiana*
- *Barriopsis tectonae*
- *Barriopsis thailandica*

Botryosphaeria
- *Botryosphaeria agaves*
- *Botryosphaeria corticis*
- *Botryosphaeria dothidea*
  - syn. *Botryosphaeria auasmontanum*
  - syn. *Botryosphaeria minutispermatia*
  - syn. *Botryosphaeria qinlingensis*
  - syn. *Botryosphaeria quercus*
  - syn. *Botryosphaeria sinensis*
  - syn. *Botryosphaeria wangensis*
- *Botryosphaeria fabicerciana*
  - syn. *Botryosphaeria fusispora*
- *Botryosphaeria kuwatsukai*
  - syn. *Botryosphaeria rosaceae*
- *Botryosphaeria qingyuanensis*
- *Botryosphaeria ramosa*
  - syn. *Botryosphaeria pseudoramosa*
- *Botryosphaeria scharifii*

Diplodia
- *Diplodia africana*
- *Diplodia afrocarpi*
- *Diplodia agrifolia*
- *Diplodia allocellula*
- *Diplodia arengae*
- *Diplodia bulgarica*
- *Diplodia corticola*
- *Diplodia crataegicola*
- *Diplodia cupressi*
- *Diplodia eriobotryicola*
- *Diplodia estuarina*
- *Diplodia fraxini*
- *Diplodia galiicola*
- *Diplodia gallae*
- *Diplodia malorum*
- *Diplodia mutila*
  - syn. *Diplodia magnoliigena*
  - syn. *Diplodia pyri*
- *Diplodia neojuniperi*
- *Diplodia olivarum*
- *Diplodia pseudoseriata*
  - syn. *Diplodia alatafructa*
  - syn. *Diplodia insularis*
  - syn. *Diplodia pseudoplatani*
- *Diplodia quercicola*
- *Diplodia quercivora*
- *Diplodia rosulata*
- *Diplodia sapinea*
  - syn. *Diplodia intermedia*
  - syn. *Diplodia italica*
  - syn. *Diplodia rosacearum*
- *Diplodia scrobiculata*
  - syn. *Diplodia guayanensis*
- *Diplodia seriata*
  - syn. *Diplodia huaxii*
- *Diplodia subglobosa*
- *Diplodia tsugae*

Dothiorella
- *Dothiorella acacicola*
- *Dothiorella acericola*
- *Dothiorella alpina*
- *Dothiorella brevicollis*
- *Dothiorella capri-amissi*
- *Dothiorella casuarini*
- *Dothiorella citricola*
- *Dothiorella diospyri*
- *Dothiorella dulcispinae*
  - syn. *Dothiorella oblonga*
- *Dothiorella iranica*
- *Dothiorella longicollis*
- *Dothiorella magnoliae*
- *Dothiorella mangifericola*
  - syn. *Dothiorella rosulata*
- *Dothiorella moneti*
- *Dothiorella plurivora*
- *Dothiorella pretoriensis*
- *Dothiorella prunicola*
- *Dothiorella rhamni*
  - syn. *Dothiorella eriobotryae*

Dothiorella (cont.)
- *Dothiorella santali*
- *Dothiorella sarmentorum*
  - syn. *Dothiorella americana*
  - syn. ?*Dothiorella californica*
  - syn. ?*Dothiorella guttulata*
  - syn. ?*Dothiorella iberica*
  - syn. *Dothiorella italica*
  - syn. ?*Dothiorella omnivora*
  - syn. ?*Dothiorella parva*
  - syn. ?*Dothiorella sempervirentis*
  - syn. ?*Dothiorella symphoricarpicola* (as '*symphoricarposicola*')
  - syn. ?*Dothiorella vidmadera*
- *Dothiorella striata*
  - syn. *Dothiorella neclivora* (as '*neclivorem*')
- *Dothiorella tectonae*
- *Dothiorella thailandica*
- *Dothiorella thripsita*
- *Dothiorella ulmacea*
- *Dothiorella uruguayensis*
- *Dothiorella vinea-gemmae*
- *Dothiorella viticola*
  - syn. *Dothiorella westralis*
- *Dothiorella yunnana*

Lasiodiplodia
- *Lasiodiplodia acaciae*
- *Lasiodiplodia aquilariae*
- *Lasiodiplodia avicenniae*
- *Lasiodiplodia brasiliensis* (as '*brasiliense*')
- *Lasiodiplodia bruguierae*
- *Lasiodiplodia cinnamomi*
- *Lasiodiplodia citricola*
  - syn. *Lasiodiplodia vaccinii*
- *Lasiodiplodia crassispora*
  - syn. *Lasiodiplodia pyriformis*
- *Lasiodiplodia euphorbiaceicola*
- *Lasiodiplodia gilanensis*
  - syn. *Lasiodiplodia missouriana*
- *Lasiodiplodia gonubiensis*
- *Lasiodiplodia gravistriata*
- *Lasiodiplodia hormozganensis*
- *Lasiodiplodia iraniensis*
  - syn. *Lasiodiplodia jatrophicola*
- *Lasiodiplodia laeliocattleyae*
  - syn. *Lasiodiplodia egyptiaca* (as '*egyptiacae*')
- *Lasiodiplodia lignicola*
  - syn. *Lasiodiplodia chinensis*
  - syn. *Lasiodiplodia sterculiae*
  - syn. *Lasiodiplodia tenuiconidia*
- *Lasiodiplodia macrospora*
- *Lasiodiplodia mahajangana*
  - syn. *Lasiodiplodia caatinguensis*
  - syn. *Lasiodiplodia curvata*
  - syn. *Lasiodiplodia exigua*
  - syn. *Lasiodiplodia irregularis*
  - syn. *Lasiodiplodia macroconidia*
  - syn. *Lasiodiplodia pandanicola*
- *Lasiodiplodia margaritacea*
- *Lasiodiplodia mediterranea*
- *Lasiodiplodia microconidia*
- *Lasiodiplodia parva*
- *Lasiodiplodia plurivora*
- *Lasiodiplodia pontae*
- *Lasiodiplodia pseudotheobromae*
- *Lasiodiplodia rubropurpurea*
- *Lasiodiplodia subglobosa*
- *Lasiodiplodia syzygii*
- *Lasiodiplodia thailandica*
  - syn. *Lasiodiplodia hyalina*
  - syn. *Lasiodiplodia swieteniae*
- *Lasiodiplodia theobromae*
  - syn. *Lasiodiplodia laosensis*
- *Lasiodiplodia tropica*
- *Lasiodiplodia venezuelensis*
- *Lasiodiplodia viticola*
- *Lasiodiplodia vitis*

Neofusicoccum
- *Neofusicoccum arbuti*
  - syn. *Neofusicoccum andinum*
- *Neofusicoccum australe*
- *Neofusicoccum braziliense*
- *Neofusicoccum buxi*
- *Neofusicoccum cordaticola*
- *Neofusicoccum cryptoaustrale*

Neofusicoccum (cont.)
- *Neofusicoccum eucalypticola*
- *Neofusicoccum eucalyptorum*
- *Neofusicoccum euphorbiaceicola*
- *Neofusicoccum grevilleae*
- *Neofusicoccum hellenicum*
- *Neofusicoccum hongkongensis*
- *Neofusicoccum ilicii*
- *Neofusicoccum kwambonambiense*
- *Neofusicoccum lumnitzerae*
- *Neofusicoccum luteum*
  - syn. *Neofusicoccum mangroviorum*
- *Neofusicoccum macroclavatum*
- *Neofusicoccum mangiferae*
- *Neofusicoccum mediterraneum*
  - syn. *Neofusicoccum pistaciarum*
  - syn. *Neofusicoccum pistaciicola*
- *Neofusicoccum microconidium*
- *Neofusicoccum nonquaesitum*
- *Neofusicoccum occulatum*
- *Neofusicoccum parvum*
  - syn. *Neofusicoccum algeriense*
  - syn. *Neofusicoccum italicum*
  - syn. *Neofusicoccum pandanicola*
- *Neofusicoccum pennatisporum*
- *Neofusicoccum pistaciae*
- *Neofusicoccum podocarpi*
- *Neofusicoccum protearum*
- *Neofusicoccum rapaneae*
- *Neofusicoccum ribis*
  - syn. *Neofusicoccum batangarum*
  - syn. *Neofusicoccum umdonicola*
- *Neofusicoccum sinense*
- *Neofusicoccum sinoeucalypti*
- *Neofusicoccum stellenboschiana*
- *Neofusicoccum terminaliae*
- *Neofusicoccum ursorum*
- *Neofusicoccum viticlavatum*
- *Neofusicoccum vitifusiforme*
  - syn. *Neofusicoccum corticosae*
  - syn. *Neofusicoccum pruni*

Neoscytalidium
- *Neoscytalidium dimidiatum*
  - syn. *Neoscytalidium novaehollandiae*
  - syn. *Neoscytalidium orchidacearum*

Phaeobotryon
- *Phaeobotryon cupressi*
- *Phaeobotryon mamane*
- *Phaeobotryon negundinis*
- *Phaeobotryon rhoinum*
- *Phaeobotryon rhois*
- *Phaeobotryon ulmi*

Pseudofusicoccum
- *Pseudofusicoccum adansoniae*
- *Pseudofusicoccum ardesiacum*
- *Pseudofusicoccum artocarpi*
- *Pseudofusicoccum kimberleyense*
- *Pseudofusicoccum olivaceum*
- *Pseudofusicoccum stromaticum*
- *Pseudofusicoccum violaceum*

Saccharata
- *Saccharata acaciae*
- *Saccharata banksiae*
- *Saccharata capensis*
- *Saccharata daviesiae*
- *Saccharata epacridis*
- *Saccharata eucalypti*
- *Saccharata eucalyptorum*
- *Saccharata grevilleae*
- *Saccharata hakeae*
- *Saccharata hakeicola*
- *Saccharata hakeigena*
- *Saccharata hakeiphila*
- *Saccharata hawaiiensis*
  - syn. *Saccharata protearum*
- *Saccharata intermedia*
- *Saccharata kirstenboschensis*
- *Saccharata lambertiae*
- *Saccharata leucospermi*
- *Saccharata petrophiles*
- *Saccharata petrophilicola*
- *Saccharata proteae*

from each other using these characteristics, and presently more than 30 species are recognised in the genus (Slippers et al. 2017). More than 200 *Neofusicoccum* strains were considered in the present study applying a multigene ITS-*tef1*-*tub2*-*rpb2* dataset. The resulting phylogeny presented a polytomy in the *N. parvum*/*N. ribis* species complex. Ten cryptic species have been described in this complex (Pavlic et al. 2009, Begoude et al. 2010, Sakalidis et al. 2013, Slippers et al. 2017), several of which are reduced to synonymy here (Fig. 6). An addition, two species, *N. podocarpi* and *N. rapaneae* are newly introduced, leading to 37 accepted species (Table 3).

Phaeobotryon, based on *P. cercidis*, presently accommodates seven species. Of these, *P. ulmi* has recently been described as a canker pathogen of *Ulmus* occurring in Europe and the USA, having frequently been confused in older literature as *Botryodiplodia hypodermia*. *Pseudofusicoccum*, based on *P. stromaticum*, presently includes nine accepted species. Species in the genus mostly occur in tropical or subtropical parts of the world, and are commonly isolated as endophytes from woody plants. *Saccharata*, based on *S. proteae*, is a genus associated with twigs and leaves of woody plants that occur in the Southern Hemisphere. Presently 20 species are recognised in the genus, with two new taxa, *S. grevilleae* and *S. hakeiphila* described in this study.

The majority of members in *Botryosphaeriales* considered in this study are plant-associated fungi. Only a few species have been reported from other substrates and these for example include *Lasiodiplodia parva* (CBS 456.78 and CBS 494.78) from soil (Alves et al. 2008), *Lasiodiplodia theobromae* (CBS 139728) from a human knee, *L. hormozganensis* (CBS 133510) from a human eye, *Neoscytalidium dimidiatum* (CBS 137.77, CBS 312.90) from cow and human blood and (CBS 125610) from human tissue. The tree canker pathogen *Neoscytalidium* (Polizzi et al. 2011) is also known to cause chronic dermatomycosis and onychomycosis in humans, mainly involving foot infections. There is no established duration of therapy for this disease, but patients that survive generally require surgical intervention along with antifungal therapy (Dionne et al. 2015). In the present study, *Neoscytalidium* is reduced to a single species, *N. dimidiatum*.

A significant increase in the number of species of *Botryosphaeriales* recognised in recent phylogenetic studies, shows clearly that using morphological data for species identification in this order is becoming increasingly difficult. This problem was highlighted in studies by Slippers et al. (2014, 2017) who also provided the argument that examination of dried herbarium specimens has little value when describing new taxa in the order. Furthermore, phylogenetic inference is revealing cryptic species complexes that cannot be distinguished based on morphology alone (Pavlic et al. 2009, Sakalidis et al. 2011). In this regard, Phillips et al. (2013) recommended that at least two loci (ITS and *tef1*) are used for species separation in the *Botryosphaeriaceae*, while data for the *tub2*, *rpb2* regions and other loci have subsequently been shown as useful to separate cryptic species (Li et al. 2018). However, in the present study we have found the vast majority of species to be based on *tef1* only. Care should also be taken when interpreting phylogenetic trees, as seemingly clear lineages in the phylogenetic trees might actually be based on very minute differences and then even a small number of errors in the sequence or alignment might result in a lineage wrongly being described as new. Therefore it is essential to always check the alignment and sequence quality for species that belong to complexes where interspecific variation is low.

Sequence data for the ITS, *tef1* and *tub2* regions are widely used to distinguish species of *Botryosphaeria*, *Diplodia*, *Dothiorella* and *Pseudofusicoccum* (Phillips et al. 2013, Chen et al. 2015, Linaldeddu et al. 2015, Coutinho et al. 2017, Yang et al. 2017), while ITS, LSU, *tef1*, *tub2* and *rpb2* have been used for species identification in *Neofusicoccum*, *Lasiodiplodia*, *Saccharata*, *Phaeobotryon* and *Neoscytalidium* (Sakalidis et al. 2011, Cruywagen et al. 2017, Dou et al. 2017, Osorio et al. 2017, Yang et al. 2017). In the present study ITS, *tef1*, *tub2*, LSU and *rpb2* sequences were generated to identify and distinguish five new species of *Botryosphaeriales* (Table S1). However, comparisons of sequences for closely related species raises the question of whether phylogenetic species are being recognised based on only minute differences. In that regard, there is a danger that species names are being provided for genotypes rather than for species that represent biologically discrete entities. Such species boundaries will need to be considered using a population genetics approach.

Wherever possible in this study, we have built on the framework of previously published data. Genetic variation presented in the phylogenetic trees in those studies have also been taken into consideration when deciding on whether novel species should be introduced or not. Distinct nucleotide differences in two or more gene regions were present for the species newly described in this study. Where species have been reduced to synonymy, details regarding the nucleotide differences have been provided in the notes and are also outlined in the supplementary individual gene trees, which together with comparisons of pairwise and blast2-based nucleotide similarities proved crucial to evaluate the status of new and established species names.

Acknowledgements We are grateful to Arien van Iperen (cultures), as well as Uwe Braun and Konstanze Bensch for helping to clarify the nomenclature of *Myxosporium hypodermium* Sacc. Michael J. Wingfield and Bernard Slippers (FABI, University of Pretoria, South Africa) are also thanked for numerous discussions about species hypotheses in the *Botryosphaeriales*. Alan J.L. Phillips acknowledges the support from UIDB/04046/2020 and UIDP/04046/2020 Centre grants from FCT, Portugal (to BioISI). Wu Zhang acknowledges the support fromThe Overseas Scholarship Program for Elite Young and Middle-aged Teachers of Lingnan Normal University.

REFERENCES

Abdollahzadeh J, Javadi A, Mohammadi Goltapeh E, et al. 2010. Phylogeny and morphology of four new species of Lasiodiplodia from Iran. Persoonia 25: 1–10.

Alves A, Correia A, Luque J, et al. 2004. Botryosphaeria corticola, sp. nov. on Quercus species, with notes and description of Botryosphaeria stevensii and its anamorph, Diplodia mutila. Mycologia 96: 598–613.

Alves A, Crous PW, Correia A, et al. 2008. Morphological and molecular data reveal cryptic speciation in Lasiodiplodia theobromae. Fungal Diversity 28: 1–13.

Bartnik C, Boroń P, Michalcewicz J, et al. 2019. The first record of Botryodiplodia canker in Poland. Forest Pathology 49: e12528.

Begoude BAD, Slippers B, Wingfield MJ, et al. 2010. Botryosphaeriaceae associated with Terminalia catappa in Cameroon, South Africa and Madagascar. Mycological Progress 9: 101–123.

Braun U, Nakashima C, Crous PW, et al. 2018. Phylogeny and taxonomy of the genus Tubakia s. lat. Fungal Systematics and Evolution 1: 41–99.

Buisman C. 1931. Three species of Botryodiplodia (Sacc.) on elm trees in the United States. Journal of the Arnold Arboretum 12: 289–296.

Burgess TI, Barber PA, Mohali S, et al. 2006. Three new Lasiodiplodia spp. from the tropics, recognized based on DNA sequence comparisons and morphology. Mycologia 98: 423–435.

Carbone I, Kohn LM. 1999. A method for designing primer sets for speciation studies in filamentous ascomycetes. Mycologia 91: 553–556.

Chen SF, Li GQ, Liu FF, et al. 2015. Novel species of Botryosphaeriaceae associated with shoot blight of pistachio. Mycologia 107: 780–792.

Coutinho IBL, Freire FCO, Lima CS, et al. 2017. Diversity of genus Lasiodiplodia associated with perennial tropical fruit plants in northeastern Brazil. Plant Pathology 66: 90–104.

Crous PW, Muller M, Sánchez RM, et al. 2015. Resolving Tiarosporella spp. allied to Botryosphaeriaceae and Phacidiaceae. Phytotaxa 202: 73–93.

Crous PW, Slippers B, Wingfield MJ, et al. 2006. Phylogenetic lineages in the Botryosphaeriaceae. Studies in Mycology 55: 235–253.
Crous PW, Verkley GJM, Groenewald JZ, et al. 2019. Fungal Biodiversity. Westerdijk Laboratory Manual Series 1: 1–425. Westerdijk Fungal Biodiversity Institute, Utrecht, Netherlands.
Crous PW, Wingfield MJ, Burgess TI, et al. 2016. Fungal Planet description sheets: 469–557. Persoonia 37: 218–403.
Crous PW, Wingfield MJ, Burgess TI, et al. 2017. Fungal Planet description sheets: 625–715. Persoonia 39: 270–467.
Crous PW, Wingfield MJ, Guarro J, et al. 2013. Fungal Planet description sheets: 154–213. Persoonia 31: 188–296.
Cruywagen EM, Slippers B, Roux J, et al. 2017. Phylogenetic species recognition and hybridisation in Lasiodiplodia: A case study on species from baobabs. Fungal Biology 121: 420–436.
Daranagama D, Thambugala K, Campino B, et al. 2016. Phaeobotryon negundinis sp. nov. (Botryosphaeriales) from Russia. Mycosphere 7: 933–941.
De Hoog GS, Guarro J, Gené J, et al. 2000. Atlas of Clinical Fungi, 2nd edn. Centraalbureau voor Schimmelcultures/Universitat Rovira i Virgili, Utrecht/Reus.
Denman S, Crous PW, Taylor JE, et al. 2000. An overview of the taxonomic history of Botryosphaeria and a re-evaluation of its anamorphs based on morphology and ITS rDNA phylogeny. Studies in Mycology 45: 129–140.
Dionne B, Neff L, Lee SA, et al. 2015. Pulmonary fungal infection caused by Neoscytalidium dimidiatum. Journal of Clinical Microbiology 53: 2381–2384.
Dou ZP, He W, Zang Y. 2017. Does morphology matter in taxonomy of Lasiodiplodia? An answer from Lasiodiplodia hyalina sp. nov. Mycosphere 8: 1014–1027.
Fan XL, Hyde KD, Liu JK, et al. 2015. Multigene phylogeny and morphology reveal Phaeobotryon rhois sp. nov. (Botryosphaeriales, Ascomycota). Phytotaxa 205: 90–98.
Fuckel L. 1870. Symbolae mycologicae. Beiträge zur Kenntniss der Rheinischen Pilze. Jahrbücher des Nassauischen Vereins für Naturkunde 23–24: 1–459.
Glass NL, Donaldson GC. 1995. Development of primer sets designed for use with the PCR to amplify conserved genes from filamentous ascomycetes. Applied and Environmental Microbiology 61: 1323–1330.
González-Domínguez E, Alves A, León M, et al. 2017. Characterization of Botryosphaeriaceae species associated with diseased loquat (Eriobotrya japonica) in Spain. Plant Pathology 66: 77–89.
Huelsenbeck JP, Ronquist F. 2001. MrBayes: Bayesian inference of phylogeny Bioinformatics 17: 754–755.
Jami F, Marincowitz S, Slippers B, et al. 2018. New Botryosphaeriales on native red milkwood (Mimusops caffra). Australasian Plant Pathology 47: 475–484.
Jami F, Slippers B, Wingfield MJ, et al. 2012. Five new species of the Botryosphaeriaceae from Acacia karroo in South Africa. Cryptogamie, Mycologie 33: 245–266.
Jayasiri SC, Hyde KD, Jones EBG, et al. 2019. Diversity, morphology and molecular phylogeny of Dothideomycetes on decaying wild seed pods and fruits. Mycosphere 10: 1–186.
Katoh K, Standley DM. 2013. MAFFT Multiple sequence alignment software version 7: improvements in performance and usability. Molecular Biology and Evolution 30: 772–780.
Krupinsky JM. 1981. Botryodiplodia hypodermia and Tubercularia ulmea in cankers on Siberian elm in northern great plains windbreaks. Plant Disease 65: 677–678.
Krupinsky JM, Cunningham RA. 1993. Response of Siberian elm to inoculations with Sphaeropsis ulmicola. Plant Disease 77: 678–681.
Kumar S, Stecher G, Tamura K. 2016. MEGA7: Molecular Evolutionary Genetics Analysis version 7.0 for bigger datasets. Molecular Biology and Evolution 33: 1870–1874.
Lawrence DP, Peduto Hand F, Gubler WD, et al. 2017. Botryosphaeriaceae species associated with dieback and canker disease of bay laurel in northern California with the description of Dothiorella californica sp. nov. Fungal Biology 121: 347–360.
Li GQ, Liu FF, Li JQ, et al. 2018. Botryosphaeriaceae from Eucalyptus plantations and adjacent plants in China. Persoonia 40: 63–95.
Liang LY, Jiang N, Chen WY, et al. 2019. Botryosphaeria qinlingensis sp. nov. causing oak frogeye leaf spot in China. Mycotaxon 134: 463–473.
Linaldeddu BT, Alves A, Phillips AJL. 2016a. Sardiniella urbana gen. et sp. nov., a new member of the Botryosphaeriaceae isolated from declining Celtis australis trees in streetscapes. Mycosphere 7: 893–905.
Linaldeddu BT, Dedda A, Scanu B, et al. 2015. Diversity of Botryosphaeriaceae species associated with grapevine and other woody hosts in Italy, Algeria and Tunisia, with descriptions of Lasiodiplodia exigua and Lasiodiplodia mediterranea sp. nov. Fungal Diversity 71: 201–214.
Linaldeddu BT, Maddau L, Franceschini A, et al. 2016b. Botryosphaeriaceae species associated with lentisk dieback in Italy and description of Diplodia insularis sp. nov. Mycosphere 7: 962–977.
Liu JK, Phookamsak R, Doilom M, et al. 2012. Towards a natural classification of Botryosphaeriales. Fungal Diversity 57: 149–210.
Liu YJ, Whelen S, Hall BD. 1999. Phylogenetic relationships among ascomycetes: evidence from an RNA polymerase II subunit. Molecular Biology and Evolution 16: 1799–1808.
Lopes A, Phillips AJL, Alves A. 2017. Mating type genes in the genus Neofusicoccum: Mating strategies and usefulness in species delimitation. Fungal Biology 121: 394–404.
Machado AR, Pinho DB, Pereira OL. 2014. Phylogeny, identification and pathogenicity of the Botryosphaeriaceae associated with collar and root rot of the biofuel plant Jatropha curcas in Brazil, with a description of new species of Lasiodiplodia. Fungal Diversity 67: 231–247.
Meng C-R, Zhang Q, Yang Z-F, et al. 2021. Lasiodiplodia syzygii sp. nov. (Botryosphaeriaceae) causing post-harvest water-soaked brown lesions on Syzygium samarangense in Chiang Rai, Thailand. Biodiversity Data Journal 9: e60604.
Miller MA, Pfeiffer W, Schwartz T. 2012. The CIPRES science gateway: enabling high-impact science for phylogenetics researchers with limited resources. Paper presented at: Proceedings of the 1st Conference of the Extreme Science and Engineering Discovery Environment: Bridging from the extreme to the campus and beyond (ACM).
Minnis A, Kennedy A, Grenier D, et al. 2012. Phylogeny and taxonomic revision of the Planistromellaceae including its coelomycetous anamorphs: contributions towards a monograph of the genus Kellermania. Persoonia 29: 11–28.
Mohali S, Slippers B, Wingfield MJ. 2006. Two new Fusicoccum species from Acacia and Eucalyptus in Venezuela, based on morphology and DNA sequence data. Mycological Research 110: 405–413.
Mohali S, Slippers B, Wingfield MJ. 2007. Identification of Botryosphaeriaceae from Eucalyptus, Acacia and Pinus in Venezuela. Fungal Diversity 25: 103–125.
Nylander JAA. 2004. MrModeltest v2. Program distributed by the author. Evolutionary Biology Centre, Uppsala University, Sweden.
Osorio JA, Crous CJ, De Beer ZW, et al. 2017. Endophytic Botryosphaeriaceae, including five new species, associated with mangrove trees in South Africa. Fungal Biology 121: 361–393.
Pavlic D, Slippers B, Coutinho TA, et al. 2009. Multiple gene genealogies and phenotypic data reveal cryptic species of the Botryosphaeriaceae: a case study on the Neofusicoccum parvum/N. ribis complex. Molecular Phylogenetics and Evolution 51: 259–268.
Pavlic D, Wingfield MJ, Barber P, et al. 2008. Seven new species of the Botryosphaeriaceae from baobab and other native trees in Western Australia. Mycologia 100: 851–866.
Petrak F, Sydow H. 1927. Die Gattungen der Pyrenomyzeten, Sphaeropsideen und Melanconieen. 1. Die phaeosporen Sphaeropsideen und die Gattung Macrophoma. Repertorium Specierum Novarum Regni Vegetabilis Beihefte 42: 1–551.
Phillips AJL, Alves A, Abdollahzadeh J, et al. 2013. The Botryosphaeriaceae: genera and species known from culture. Studies in Mycology 76: 51–167.
Phillips AJL, Alves A, Correia ACM, et al. 2005. Two new species of Botryosphaeria with brown, 1-septate ascospores and Dothiorella anamorphs. Mycologia 97: 513–529.
Phillips AJL, Hyde KD, Alves A, et al. 2019. Families in Botryosphaeriales: a phylogenetic, morphological and evolutionary perspective. Fungal Diversity 94: 1–22.
Pitt WM, Úrbez-Torres JR, Trouillas FP. 2015. Dothiorella and Spencermartinsia, new species and records from grapevines in Australia. Australasian Plant Pathology 44: 43–56.
Polizzi G, Aiello D, Castello I, et al. 2011. Occurrence, molecular characterisation, and pathogenicity of Neoscytalidium dimidiatum on Citrus in Italy. Acta Horticulturae 892: 237–243.
Rayner RW. 1970. A mycological colour chart. CMI and British Mycological Society, Kew, Surrey, UK.
Rehner SA, Samuels GJ. 1994. Taxonomy and phylogeny of Gliocladium analysed from nuclear subunit ribosomal DNA sequences. Mycological Research 95: 625–634.
Rodríguez-Gálvez E, Guerrero P, Barradas C, et al. 2017. Phylogeny and pathogenicity of Lasiodiplodia species associated with dieback of mango in Peru. Fungal Biology 121: 452–465.
Ronquist F, Huelsenbeck JP. 2003. MrBayes 3: Bayesian phylogenetic inference under mixed models. Bioinformatics 19: 1572–1574.
Saccardo PA. 1877. Fungi Veneti novi vel critici vel Mycologiae Venetae addendi. Series VI. Michelia 1 (1): 1–72.
Saccardo PA. 1882. Sylloge Pyrenomycetum, Vol. I. Sylloge Fungorum 1: 1–768.

Saccardo PA. 1884. Sylloge Fungorum: Sylloge Sphaeropsidearum et Melanconiearum. Sylloge Fungorum 3: 1–840.
Sakalidis ML, Hardy GEStJ, Burgess TI. 2011. Use of the Genealogical Sorting Index (GSI) to delineate species boundaries in the Neofusicoccum parvum-Neofusicoccum ribis species complex. Molecular Phylogenetics and Evolution 60: 333–344.
Sakalidis ML, Slippers B, Wingfield BD, et al. 2013. The challenge of understanding the origin, pathways and extent of fungal invasions: global populations of the Neofusicoccum parvum – N. ribis species complex. Diversity and Distributions 19: 873–883.
Sakayaroj J, Preedanon S, Supaphon O, et al. 2010. Phylogenetic diversity of endophyte assemblages associated with the tropical seagrass Enhalus acoroides in Thailand. Fungal Diversity 42: 27–45.
Sarr MP, Ndiaya M, Groenewald JZ, et al. 2014. Genetic diversity in Macrophomina phaseolina, the causal agent of charcoal rot. Phytopathologia Mediterranea 53: 250–268.
Scarlett KA, Shuttleworth LA, Collins D, et al. 2018. Botryosphaeriales associated with stem blight and dieback of blueberry (Vaccinium spp.) in New South Wales and Western Australia. Australasian Plant Pathology 48: 45–57.
Schoch CL, Shoemaker RA, Seifert KA, et al. 2006. A multigene phylogeny of the Dothideomycetes using four nuclear loci. Mycologia 98: 1041–1052.
Slippers B, Boissin E, Phillips AJ, et al. 2013. Phylogenetic lineages in the Botryosphaeriales: a systematic and evolutionary framework. Studies in Mycology 76: 31–49.
Slippers B, Crous PW, Jami F, et al. 2017. Diversity in the Botryosphaeriales: Looking back, looking forward. Fungal Biology 121: 307–321.
Slippers B, Roux J, Wingfield MJ, et al. 2014. Confronting the constraints of morphological taxonomy in the Botryosphaeriales. Persoonia 33: 155–168.
Slippers B, Wingfield MJ. 2007. Botryosphaeriaceae as endophytes and latent pathogens of woody plants: diversity, ecology and impact. Fungal Biology Reviews 21: 90–106.
Smith H, Wingfield MJ, Crous PW, et al. 1996. Sphaeropsis sapinea and Botryosphaeria dothidea endophytic in Pinus spp. and Eucalyptus spp. in South Africa. South African Journal of Botany 62: 86–88.
Stamatakis A. 2014. RAxML version 8: a tool for phylogenetic analysis and post-analysis of large phylogenies. Bioinformatics 30: 1312–1313.
Swofford DL. 2003. PAUP*: phylogenetic analysis using parsimony. (*and other methods). Version 4.0b10. Sinauer Associates, Sunderland.
Theissen F, Sydow H. 1918. Vorentwürfe zu den Pseudosphaeriales. Annales Mycologici 16: 1–34.
Trakunyingcharoen T, Lombard L, Groenewald JZ, et al. 2015. Caulicolous Botryosphaeriales from Thailand. Persoonia 34: 87–99.
Vilgalys R, Hester M. 1990. Rapid genetic identification and mapping of enzymatically amplified ribosomal DNA from several Cryptococcus species. Journal of Bacteriology 172: 4238–4246.
White TJ, Bruns T, Lee S, et al. 1990. Amplification and direct sequencing of fungal ribosomal RNA genes for phylogenetics. In: Innis MA, Gelfand DH, Sninsky JJ, et al. (eds), PCR Protocols: a guide to methods and applications: 315–322. Academic Press, San Diego, CA, USA.
Wijayawardene NN, Hyde KD, Wanasinghe DN, et al. 2016. Taxonomy and phylogeny of dematiaceous coelomycetes. Fungal Diversity 77: 1–316.
Wikee S, Lombard L, Nakashima C, et al. 2013. A phylogenetic re-evaluation of Phyllosticta (Botryosphaeriales). Studies in Mycology 76: 1–29.
Wyka SA, Broders KD. 2016. The new family Septorioideaceae, within the Botryosphaeriales and Septorioides strobi as a new species associated with needle defoliation of Pinus strobus in the United States. Fungal Biology 120: 1030–1040.
Xu C, Wang CS, Ju LL, et al. 2015. Multiple locus genealogies and phenotypic characters reappraise the causal agents of apple ring rot in China. Fungal Diversity 71: 215–231.
Yang T, Groenewald JZ, Cheewangkoon R, et al. 2017. Families, genera, and species of Botryosphaeriales. Fungal Biology 121: 322–346.
Zhou S, Stanosz GR. 2001. Relationships among Botryosphaeria species and associated anamorphic fungi inferred from the analyses of ITS and 5.8S rDNA sequences. Mycologia 93: 516–527.
Zhou YP, Dou ZP, He W, et al. 2016. Botryosphaeria sinensia sp. nov., a new species from China. Phytotaxa 245: 43–50.
Zhou YP, Zhang M, Dou ZP, et al. 2017. Botryosphaeria rosaceae sp. nov. and B. ramosa, new botryosphaeriaceous taxa from China. Mycosphere 8: 162–171.
Zhu HY, Tian CM, Fan XL. 2018. Studies of botryosphaerialean fungi associated with canker and dieback of tree hosts in Dongling Mountain of China. Phytotaxa 348: 63–76.
Zlatkovic M, Keca N, Wingfield MJ, et al. 2016. Botryosphaeriaceae associated with the die-back of ornamental trees in the Western Balkans. Antonie Van Leeuwenhoek 109: 543–564.

Supplementary material

Table S1 Collection details and GenBank accession numbers of isolates included in the phylogenetic analyses. Novel species, strains with type status and GenBank accession numbers of novel sequences are highlighted with **bold** font. A question mark in front of a previous species name means that this is a putative synonym of the current species name.

Table S2 Statistical parameters describing the sequence alignments and phylogenetic analysis (supplementary data) of the individual genes of the studied genera. For the Bayesian analyses, the same models were used as those used for the corresponding partitions in the combined alignments. Locus abbreviations follow Table 1.

Fig. S1 Phylogenetic tree of *Botryosphaeria* resulting from a Bayesian analysis of the individual ITS, *tef1* and *tub2* (A–C) sequence alignments. Bayesian posterior probabilities (PP > 0.90) are shown at the nodes. Taxonomic novelties are indicated in **bold** font. The tree was rooted to *Cophinforma eucalypti* (CBS 134651).

Fig. S2 Phylogenetic tree of *Diplodia* resulting from a Bayesian analysis of the individual ITS, *tef1* and *tub2* (A–C) sequence alignments. Bayesian posterior probabilities (PP > 0.89) are shown at the nodes. Taxonomic novelties are indicated in **bold** font. The tree was rooted to *Lasiodiplodia theobromae* (CBS 164.96).

Fig. S3 Phylogenetic tree of *Dothorella* resulting from a Bayesian analysis of the individual ITS, *tef1* and *tub2* (A–C) sequence alignments. Bayesian posterior probabilities (PP > 0.90) are shown at the nodes. Taxonomic novelties are indicated in **bold** font. The tree was rooted to *Neofusicoccum luteum* (CBS 121482).

Fig. S4 Phylogenetic tree of *Lasiodiplodia* resulting from a Bayesian analysis of the individual ITS, *rpb2*, *tef1* and *tub2* (A–D) sequence alignments. Bayesian posterior probabilities (PP > 0.90) are shown at the nodes. Taxonomic novelties are indicated in **bold** font. The tree was rooted to *Neodeightonia phoenicum* (CBS 122528).

Fig. S5 Phylogenetic tree of *Neofusicoccum* resulting from a Bayesian analysis of the individual ITS, *rpb2*, *tef1* and *tub2* (A–D) sequence alignments. Bayesian posterior probabilities (PP > 0.90) are shown at the nodes. Taxonomic novelties are indicated in **bold** font. The tree was rooted to *Botryosphaeria dothidea* (CBS 115476).

Fig. S6 Phylogenetic tree of *Neofusicoccum parvum species* complex resulting from a Bayesian analysis of the individual ITS, *rpb2*, *tef1* and *tub2* (A–D) sequence alignments. Bayesian posterior probabilities (PP > 0.90) are shown at the nodes. Taxonomic novelties are indicated in **bold** font. The tree was rooted to *Botryosphaeria dothidea* (CBS 115476).

Fig. S7 Phylogenetic tree of *Neoscytalidium* resulting from a Bayesian analysis of the individual ITS, *tef1* and *tub2* (A–C) sequence alignments. Bayesian posterior probabilities (PP > 0.90) are shown at the nodes. Taxonomic novelties are indicated in **bold** font. The tree was rooted to *Botryosphaeria dothidea* (CBS 117451).

Fig. S8 Phylogenetic tree of *Phaeobotryon*, *Alanphillipsia*, *Barriopsis*, *Oblongocollomyce* and *Sphaeropsis* resulting from a Bayesian analysis of the individual ITS, LSU and *tef1* (A–C) sequence alignments. Bayesian posterior probabilities (PP > 0.90) are shown at the nodes. Taxonomic novelties are indicated in **bold** font. The tree was rooted to *Cophinforma eucalypti* (CBS 117451).

Fig. S9 Phylogenetic tree of *Pseudofusicoccum* resulting from a Bayesian analysis of the individual ITS, *tef1* and *tub2* (A–C) sequence alignments. Bayesian posterior probabilities (PP > 0.90) are shown at the nodes. Taxonomic novelties are indicated in **bold** font. The tree was rooted to *Dothiorella parva* (CBS124720).

Fig. S10 Phylogenetic tree of *Saccharata* resulting from a Bayesian analysis of the individual ITS, *rpb2* and *tef1* (A–C) sequence alignments. Bayesian posterior probabilities (PP > 0.90) are shown at the nodes. Taxonomic novelties are indicated in **bold** font. The tree was rooted to *Aplosporella hesperidiaca* (CBS732.79).